Computational assessment of the feasibility of an ATES triplet system
Case study: Mijnbouwstraat 120, Delft

Wasman, Raymon J.

Award date:
2023

Computational assessment of the feasibility of an ATES triplet system

Case study: Mijnbouwstraat 120, Delft

MSc graduation thesis

R.J. Wasman

March 2023

EINDHOVEN
UNIVERSITY OF
TECHNOLOGY

Computational assessment of the feasibility of an ATES triplet system

Case study: Mijnbouwstraat 120, Delft

MSc graduation thesis
for master's track Building Physics and Services
of the master Architecture, Building and Planning

Student:
R.J. (Raymon) Wasman
1613111

Graduation supervision committee:

Dr. Ir. T.A.J. van Hooff	(Chair)
Dr. Ir. R.P. Kramer	(Daily supervisor)
Ir. W.H. Maassen EngD	(Advisor, TU/e & Royal HaskoningDHV)
Ir. M.P.E. Maas	(External advisor, Royal HaskoningDHV)

March 2023

Course: 7S45M0, 45 ECTS
Date of graduation: April 6, 2023

Eindhoven University of Technology
Department: Built environment
Unit: Building Physics and Services
Chair: Building Services

This master's thesis has been carried out in accordance to the TU/e code of scientific conduct

EINDHOVEN UNIVERSITY OF TECHNOLOGY

Preface

This thesis has been written for my research graduation project for the Master's track Building Physics and Services at the Eindhoven University of Technology. The topic of this research is a feasibility study of a potential way to save energy in buildings, in the form of an ATES triplet system.

This graduation project is the final project before getting my Master's degree. I started in September 2020 with the premaster. In February 2021, I started with the Master's degree, which will come to an end in April 2023. During this study, my focus was always on building services, which was the reason for choosing this Master's in the first place. I was pleased when this specific graduation topic came to my attention, as this topic includes almost all facets of building services. This gave me the further possibility to develop myself wider within the building services field.

I want to thank my daily supervisors Marco Maas and Rick Kramer, respectively of Royal HaskoningDHV and the Eindhoven University of Technology, for their guidance, time, and knowledge. I also want to thank Wim Maassen for his supervision during this project, and for being able to assign me this specific research topic. Also, I want to thank Twan van Hooff, for being able to complete the graduation committee as chair at the last moment. The last person I want to thank is Jan Bakker, for his help regarding hydraulic design and control questions. Also, I want to thank Royal HaskoningDHV for providing the opportunity to collaborate on this project.

Raymon Wasman

Schiedam, March 13, 2023

Abstract

Large energy savings are already being achieved relative to conventional systems with ATES doublet systems. However, the majority of the energy in such a system is consumed by the heat pump. The energy consumption of the heat pump still is substantial and creates a significant load on the electricity grid. An ATES triplet system can reduce energy consumption and grid load. In an ATES triplet system, heat is generated by solar collectors and cold is generated by a dry cooler. Generated heat and cold that cannot directly be delivered to the building are stored in a hot and cold ATES well. These well temperatures are directly at building supply level. The third well, the buffer well, is introduced to prevent thermal pollution of the two other wells.

This research uses a dynamic integral simulation model to investigate the feasibility of an ATES triplet system for a specific case. The case is Mijnbouwstraat 120 in Delft. This will be the first Paris Proof monumental building in The Netherlands and is being renovated into an office. The monumental status of the building has not been taken into account. The building consumers and heat and cold generators are modeled in detail. The ATES wells are modeled in less detail.

The simulations show that a monovalent ATES triplet system for the Mijnbouwstraat case is not technically feasible. The reason for this is that the solar collectors cannot generate enough heat to overcome the demand and losses in the system. Therefore, an additional heat source must be introduced. In this research, this additional heat source is in the form of a water-water heat pump. The heat consumption of the building is 561 MWh. The heat pump has to generate 29 MWh (5%) of the heat demand, while the other 532 MWh (95%) comes from the triplet system. Relative to the doublet, 150 MWh (82%) of energy is saved. The electricity grid peak load reduces by 312 kW (94%). With a heat pump capacity of 125 kW, the triplet system can be made reliable to withstand extreme consecutive cold weather years. The financial performance of the triplet system is worse than the doublet. The higher investment costs of the triplet cannot be made up by the reduction in operational costs. This results in a higher total cost of ownership for the triplet of €537k (11%) over a doublet system over a 30-year period. Subsidies have not been considered, but can possibly improve the financial performance. An approximate 73% CO_2 reduction is achieved relative to the doublet.

The conflict of a triplet system with PV panels can have a large impact on feasibility. A triplet system requires all available roof space to be filled with solar collectors, which leaves no room left for PV panels. However, the energy consumption reduction realized by the triplet system is smaller than the electricity generation of the originally installed PV panels for the Mijnbouwstraat case. This would result in a higher net energy consumption when implementing a triplet, which makes it unfeasible. A solution for this is to (partially) install PVT collectors. However, PVT collectors have a significant reduced thermal performance relative to solar collectors. This causes the energy savings to reduce to 112 MWh (61%) and the heat pump share to rise to 38%. The difference in total cost of ownership grows to €833k (17%) relative to the doublet. With 300 kW (91%), the reduction in peak electricity grid load still is significant, and can potentially play an important role in reducing grid congestion.

The conclusion is that an ATES triplet system can be technically feasible in bivalent form, but the total cost of ownership is higher than for a doublet system. The system can provide great benefits by reducing energy consumption, CO_2 emissions, and electricity grid load.

Samenvatting

Er worden al grote energiebesparingen behaald ten opzichte van conventionele systemen met WKO doublet systemen. Echter, het grootste gedeelte van de energie in zo'n systeem wordt verbruikt door de warmtepomp. Het energieverbruik van deze warmtepomp is nog steeds substantieel, en creëert een significante belasting op het elektriciteitsnet. Een WKO triplet systeem kan het energieverbruik en de netbelasting verminderen. In een WKO triplet systeem wordt warmte opgewekt door zonnecollectoren en koude door een droge koeler. Opgewekte warmte en koud die niet rechtstreeks aan het gebouw geleverd kan worden wordt opgeslagen in een warme en koude WKO bron. Deze brontemperaturen zijn direct op gebouw aanvoertemperatuur niveau. De derde bron, de bufferbron, is geïntroduceerd om thermische vervuiling in de andere twee bronnen te voorkomen.

Dit onderzoek gebruikt een dynamisch integraal simulatiemodel om de haalbaarheid van een WKO triplet systeem te onderzoeken voor een specifieke casus. Deze casus is Mijnbouwstraat 120 in Delft. Dit zal het eerste Paris Proof monumentale gebouw in Nederland zijn, en wordt gerenoveerd tot een kantoorgebouw. De monumentale status van het gebouw is niet meegenomen in het onderzoek. De afnemers en warmte en koude opwekkers zijn in detail gemodelleerd. De WKO bronnen zijn met minder detail gemodelleerd.

De simulaties laten zien dat een monovalent WKO triplet systeem voor de Mijnbouwstraat casus niet technisch haalbaar is. De reden hiervoor is dat de zonnecollectoren niet genoeg warmte op kunnen wekken om de vraag en verliezen te boven te komen. Daarom moet er een additionele warmtebron worden geïntroduceerd. Voor dit onderzoek is de toegepaste additionele warmtebron een water-water warmtepomp. De warmtevraag van het gebouw is 561 MWh. De warmtepomp moet 29 MWh (5%) van de warmtevraag opwekken, terwijl de andere 532 MWh (95%) van het tripletsysteem komt. Relatief aan de doublet wordt er 150 MWh (82%) aan energie bespaard. De piek op het elektriciteitsnet wordt verminderd met 312 kW (94%). Met een warmtepompcapaciteit van 125 kW kan het triplet systeem betrouwbaar worden gemaakt voor opeenvolgende extreem koude jaren. De financiële prestatie van de triplet is slechter dan de doublet. De hogere investeringskosten van de triplet kunnen niet worden goedgemaakt door de lagere operationele kosten. Dit resulteert in een hogere totale eigendomskosten voor de triplet van €537k (11%) ten opzichte van een doublet in een periode van 30 jaar. Subsidies zijn niet meegenomen, maar kunnen de financiële prestatie mogelijk verbeteren. Er wordt een CO_2 emissie reductie behaald van ongeveer 73% relatief aan de doublet.

Het conflict van een triplet met PV panelen kan een grote impact hebben op de haalbaarheid. Een triplet systeem heeft alle dak ruimte nodig om te beleggen met zonnecollectoren, waardoor een geen ruimte over is voor PV panelen. Echter is de energiebesparing die gerealiseerd wordt door de triplet kleiner dan de elektrische opbrengst van de origineel geïnstalleerde PV panelen voor de Mijnbouwstraat casus. Dit zou resulteren in een hoger netto energieverbruik als er een triplet geïmplementeerd zou worden, wat onhaalbaar is. Een oplossing hiervoor is om (gedeeltelijk) PVT collectoren te installeren. Echter, PVT collectoren hebben een significant verminderde thermische prestatie relatief aan zonnecollectoren. Dit zorgt ervoor dat de energiebesparing wordt verlaagt naar 112 MWh (61%), en het warmtepomp aandeel stijgt naar 38%. Het verschil in totale eigendomskosten groeit naar €833k (17%) relatief aan de doublet in deze situatie. Met 300 kW (91%) is de reductie in elektriciteitsnet belasting nog steeds significant, en kan mogelijk een belangrijke rol spelen in het verminderen van net congestie.

De conclusie is dat een WKO triplet systeem technisch haalbaar kan zijn in bivalente vorm, maar dat de totale eigendomskosten hoger zijn dan voor een doublet systeem. Een WKO triplet systeem kan grote voordelen brengen, door vermindering in energieverbruik, CO_2 emissies en elektriciteitsnet belasting.

Table of contents

1 Introduction

To mitigate global warming, CO_2 emission reduction must be accomplished sector-wide. This includes the built environment. The first step in the Trias Energetica is the reduction in energy demand. A widely applied method to reduce this energy demand for buildings in The Netherlands is to apply ATES doublet systems in combination with a heat pump, for both new and renovated utility buildings. The energy consumption and CO_2 emissions of an ATES doublet system are already a big step forward relative to the conventional solution with a gas-fired boiler and chiller. However, in this relatively energy-efficient doublet system, the majority of the energy is consumed by the heat pump. This makes the heat pump responsible for considerable energy consumption and CO_2 emissions. Also, the electrification of heating and cooling by heat pumps, in combination with electrification in all other sectors puts an increasingly large strain on the electricity grid [1]. This can delay the implementation of sustainable solutions and therefore delays achieving the set climate goals.

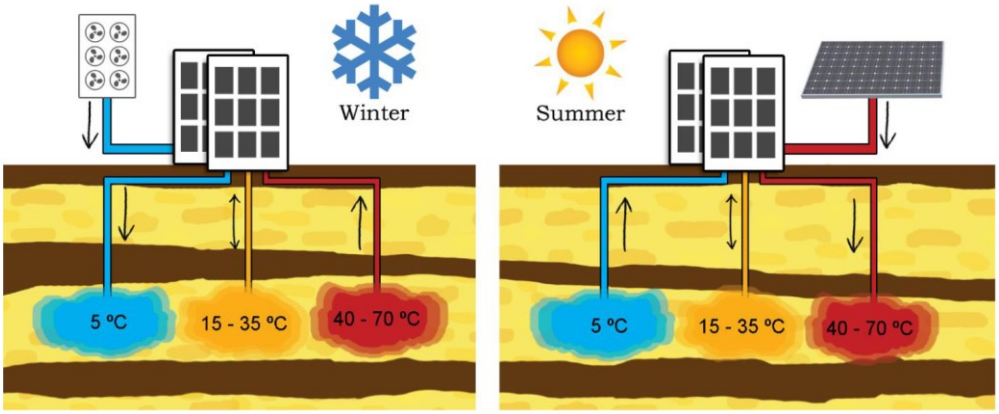

Figure 1 Indication of the basics of an ATES triplet system [2]

The basics of an ATES triplet system are visible in Figure 1. In an ATES triplet system, heat is generated by solar collectors and cold is generated by a dry cooler. Energy that cannot be directly supplied to the building is stored in aquifers, just like in normal ATES doublet systems [3]. However, where normal ATES doublet systems do incorporate a heat pump to increase the hot well water temperature to a usable level in the building, a triplet system does not incorporate a heat pump. Therefore, hot and cold water have to be generated and stored in the aquifer at a temperature level that is directly usable in the building. This means that the storage temperature of the water in the hot well has to be much higher than in a conventional doublet system, where this is mostly around 17°C. For a triplet, this would mostly be at 50°C or above. The name triplet comes from the fact that there are three wells present. The extra well is called the buffer well. When water from the hot well is extracted but cannot directly be injected into the cold well, due to lack of cold generation, the return water coming from the hot well is injected into the buffer well. This works also the other way around when the cold well is extracting water. The reason for doing this is to prevent thermal pollution in the hot and cold wells.

An ATES triplet system has potential advantages over an ATES doublet system. The concept of an ATES triplet system does not incorporate a heat pump. The only energy it consumes comes from pumps and fans. The result of this is a decrease in energy consumption, CO_2 emission, and electricity grid loads. Another advantage that an ATES triplet system can bring over an ATES doublet system is that heat and cold demand are mostly uncoupled. For a doublet

system, a too large difference in heat and cold demand can make a doublet unfeasible, and decrease its performance. In a triplet system, the difference between heat and cold demand plays a smaller role. This is because in a doublet system, when the hot well is discharging, it simultaneously charges the cold well, and vice versa. In a triplet system, because of the buffer well in between, discharging the hot well does not by definition result in simultaneously charging the cold well and vice versa, and therefore the hot and cold wells charging can be controlled individually. Another potential advantage is that a triplet system may be able to handle higher hot water supply temperatures than a doublet system, which makes it more applicable for older buildings, where low-temperature heating is no option.

There are many obstacles to overcome and questions to be answered before an ATES triplet system can be implemented. Up until now, only one research on ATES triplet systems has been done, performed by Pape [3]. That research's main focus lies on the sub-subsurface side of the system, and not so much on the generation and building side. The research shows the promise of ATES triplet systems, but due to the lack of detail in the generation and building side, no complete picture can be drawn. Due to the fact that there is only one research available on the triplet, there is almost no knowledge about the functioning of the system. In principle, an ATES triplet system is built up from all mature developed components. However, in a triplet system, those components are used in a different combination and with other functions than normal. Large-scale solar collector applications for buildings are as of yet not very common in The Netherlands. As heat and cold generation are dependent on uncontrollable factors in a triplet system, the weather, the question is how reliable a triplet system is. And how financially feasible it is. Currently, there are also regulatory restrictions that would currently prevent the implementation of a triplet system. This is because the maximum allowed ATES well injection temperature is 25°C, and a heat surplus in the subsurface is not allowed [4]. The first restriction surely conflicts with the functioning of a triplet system, and the second restriction can be a conflict, depending on the situation. Potentially, the heat and cold generation sources can also be different than solar collectors and a dry cooler, but has not been investigated in this research.

This research assesses the feasibility of an ATES triplet system, both technical and financial feasibility. It also gains insight into the dynamics of the system, by for example investigating the losses in the system. A specific case is used for this research: Mijnbouwstraat 120 in Delft. This is a former TU Delft faculty building, built in 1912. It has the status of national monument and is currently being transformed into an office building. The building design incorporates an ATES doublet system, and is aimed to be the first Paris Proof monumental building in The Netherlands. Important to notice is that during this research, the monumental status of the building is not considered to make it a more representative case.

1.1 Research questions

The main research question is the following:

What is the feasibility of an ATES triplet system for the Mijnbouwstraat case, and what factors influence the general feasibility of an ATES triplet system?

Multiple sub-questions have been formulated:

1 *Which aspects/components are important to model, to what level of detail, and how can they be modeled?"*

2 *What are the effects of the dynamics of an ATES triplet system for the Mijnbouwstraat?*

3 *What is the technical feasibility of an ATES triplet system for the Mijnbouwstraat?*

4 *What is the financial feasibility of an ATES triplet system for the Mijnbouwstraat?*

5 *What lessons can be learned from the Mijnbouwstraat case to indicate the general feasibility of an ATES triplet system?*

1.2 Approach

The approach of this research is globally displayed in Figure 2. The research starts by analyzing the triplet concept and looking into the functionalities the system must include. Based on this, a hydraulic design is created. From the triplet concept and the hydraulic design comes clear what components are included in the system, and therefore what components must be modeled for the simulation model. Then is determined on what level of detail and with what functionalities each component must be modeled, and how the total simulation model must be built. The next step is to create the simulation model, and then apply the parameters of the case to the model, and where possible calibrate it based on available design data. The model is built in the Matlab Simulink environment.

When the simulation model is completed, it is used to simulate different scenarios. The main focus is on the basis scenario, which is the scenario most applicable to the case. Based on this scenario, the system dynamics are visualized. Also, alternative scenarios are simulated to investigate the influence of uncertainties and other system configurations. The first alternative is a scenario with a lower assumed hot well efficiency, to investigate the effect on the system performance. Another simulated scenario is a quadruplet layout instead of a triplet layout, which can potentially improve system efficiency. The last simulated alternative scenario that is investigated is a scenario where the available roof space is assumed to not be a constraint for the solar collector placement, to get better insight into the possibility of a monovalent system.

Important to note is that all simulated scenarios are started during the operational phase. This means that the ATES wells do not start empty, but are already filled to a nominal energy level and temperature. The reason for this is the fact that the system performance and dynamics during the startup phase are vastly different than in the operational phase. While the startup phase only lasts for a short time (a few years), the operational period last much longer (decades), and is therefore more representative for the functioning of the system. The startup phase itself is simulated separately to also gain insight into this, and is the only simulated scenario that starts with empty wells.

Based on the simulated scenarios, the technical feasibility of the system is assessed. This is for example done by examining thermal power delivery, indoor comfort, and reliability, and is compared to a doublet system. The financial feasibility is assessed by a total cost of ownership calculation and is also compared to a doublet system. Also, calculations are made regarding the conflict between a triplet system and placed PV panels. With all results considered, this leads to the discussion, conclusion, and recommendations.

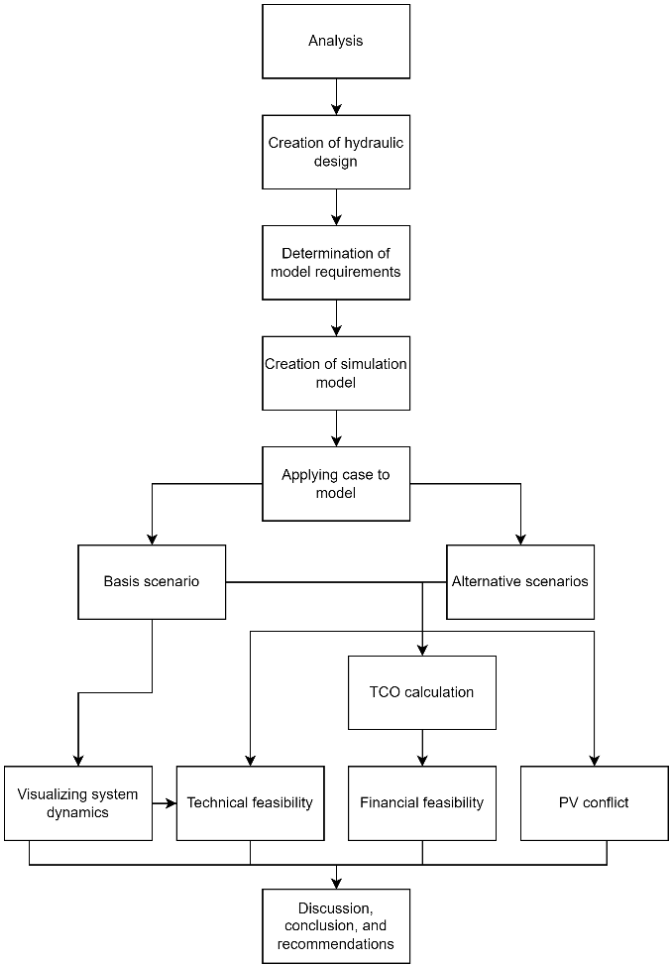

Figure 2 Global overview of the approach used during this research

1.3 Report structure

The next chapter provides more insight into the concept of a triplet system, and a hydraulic design for the triplet system is created and explained. Chapter 3 describes the use case of the Mijnbouwstraat. Chapter 4 elaborates on the details of the simulation model. Then in Chapter 5, all the results are presented and discussed. Chapter 6 presents the general discussion, conclusions, and recommendations for further research.

2 Concept and hydraulic design

The research of Pape [3] establishes the concept of the triplet. However, on the building and generation side, it lacks detail and functionality. With the used hydraulic layout in that study, simultaneous heat and cold delivery to the buildings from the wells is not possible. Also, the generation circuits are hydraulically coupled to the building, while this is not desired (because of the necessity of an antifreeze medium in the generation circuits). Another shortcoming of that design is that the CH (central heating) and CW (chilled water) circuits are hydraulically coupled, while in reality they have separate circuits. In this section of the report, a new hydraulic layout for a triplet system is proposed, and the concept of the triplet is further explained.

In a triplet system, the following independent processes can occur:

- Heating demand being fulfilled
- Cooling demand being fulfilled
- Heat being generated
- Cold being generated

From current buildings, it is already clear that heating and cooling demands can occur simultaneously. Solar collectors can produce heat, even at relatively low outdoor temperatures and irradiation levels. Therefore, it is likely that heating demand and heat generation can also occur simultaneously. Cold generation can only start with low outdoor temperatures. However, in rooms within buildings with a high internal load or with servers in it, a cold demand can also occur during low outdoor temperatures, which means that cold demand and cold generation can occur simultaneously. The starting point of each installation must always be to provide comfort to the building occupants, meaning fulfilling the heating and cooling demand must be the first priority of the triplet. When simultaneous demand and generation would not be possible, this would mean that the generation installations must always be turned off when there is a demand. This results in a lower generation yield, which would require higher generation capacity to generate the required amount of energy. This is ineffective and expensive. Therefore, is decided that the starting point of the hydraulic triplet design must be that all four of the above processes can occur simultaneously. Another function of the triplet is of course that the wells must be able to be charged and discharged.

Combining the requirements with common hydraulic design rules, a basic hydraulic design for an ATES triplet system is created. The basics of this design are applicable to all ATES triplet system applications. It is a simple, yet useful, design, providing maximum functionality.

2.1 Hydraulic design

The created hydraulic design is displayed in Figure 3, and is described in this section.

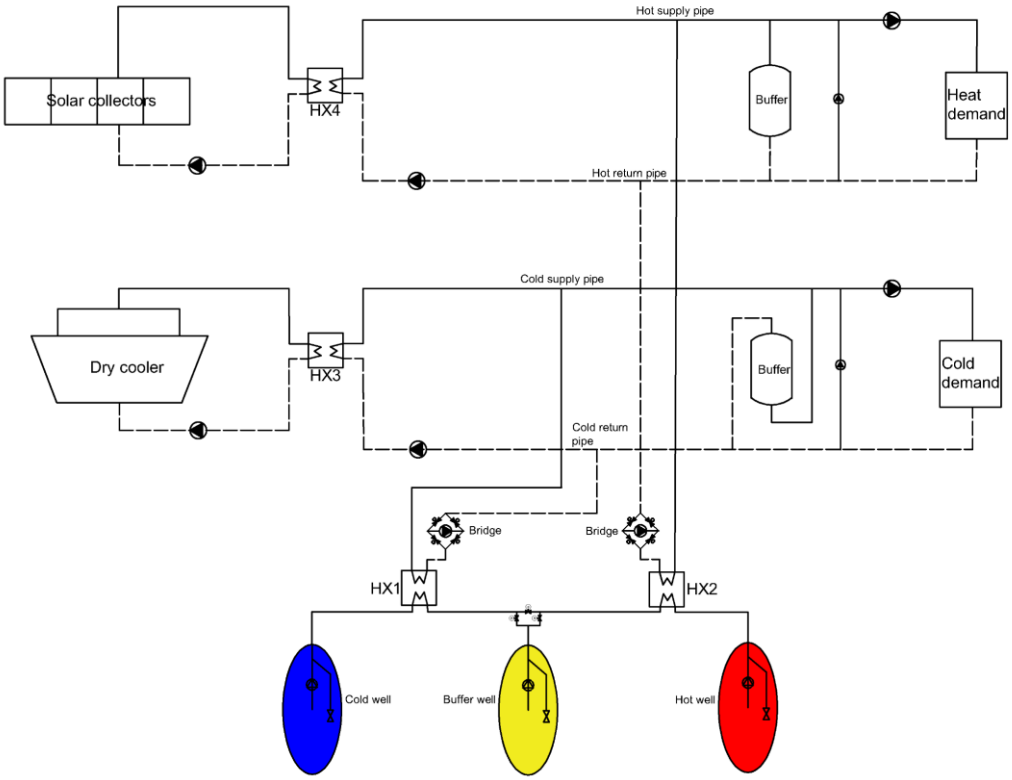

Figure 3 Overview of the created hydraulic design of an ATES triplet system

Subsurface wells

The explanation of the hydraulic design will be done from bottom to top. On the bottom are the three wells. Each well has a pump and an injection point. The cold and hot well both flow through a counter-flow heat exchanger (further referred to as HX). In the middle is the buffer well. In the piping from the buffer well to the other wells, control valves are placed. These control valves are used to direct the flows underground to the right place, and with the correct flow rate. The HXs are placed to hydraulically disconnect the subsurface circuit from the building circuit, which is conventional for ATES systems [5].

Main hydraulic circuit

Above the HXs, a pump is placed within a flow reversal module. This is because the flow at this place can be bi-directional, depending on if the well is charging or discharging. In the remainder of this report, the term 'bridge' is used to refer to the flow reversal modules. The solid lines going from HX1 and HX2 up vertically are connected to the main supply pipes, into a three-way connection. When the well is discharging, the water flows up in the pipe, carrying the energy delivered by the well, and then flows to the right, to the building demand section. When the wells are charging, the water flows down via this pipe, carrying the energy generated by the generators. This is also the reason for the flow reversal module around the pump. Parallel to this vertically drawn supply pipes are the (dotted) return pipes. When discharging, return water from the building flows through this pipe. When charging, energy coming from the return water or buffer well water from the underground circuit is transferred via the HX to this pipe.

Generators
When the generators (solar collectors or dry cooler) are active, water starts flowing in the closed generation circuit. This water flows then through the solar collectors or dry cooler, and through the HX. When there is a flow on one side of the HX (3 or 4), the pump on the other side will also become active. When there is a building demand at this moment, the water flows directly via the supply pipe to the building consumers. If the generated water flow is higher than demanded by the building, this water is used to charge the well, and then flows down via the solid vertical supply pipe. If there is generation, but this generation is less than the building demand, the remaining difference is supplied by the well. The well discharges, exchanges heat via the HX, and water flows up via the vertical supply pipe, and mixes with the water coming from the generator before it flows to the building consumers.

Temperature control
Near the building demand side, a shortcut between the supply and return is made, with a pump in it. This is to control the supply temperature to the building so that the supply water temperature setpoint can be followed. This supply temperature control for example has to act during the moment that there is a solar collector generation surplus. Because of the well inefficiencies, the injection temperature has to be higher than the desired well temperature. If for example 70°C is generated by the solar collector and injected into the well, but only 50°C is desired in the building, the shortcut mixes water from the return with the water of 70°C, to get a supply water temperature to the building of 50°C. This pre-temperature control of the water helps the control valves elsewhere in the building to be kept within their controllable operation point. The proposed solution for this temperature control is not the only possible solution. However, from a control perspective, this seems to be the simplest solution, but might be more expensive (hardware-wise) than other possible solutions.

Buffer vessel
The reason for placing buffer vessels is for one part the same as with conventional systems. This is mainly because pumps do have a minimum and maximum operating limit, and pumps cannot instantly achieve their setpoint, which can cause short-lasting differences between pumps. The buffer then helps to keep the flow consistent and prevents too frequent on/off switching of the pumps. In a triplet system, the buffer can have an additional function. It is more effective to supply power directly by the generators to the building than to first charge the well, and then discharge the well. This is because the wells, especially the hot well, lose a significant amount of energy. When charging the buffer vessels with water supplied by the generators until the buffer is full, and then discharging the buffer vessels when there is no generation surplus anymore, it is possible to save some energy. However, the buffer vessels volume will be limited, so the savings will also be limited.

This layout has been tested to check if it can perform in all possible operational modes. Over 30 operational modes are identified. An operational mode in this context is specified as the combination of flow directions at each point in the system. If the flow direction in one point in the system is different than in another specified operational mode, this is seen as a new operational mode. To make the concept more clear, two operational modes are shown and explained in the next figures. All possible operational modes are checked and it is concluded that the hydraulic design is able to support each operational mode.

2.2 Example operational mode 1

Example operational mode 1 is a typical situation one can find during the transition season. The outdoor temperature is 12°C and there is limited sunshine which generates some heat with the solar collectors. The building does have a heat demand larger than that is generated by the solar collectors and the building also does have a cold demand.

The water flow directions in this operational mode are displayed in Figure 4. To fulfill the building demands, and to make use of the generated heat by the solar collector, all generated heat is directly fed into the building. As the generated heat alone is not enough, also the hot well is discharged. At the top, the flow from the hot well and the solar collector water (not the actual water, as there are HXs in between) mixes, and then flows to the building consumers. There is also a cold demand, but no cold generation (as 12°C outdoor temperature is too high to generate any usable cold). This means all the cold required in the building has to be extracted from the cold well, so the cold well must discharge. This then flows into the building. At the HXs of both the cold well and the hot well, return water flows from the building consumers and is exchanged in the HX, and then flows underground, both into the buffer well.

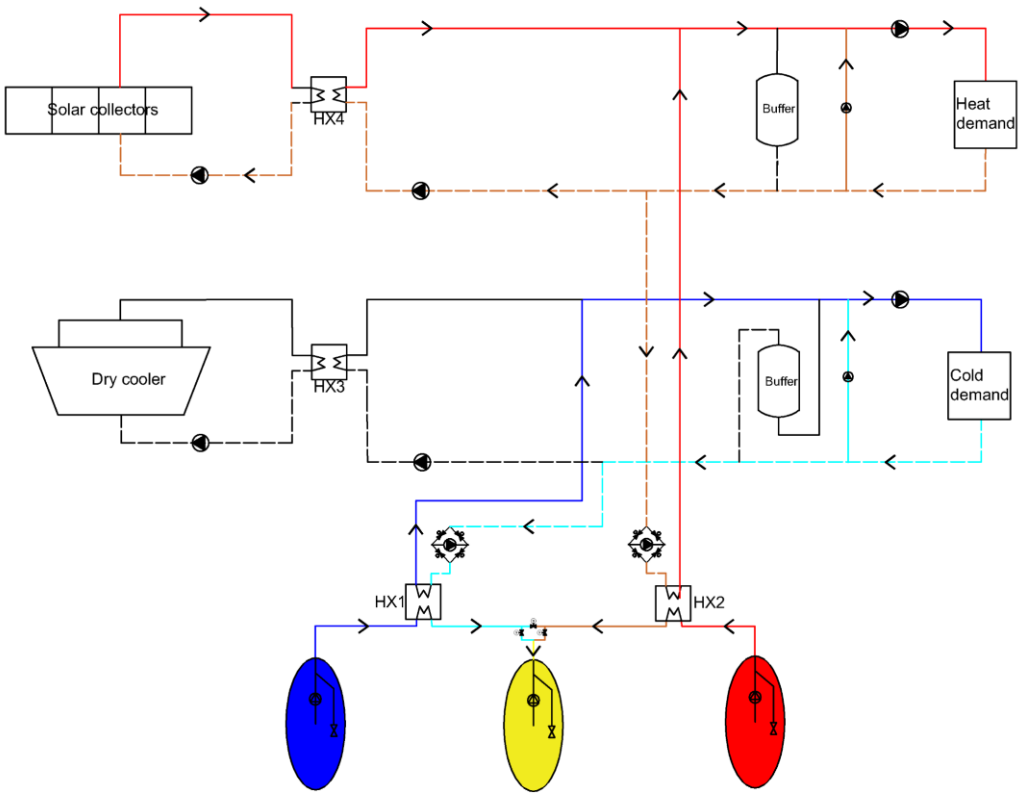

Figure 4 Display of example operational mode 1

2.3 Example operational mode 2

Example operational mode 2 is a situation that might occur during an afternoon in the winter. It is 3°C outside, and the sun is shining. For the generation side, this means that cold can be generated by the dry cooler, and a little bit of heat can be generated by the solar collector. From the demand side, this means that there is a large heating demand which is larger than generated, and a small cooling demand, which is smaller than generated.

The water flow directions in this operational mode are displayed in Figure 5. The small amount of heat generated by the solar collectors is directly supplied to the building. The remaining part of the heat demand is fulfilled by the hot well. The cold demand is directly fulfilled by the generated cold. The surplus of the generated cold is used to charge the cold well. It is assumed that the water flow from the hot well is smaller than the water flow that is required to charge the cold well. What this means is that all the return water coming from the hot well alone is not enough, so also water from the buffer well has to be extracted, to get enough water to the cold well. At HX1, this water mixture is then cooled down and injected into the cold well.

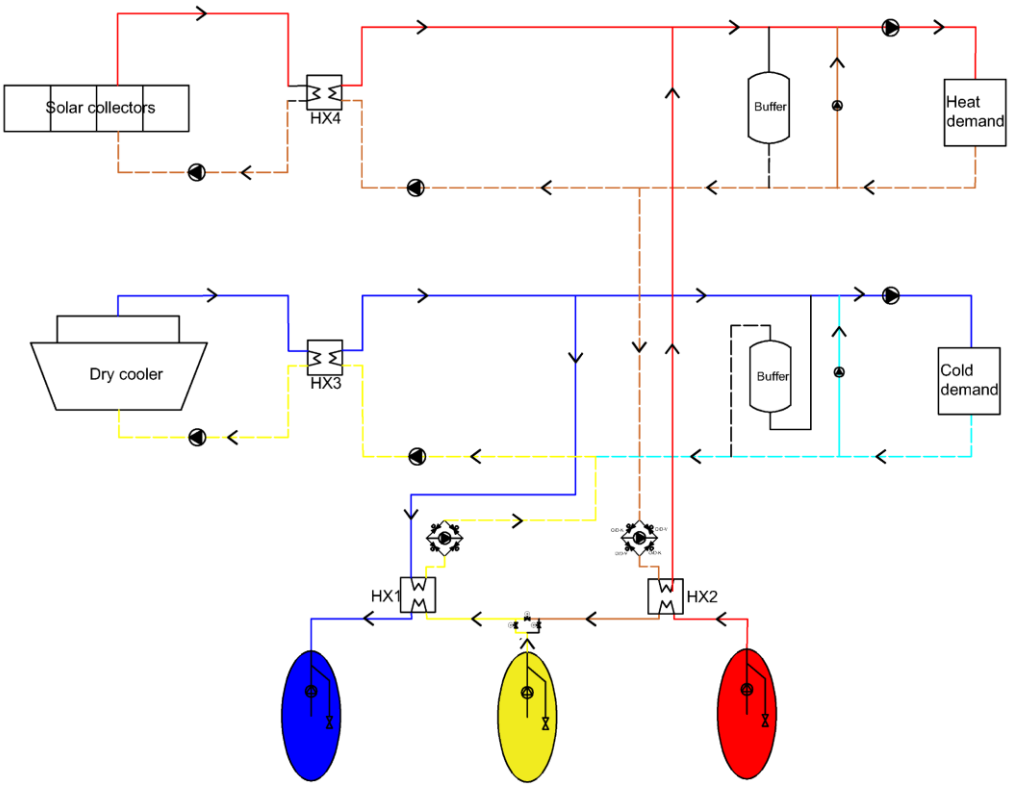

Figure 5 Display of example operational mode 2

3 Case

The building used as case during this research is the Mijnbouwstraat 120 in Delft, which was built in 1912. This is a former faculty building of the TU Delft and has the status as national monument. Now, it is being renovated into an office for Royal HaskoningDHV. After the renovation, it will be the first Paris Proof national monumental building in The Netherlands [6]. When an office is Paris Proof, it has a total net energy consumption below 70 kWh/m^2. This is the maximum calculated net energy consumption for offices in order to reach the climate goals for 2050 set at the 2015 Climate Agreement in Paris [7]. It will have energy label A+++. With the renovation, the two courtyards will be covered by a high roof, creating two atria. The figures below give an impression of the geometry before and after the renovation. The rough dimensions of the building are 120 m wide, 60 m deep, and 17 m high. Above ground, there are three usable levels (ground floor, first floor, and second floor), and there is some storage space in the attic on the third floor. Under the north wing, there is a usable basement. Under the west wing, bike storage will be created in the basement, and under most of the remainder of the building the basement is not usable as it is crawl space. The situation before the renovations is displayed in Figure 6 and Figure 7, while the situation after the renovation is displayed in Figure 8 and Figure 9.

Figure 6 Aerial view of the Mijnbouwstraat 120 before the renovation. Source: Google Earth

Figure 7 Top view of the Mijnbouwstraat 120 before the renovation. Source: Google Earth

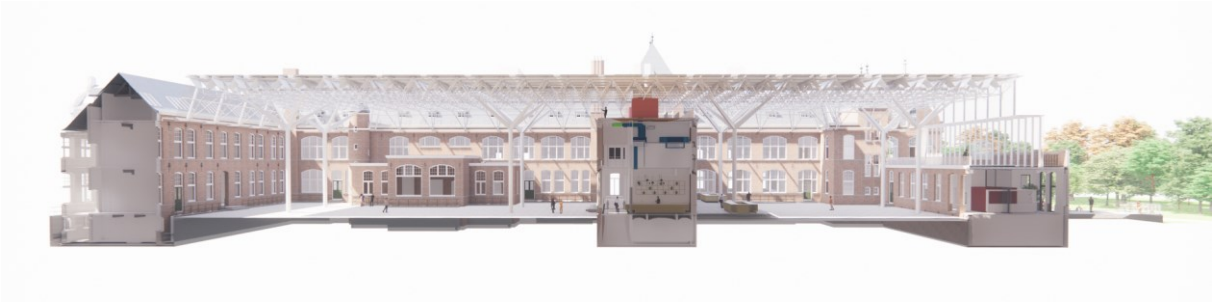

Figure 8 Render cross-section of the building after the renovation. Source: internal RHDHV design

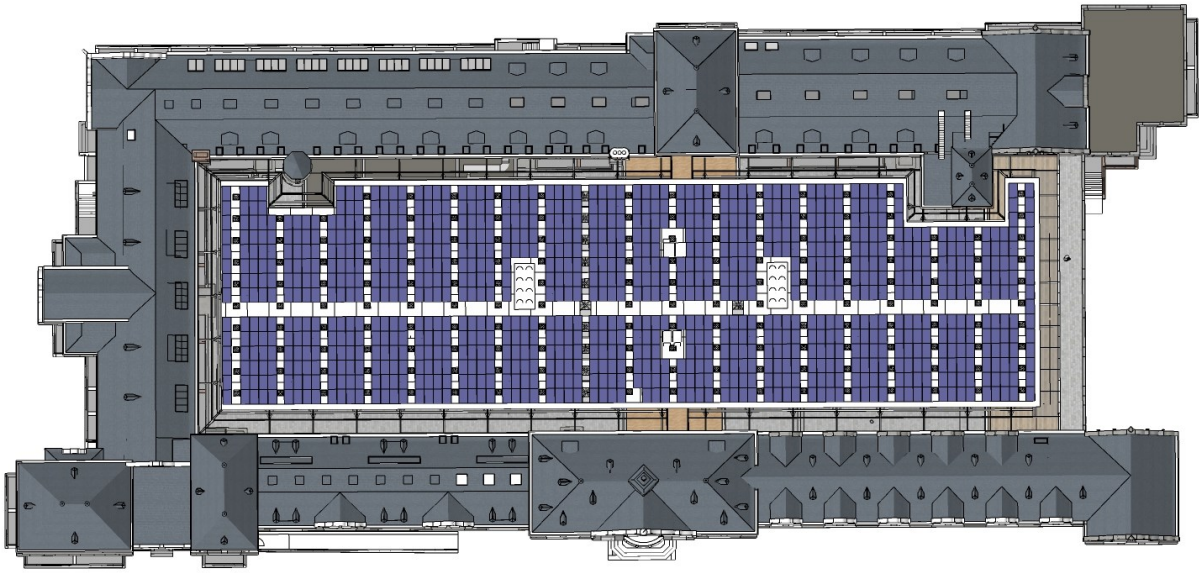

Figure 9 Render of top view after the renovation. Source: internal RHDHV design

The roofing over the courtyard is the main change that will be made to the geometry. Most other parts of the building are not changed externally. This is mainly due to the fact that the building is a monument, and therefore the external view must be kept intact. After the renovation, the gross floor area will be approximately 16,350 m^2. The usable floor area is 12,607 m^2.

Renovation

The most important points of the renovation are the following:

- Creation of two atria by putting a roof over the courtyards
- Changing the windows to HR++ glass
- Insulate the ground floor and the roofs. The tilted roof is insulated to an RC value of 6.1 m^2K/W, and the ground floors to an RC value of 3.5 m^2K/W. The façade is not extra insulated during the renovation on most places, and will keep the current RC value of 0.87 m^2K/W.
- New HVAC installations
- New energy plant (ATES doublet system with heat pumps)
- Placement of 1,500 m^2 of PV panels

3.1 HVAC design concept

The most important factors for the HVAC installation design concept of the original Mijnbouwstraat design are explained below.

3.1.1 Air handling units

The renovation design does include three air handling units (AHUs). The core function of the AHUs is to supply fresh air to the rooms, and does not have a core function in the heat or cold supply to rooms. To save energy, most rooms connected to the AHU have VAV units that control the airflow to each room based on CO_2 level. The AHU incorporates a heat recovery wheel, heating coil, and cooling coil. There is no recirculation within the AHU. The air supply temperature is controlled based on a heating curve, which relates the supply temperature setpoint to the (running mean) outdoor air temperature. The air supply temperature in this heating curve ranges from 16°C to 21°C. Ventilation air is supplied to rooms and then is transferred via grills to the hallways where it is extracted again.

3.1.2 Office and conference rooms

The main device to supply heat and cold to office and conference rooms are climate ceilings. This is a switchover system. The design water inlet temperature is 45°C for heating and 15°C for cooling. The hot water inlet temperature setpoint is based on a heating curve.

In office and conference rooms, also radiators are present. They are placed below most external windows. The function of these radiators is to prevent comfort complaints by draft from the windows. The radiators are equipped with thermostatic radiator valves. The design supply temperature is 50°C and is controlled based on a heating curve.

3.1.3 Atria

Heating and cooling are primarily provided by the underfloor system in the atria. The design water supply temperature for heating is 42°C, and for cooling 17°C. Both supply water temperatures are controlled based on a heating curve. In the atria, also water-supplied reheaters are present in the air supply ducts.

3.1.4 Other rooms

Radiators are present in the hallways. Technical rooms and unoccupied rooms do not have a form of heating or cooling. Rooms that are occupied but are not an office, conference room or atrium do mostly have climate ceilings. There are some rooms that have a fan coil unit, but these are the exceptions.

3.2 Predicted building consumption

The available dynamic building energy simulation model that was previously developed using Vabi Elements was adjusted on some points during this research, as this model was not fully finished yet, and was not completely in line with the design goals. The adjusted Vabi Elements model yields an annual thermal heat consumption of 591 MWh and a thermal cold consumption of 194 MWh, i.e. 46.9 kWh/m^2 for heating and 15.4 kWh/m^2 for cooling.

3.3 Power plant design

This section explains the power plant design of the original case. It also briefly translates the design differences from a doublet system to a triplet system.

Doublet

The power plant in the Mijnbouwstraat uses an all-electric concept. This means natural gas is not used in the building. The power plant consists of an ATES doublet system in combination with heat pumps. The flow capacity of the ATES is 85 m^3/h. Coupled to the ATES are two 300 kW water-water heat pumps. In winter, these heat pumps are used to raise the warm well water temperature to a building supply level temperature to supply it to the building. When producing heat, simultaneously cold is generated by the evaporator of the heat pump, which is then used to charge the cold well. There are also two 200 kW air-water heat pumps present in the design. The air-water heat pumps provide the peak in heat delivery, and also can act as an instrument to influence the ATES well thermal balance. All the cooling power can be provided by the cold ATES well. The design assumes that the heat pumps do not have to turn on to provide cooling peak power during normal operation. The flow capacity of the ATES is designed for this. The thermal power delivery distribution is displayed is Figure 10.

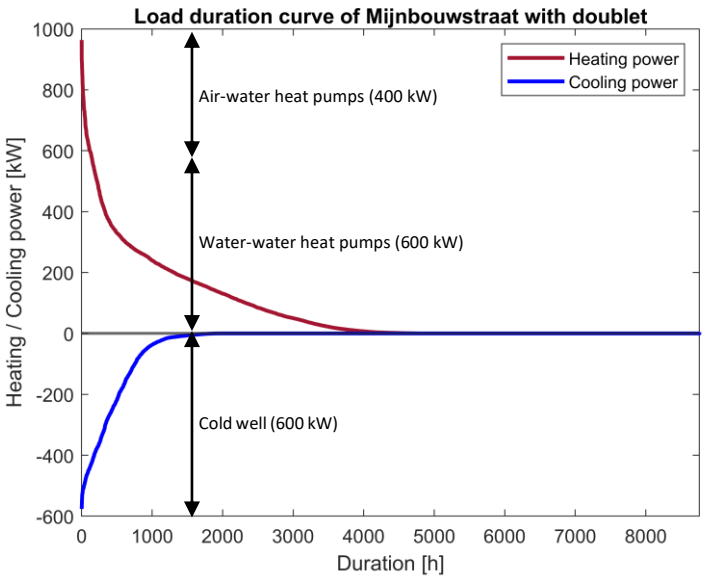

Figure 10 Indication of load duration curve of Mijnbouwstraat power plant for doublet system

The heating side will have 591 equivalent full load hours, while the cooling side will have 323 equivalent full load hours.

For heating, the designed water supply temperature is 50°C, with a designed return temperature of 40°C. For cooling, the designed water supply temperature is 12°C, with a designed return temperature of 18°C.

Triplet

The load duration curve of the triplet system will in principle be equal to that of the doublet system above, as it is a function of the building, not the energy plant. However, the triplet concept does not include heat pumps. This means that the ATES wells must be able to supply the full thermal peak power to the building. For the cold side, this is similar to the doublet

system, but for the hot side, this is different. Possibly it would require a higher well flow capacity than in the doublet.

What in the design of a triplet is also different from a doublet is that the heat and cold generation will be dependent on the weather, and available space. Especially for the hot side of the triplet system, this is important. The reason for this is the fact that the available roof space limits the solar collector area that can be placed, and therefore also the heat generation in the system. If the effective usable heat generation is lower than demand, this forms a problem. If this is the case, a monovalent system is not possible. However, good performance may still be possible with a bivalent system, by introducing an additional heat source. The Mijnbouwstraat does have relatively low heating and cooling demand, and also only has three usable floors. This would potentially make it a good contender for a triplet system, as this combination means that the required generation is relatively low, and the ratio of roof area to usable floor area is relatively high.

4 Development of dynamic building simulation model

This chapter explains all the different parts of the simulation model, and how the simulation model is tuned to the case of the Mijnbouwstraat.

4.1 Determination of required level of detail

The level of detail of the simulation model has been determined by analyzing the concept and hydraulic layout, and by testing the simplified and slightly adjusted simulation model by Pape [3]. As this model is not further used during this research, this model will not be explained. The main sub-models in a triplet system connected to a building are the consumers, the generators, the wells, and the building. For each of those sub-models, the required level of detail is indicated.

4.1.1 Heat and cold consumers

From this analysis, it appears that in triplet systems, temperature plays a bigger role than in conventional systems (like a doublet system) because of the absence of a heat pump. For a triplet, the generated temperatures by the solar collectors and the dry cooler, after intervention by the wells, are decisive for the temperatures that can be delivered to the building later on. There is no way of adjusting the temperature levels to a higher quality after the heat or cold have been generated. For systems with a heat pump, the well temperature levels are mainly important for energy consumption, as those temperatures partly determine the COP of the heat pump. For only a small part they determine the supply temperatures to the building, as for most instances the heat pump is capable of adjusting the supply temperatures to the desired levels.

Temperatures in a triplet system play an important role in two different ways. The first way is that if the supply temperatures are not appropriate, insufficient power can be delivered to the building, and therefore will have a negative effect on indoor comfort. The temperature levels in the wells vary throughout the year, and they vary more significantly if the well is closer to being empty. Because of those varying well temperatures, this can have an effect on the thermal power delivery, and therefore the indoor comfort levels. The second way are the return temperatures of the consumers. The return temperature is the product of different factors, such as the water supply temperature, the indoor air temperature, and the partial load the consumer is operating in, and therefore can vary significantly from the design conditions (which mostly considers full load operation and the maximum supply temperature of the heating curve). The return water flows of the consumers can end up in different locations in the system. For example, they can directly flow to the solar collector or dry cooler, or they can flow to the buffer well. In the buffer well, the return water flows of the heat and cold consumers will mix, causing thermal pollution. This thermal pollution is a form of energy quality loss. The quantity of this energy loss is determined by the resulting buffer well temperature, which is dependent on the water quantity and temperature of both return flows.

From the explanation above, it becomes clear that the supply and return temperature levels can have a large influence on the (successful) functioning of a triplet system, and possibly can determine the feasibility of the system. Taking this into consideration, temperatures and water flows must be modeled in detail for the heat and cold consumers.

4.1.2 Heat and cold generators

The previous section explains why temperature representation on the consumer side is important. As the solar collectors and dry cooler determine the generated temperature levels, and (with the wells in between) therefore also the supply temperature levels to the building, it is important to also represent temperature levels in detail on the generation side. Another reason for this is the fact that temperature levels (both inlet and outlet temperatures) partially determine the heat generation efficiency of the solar collectors. It is expected that the amount of available solar collector space versus the amount of solar collectors required can form a bottleneck for the implementation of the triplet system. Therefore, this adds another reason to represent temperatures in detail on the generation side.

4.1.3 Wells

The subsurface wells play an important role in the triplet system. They influence the temperature levels and energy losses, which most likely are of large influence on the feasibility of the triplet system. A detailed subsurface model is currently being developed by a PhD candidate at the TU Delft, specifically for an ATES triplet system. This detailed subsurface model will later be integrated with the simulation model used in this research. For this research now, a more simple subsurface model will be used. As the main focus of this research is more on the generation and building side, this is acceptable. The simple simulation model must be able to represent the well temperatures and energy losses.

4.1.4 Building

The building model must be able to handle the input of the consumer models in the form of supplied heating and cooling power, and give feedback to the consumer models in the form of realized room air temperatures, room radiative temperatures, and relative humidity. Geometry and specifications of the building must be represented, such as windows, insulation values, thermal mass, building layout, etc.

4.2 General model explanation

The previous section explains the required level of detail for all sub-models. In this section, the simulation model is explained in global form. In the next section, the sub-models are explained in more detail. The basis of the model is the current design of the Mijnbouwstraat, but then transformed into a triplet system.

From the analysis, it becomes clear that there are important interactions between all systems, and that those interactions are multidirectional. Taking this into consideration, it is deemed that the best and most valuable results can be achieved by creating an integral dynamic simulation model. This is displayed in Figure 11. In this model, the building installations are dynamically modeled and connected to a building simulation model, which can translate the thermal power provided by the installation into a room temperature. From the main hydraulic circuit, water flows in and out of the building installations. Also connected to this main hydraulic circuit are the dynamic solar collector model, dynamic dry cooler model, and the three dynamic subsurface wells.

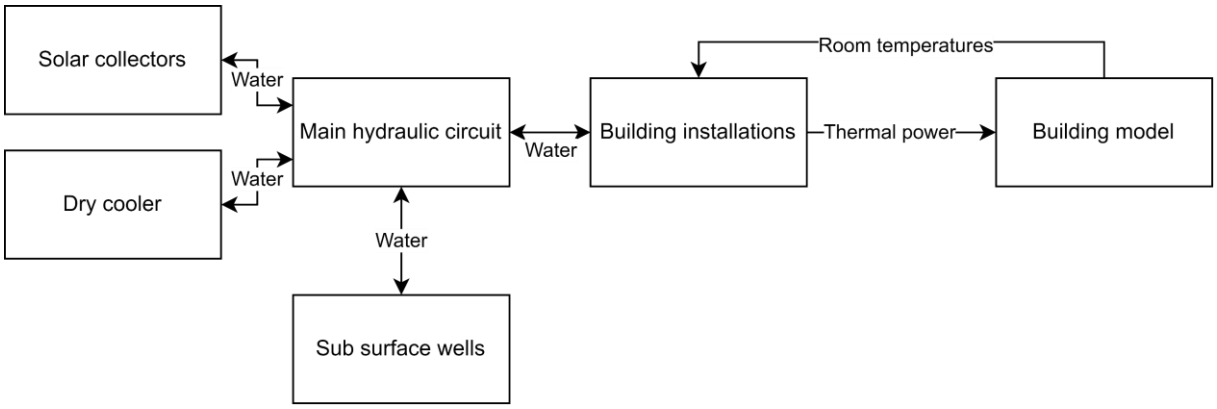

Figure 11 Simplified display of the integral dynamic simulation model

4.2.1 Deviations

The heat and cold consumers and their controls are kept the same as the original current design as much as possible. Also their temperature levels are kept the same. Some deviations have been made to the original design. These deviations can be found inAppendix IAppendix I Appendix IAppendix IAppendix I**Fout! Verwijzingsbron niet gevonden.**Appendix I.

4.2.2 Hydraulic layout

Taking the specific Mijnbouwstraat case and deviations into account, this then leads to the hydraulic layout displayed in Figure 12. Figure 13 zooms in on the hydraulic layout of the different consumer groups.

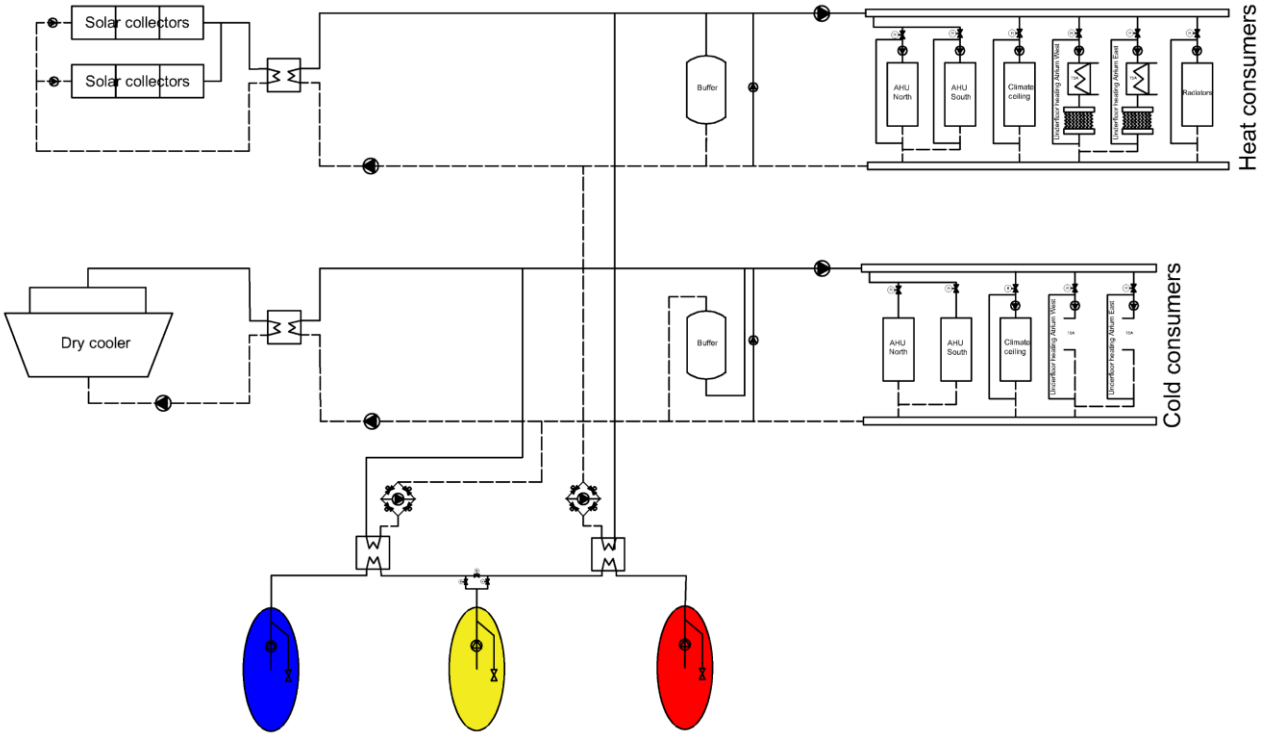

Figure 12 Hydraulic layout as used in the simulation model

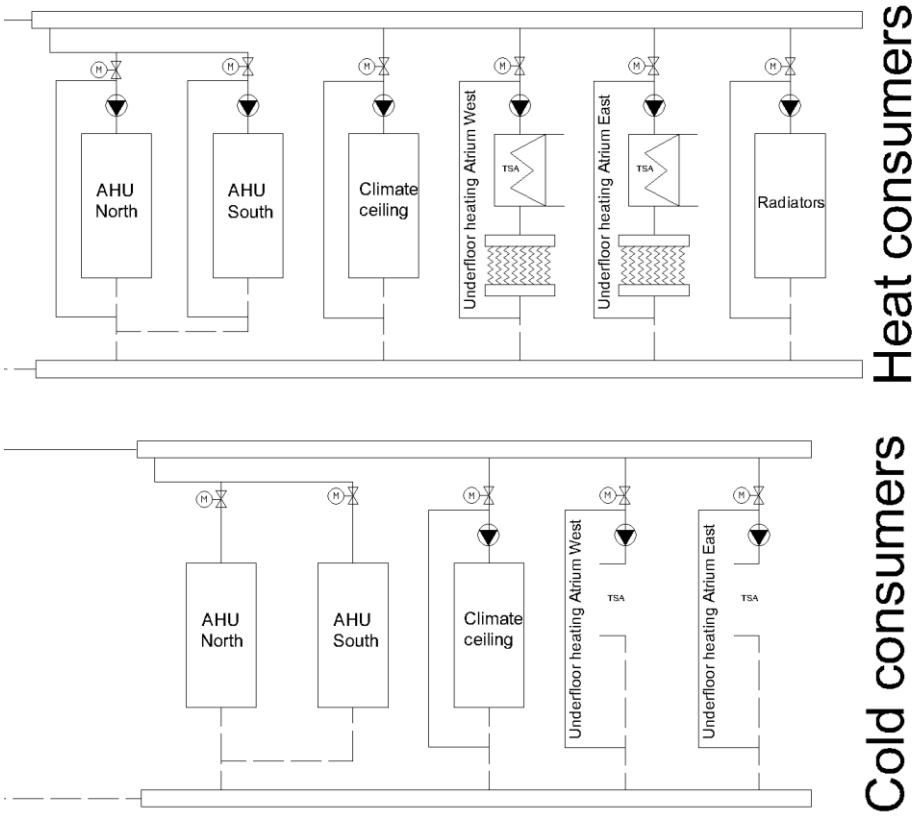

Figure 13 Detail of hydraulic layout of the consumers on group level as used in the simulation model

How each sub-system is modeled is explained in the next parts of this report. Also is explained how the sub-systems are coupled together, and how the system is controlled as a whole.

4.3 Sub-system modeling explanation

In this section, the modeling of the individual sub-systems is explained, together with their individual control. These sub-models are:

- Heat and cold consumers:
  - Underfloor system
  - Climate ceiling
  - Radiator
  - Air handling unit
- Buffer vessel
- Generators:
  - Solar collectors
  - Dry cooler
- Subsurface wells
- Building simulation model

Each consumer model, except the AHU, does have the same inputs and outputs. The difference between the different consumer models is how the output is determined, and how the input is controlled. This will be explained for each consumer in the next parts. The general block scheme for the consumers is displayed in Figure 14.

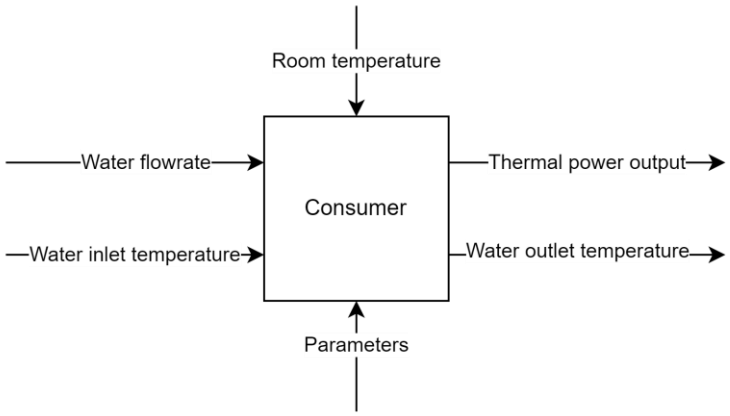

Figure 14 In and output of the consumers (with exception of the AHU coils)

4.3.1 Underfloor system

Physics model

The origin of the underfloor system physics model is the model created by Hoogervorst [8]. The control system connected to it has not been used. The model is a transient, one-dimensional electric-analog model: a network of resistances, capacities, and sources, which represent heat flows and heat resistances. The model is based on two pipes, as in most systems the supply and return pipes are next to each other. The pipes are integrated in the floor. This floor consists of different layers, each with its own thickness, thermal capacity, and heat flow resistance [8]. The model can be used for heating and cooling. The set of (differential) equations used can be found in Appendix II.

The dynamic inputs of the model are the water flow rate, the water inlet temperature, and the room temperature. The relevant dynamic outputs are the provided power to the room and the water outlet temperature. There are more outputs from the model, but those are not directly used any further in the model, only internally. Then there are static inputs, in the form of parameters. This includes information about the different material layers, pipe distance, pipe diameter, and heat transfer resistance.

Underfloor systems do have a large radiant fraction. The radiant fraction used for the underfloor system is 0.6, based on [9]–[12]. This fact has been integrated into the model by using Equation 1 to determine the room temperature input to the underfloor model.

$$Troom = T_{air} * CF + T_{radiant} * (1 - CF) \qquad 1$$

In which CF is the convection fraction (which is 1 - radiant fraction), T_{air} the room air temperature, and $T_{radiant}$ the average radiant temperature of the room.

Control

Each underfloor system does have its own connection to the distributor/collector. The system does make use of a constant water flow rate. This flow rate is different in heating or cooling mode. The supply temperature is based on a heating curve, which gives a relation between the desired water supply temperature and the (running mean) outdoor temperature. Using a control valve, the right amount of supply water is mixed with the return water, to achieve the water supply temperature to the underfloor system according to the setpoint (which is the

heating curve value at that moment). The main control of the underfloor system is an on/off control, which is done by a relay, which acts in relation to the difference between the room temperature setpoint and the actual room temperature. The cold water supply first flows through an HX. For this, a constant temperature jump of 1K is assumed. A simplified overview of the underfloor system model is displayed in Figure 15.

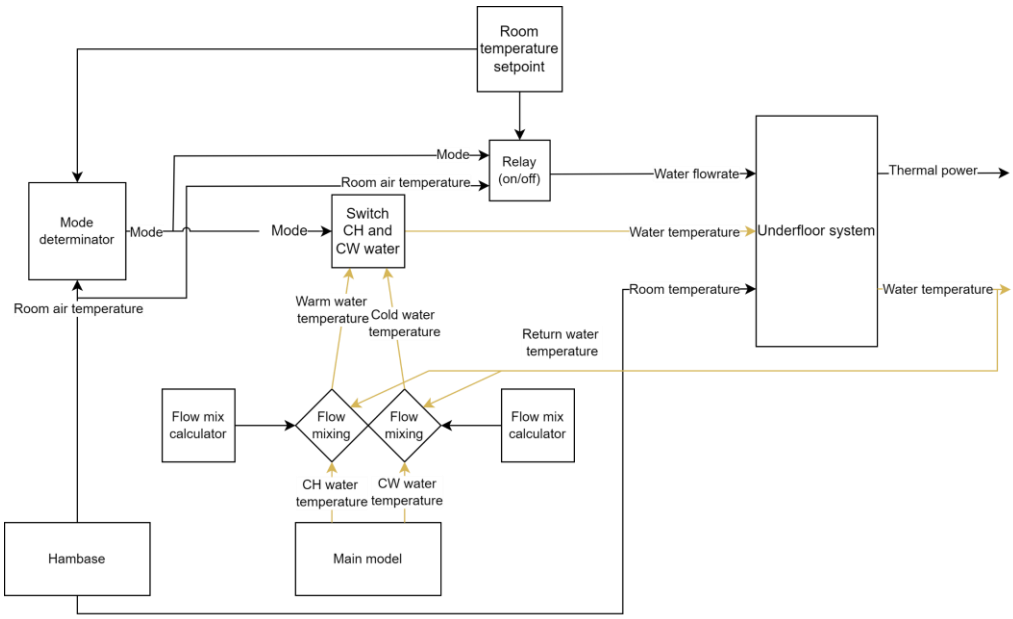

Figure 15 Display of the underfloor system model on room level

4.3.2 Climate ceiling

Different climate ceiling models have been considered to use in the simulation model. The reason this one has been selected in the end is that it requires practical (and available) model parameters, and the complexity is limited. The other considered models did require input parameters that are not available (and therefore could not be practically used), could not be fully replicated based on their papers, or were too complex to apply in this model (considering modeling work and computational demand).

Physics model

The origin of the physics model of the climate ceiling is the work of Conray and Mumma [13]. In turn, their work is based on an analogy of solar collectors, which is described in the work of Duffie and Beckman [14]. One disadvantage of this model is that it is a steady-state model and not a transient model like the other models. However, considering that the time constant of a climate ceiling is low (because of the low thermal mass), and the fact that by limiting the rate change of the flow rate the transient behavior can be somehow mimicked, this does not form a large problem, and the effect on the outcome is expected to be limited. The set of equations that describe the physical behavior of the system can be found in Appendix II. The dynamic inputs are the water inlet temperature, water mass flow rate, and room temperature. The dynamic outputs are the water outlet temperature and provided power to the room. The static input in the form of model parameters are the climate ceiling plate surface area, pipe diameter, pipe distance, plate thickness, plate thermal conductivity, and heat transfer coefficient from the plate to the room.

The assumed radiant fraction of the climate ceiling system is based on [10], [11] and the fact that the specific climate ceiling does have perforations (which increase the convection fraction). Based on this, a radiant fraction of 0.58 is used.

Control

The climate ceiling is a switch-over system, meaning it is both used for heating and cooling. If the temperature comes 0.5°C below the cooling setpoint or higher, the climate ceiling switches to cooling mode. When the climate ceiling switches to cooling mode, this does not necessarily mean that it starts cooling. This is because the climate ceiling is flow controlled. A PI controller controls the flow, based on the difference between the room temperature setpoint and the actual room temperature in each room individually. What type of water (hot water or cold water) flows in, is then dependent on the current mode.

As can be seen in Figure 13, all climate ceilings in the building are connected to one group. In this group, a temperature control is present (both in the heating and cooling group). This temperature control does have two functions. The first function is to mix the supply and return water so that the desired supply temperature of the heating curve is met. The second function is condensation protection. A condensation protection control has been created, which increases the CW supply temperature to the climate ceiling when the temperature falls below the dewpoint temperature inside the room. A simplified overview of the climate ceiling model is displayed in Figure 16.

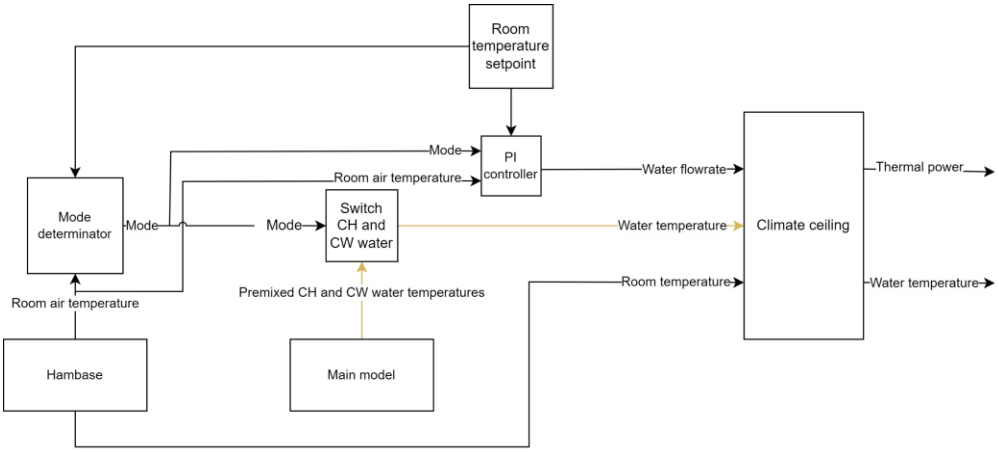

Figure 16 Display of the climate ceiling model on room level

4.3.3 Radiators

Physics model

The physics model of the radiator is based on [15]. This is a transient model and is composed of the set of (differential) equations which can be found in Appendix II. Some adjustments from [15] have been made, as that modeling approach does not take turning off the radiator into account.

The dynamic inputs of the model are the water inlet temperature, the water mass flow rate, and room temperature. The dynamic outputs are the heating power provided to the room and the return water temperature. The model parameters for the radiator are the heat exchanging area, the water and metal thermal capacitance, and the heat transfer coefficient. The assumed radiant fraction is 30%, which is based on [10], [11].

Control

All radiators are connected to one central group. In this group, there is a temperature control that controls the water supply temperature based on a heating curve. The water flow through each radiator is controlled using a thermostatic radiator valve (TRV). The numbers on a TRV correspond with a temperature setpoint. The relation between those numbers and their setpoint is modeled according to [16]. The relation between sensed temperature (by the TRV) and the mass flow rate let through the TRV is modeled according to [17]. If the room temperature is 1.5°C below the setpoint temperature (corresponding to the number on the TRV), the mass flow rate is equal to the maximum design flow rate. If the room temperature is 0.5° above the setpoint, the flow is 0. For all temperatures in between, the mass flow rate is linearly interpolated. Between the room temperature and the sensed temperature sits the thermal capacity of the TRV, which has been modeled using a differential equation as suggested by [18]. A simplified overview of the radiator model is displayed in Figure 17.

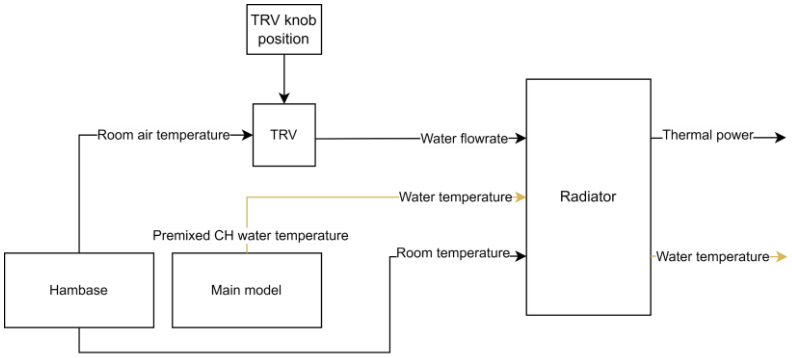

Figure 17 Display of the radiator model on room level

4.3.4 Air handling unit

Physics model

The main physical parts of the AHU consist of a heating coil and a cooling coil. The models used for this are the heating and cooling coil models of Kramer [19]. These are part of a whole air handling unit model. However, only the coil models have been used, as the functions of the AHU and controls are different than what is required for the Mijnbouwstraat. The model is validated in that research. The coils are modeled according to ASHRAE RP-1194 and make use of the NTU (Number of Transfer Units) method. It is a detailed transient model. The governing equations will not be displayed or explained in this report. For further explanation, see [19]. The dynamic inputs of the coil models are the air condition (temperature and moisture content), air flow rate, water temperature, and water flow rate. The dynamic outputs are air condition and water outlet temperature. The coils require complex parameter input.

In the AHUs, a heat recovery wheel is present. This is a sorption wheel, which means it recovers both heat and moisture. The maximum heat recovery efficiency and moisture recovery efficiency are assumed to be constant. With this assumption, the effect of the heat recovery wheel on the air that passes through it can be calculated with Equation 2 and 3.

$$T_{air,out} = \eta_{heat} * \left(T_{air,return} - T_{air,outdoor}\right) + T_{air,outdoor} \qquad 2$$

$$w_{air,out} = \eta_{moisture} * \left(w_{air,return} - w_{air,outdoor}\right) + w_{air,outdoor} \qquad 3$$

In which $T_{air,out}$ is the air temperature of the air after it passes the heat recovery wheel, η_{heat} is the heat recovery efficiency of the heat recovery wheel, $T_{air,outdoor}$ is the outdoor air temperature and $T_{air,return}$ is the return air temperature. The temperatures are in °C. Equation 3 is similar, but then uses w instead of T, which represents the absolute moisture content of the air in kg/kg. It is assumed that the fan heats up the air with 1K.

In reality, the coils are connected in series, so the air always passes through both coils. However, in the simulation, the coils have been modeled to be in parallel, which reduces the computational demand considerably. The air only passes through the coil that is active at the moment. This is translated to being in cooling mode or heating mode. If none of the coils are active, the air passes through the heating coil. It is expected that the effect of this simplification is acceptable given the overall focus on the feasibility of the triplet concept. It only would become apparent at the moment the AHU switches from cooling mode directly to heating mode (or vice versa), and the coil has not heated up yet. However, a dead band has been implemented between the mode switching. This results in the fact that most of the time, an immediate switch between the modes does not occur.

Each AHU is connected to many different rooms. The return air of all those rooms is mixed. This is done both for temperature and moisture. This then results in the $T_{air,return}$ and $w_{air,return}$ used in Equations 2 and 3.

Control

The air supply temperature setpoint is based on a heating curve, which is dependent on the (running mean) outdoor temperature. The control systems' task is to match the outlet air temperature with its given setpoint.

The first step in the control system is to control the heat recovery wheel. The heat recovery wheel can modulate its rotational speed, and in that way, it can control its outlet temperature. This can be translated to the fact that the heat recovery efficiency is adjusted by changing the rotational speed. The setpoint cannot always be met by only adjusting the heat recovery wheel speed, as it still has a maximum efficiency. By changing the speed, the heat recovery wheel can adjust its efficiency between 0 (when it is not rotating), and its maximum heat recovery efficiency. In the model, speed control is directly replaced by heat recovery efficiency control, which limits from 0 to its maximum specified heat recovery efficiency. The desired efficiency for certain inlet conditions (outdoor and return air temperatures) and outlet setpoint can then be calculated by using Equation 2. The rate of change is limited so that it can go from 0 to its maximum efficiency in 30 seconds, mimicking the inertia of the wheel, and the capabilities of its motor. It is assumed that the moisture recovery efficiency changes linearly with the change in controlled heat recovery efficiency, relative to its maximum value.

After the air passes through the heat recovery wheel, the outlet air temperature from the wheel is compared to its setpoint (based on the heating curve). If the air temperature is within 0.2°C of its setpoint, both heating and cooling coils stay inactive. If the temperature is more than 0.2°C below the heating setpoint, the AHU switches to heating mode. This means the heating coil is released, and now becomes active. If the air temperature is more than 0.2°C

above the cooling setpoint, the cooling mode becomes active. It only can switch from one mode to the other mode if for over 300 consecutive seconds a mode change is desired. This has been implemented to prevent too frequent switching.

The heating coil always uses a constant flow rate and controls its outlet air temperature using a water inlet temperature control, controlled by a PI controller. This controller controls a control valve, which mixes a certain amount of CH supply water and return water, dependent on the valve position. The cooling coil uses flow control to control its outlet air temperature. This is done by controlling a control valve using a PI controller. The airflow rate in each AHU is dependent on the sum of asked airflow rates of each room connected to that AHU. As no CO_2 control is present in the model, the airflow rates are constant during the day, and 0 during the nights and weekends. A simplified overview of the air handling unit model is displayed in Figure 18.

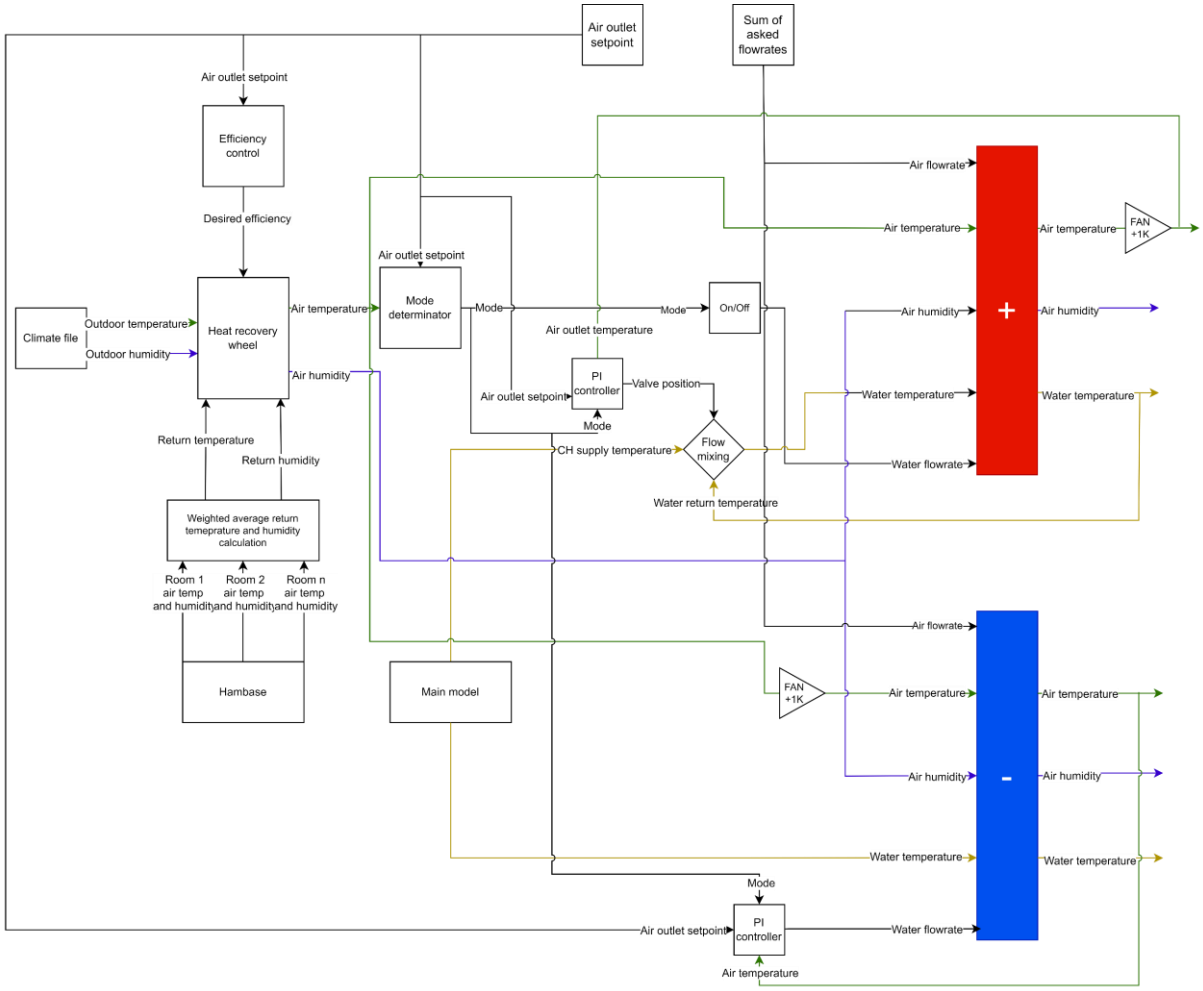

Figure 18 Display of the AHU model

4.3.5 Buffer

Physics model

A simple buffer vessel has been modeled using four differential equations. One equation for the current buffer volume level, of both the warm and cold side of the buffer, and one differential equation for the temperature level in the warm and cold side of the buffer. The model is based on the flow-weighted average injected water temperature into the buffer. The

model assumes a perfect split between the warm and cold sides of the buffer. Each side has a homogenous temperature. No heat loss to the environment and between sides is assumed.

4.3.6 Solar collector

Physics model

The physics model of the solar collector has been made by combining two different methods. The reasons for combining the selected methods is to make the simulation realistic, have the correct input and output parameters, and have practical parameter values. This has been done by combining the widely used transient differential equation for solar collector modeling according to [20], with the practically applicable solar collector properties specification of n_0, a_1, and a_2 according to [21], which can be found on (almost) every solar collector specification sheet. This combined method has been created in cooperation with EngD student Asutosh Boro. The used (differential) equation can be found in Appendix II.

The solar irradiance on the panel is not equal to the solar irradiance provided in the climate file, as this is dependent on the position of the sun relative to the panel. This conversion from climate file data to the incident solar irradiance on the panel has been done using a module from Hambase. Originally, this is used to calculate the incident irradiance on windows, but with a slight modification, this has been transformed to use for solar collectors. The direct irradiance coming out of this calculation first goes through an incident angle modifier calculation, as with smaller incident angles, more of the direct irradiance falling on the collector is reflected, and does therefore not reach the absorber. After this incident angle modifier calculation, the diffuse, reflective, and direct irradiance are summed up, and fed into the physics model.

The dynamic input parameters of the model are the water inlet temperature and mass flow rate, the outdoor air temperature, the direct normal solar irradiance, and the horizontal diffuse irradiance. The dynamic output is the water outlet temperature. The static parameters are n_0, a_1, a_2, internal water volume, gross collector area, aperture area, and the solar collector orientation.

Control

The water outlet temperature is the controlled variable. This is done by a PI controller, which compares the actual water outlet temperature with its setpoint and adjusts the water flow rate accordingly. A program has been created that switches the water outlet temperature setpoint based on the demand. If the solar collectors only supplies direct heating, a lower water outlet temperature is required. If the solar collectors are charging the hot well, a higher outlet setpoint is required and switches accordingly. A simplified overview of the solar collector model is displayed in Figure 19.

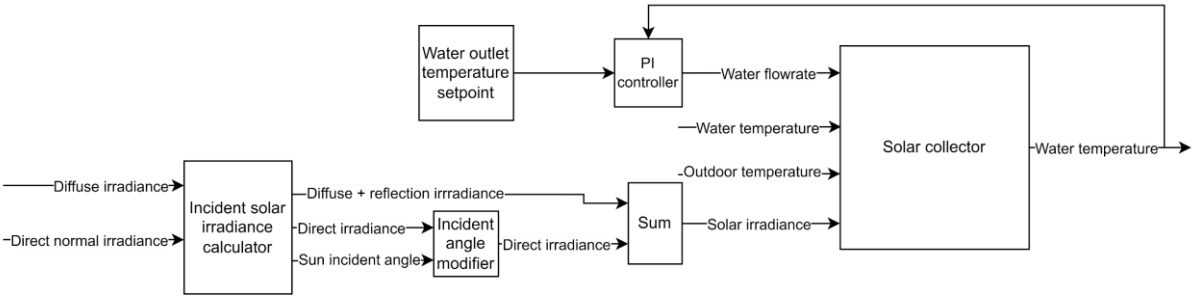

Figure 19 Display of the solar collector model

4.3.7 Dry cooler

Physics model

For the physics model of the dry cooler, the heating coil of Kramer [19] has been used, which also has been used in the AHU model. The dynamic inputs in the model are the water inlet flow rate and temperature, the outdoor air condition, and the flow rate of the outdoor air through the coil. The dynamic output is the water temperature. The input parameters are the properties of the coil, which are the same as in the AHU model. In the model, water is used instead of a water-glycol mixture, as working with two different mediums would make the model more complex.

Control

In (almost) all applications that could be found, the water outlet temperature is the controlled variable, which is the same as is required for the triplet. However, the way this variable is controlled is different from what is required in a triplet system. Normally, a certain water flow is provided to the dry cooler, and the dry cooler has to cool down that water flow to a certain temperature setpoint. The outlet temperature is controlled by controlling the fan speed, which in regard determines the air flow rate.

For the triplet, this will be different, as the dry cooler is both the generator and the unit which decides how much can be generated at the moment. In conventional dry cooler applications, the dry cooler is also the generator, but somewhere else is decided how much cold it should generate at a certain moment, and therefore the water flowrate is controlled somewhere else, and the dry cooler can only control its outlet temperature by adjusting the fan speed. For the triplet, it is desired to generate as much cold as possible with a certain dry cooler design, so that for a certain cold generation quantity, the dry cooler can be as small, cheap, and effective as possible. This can be achieved by keeping the fan speed at its maximum and controlling the outlet temperature by controlling the water flow rate. This again is done by using a PI controller. A simplified overview of the dry cooler model is displayed in Figure 20.

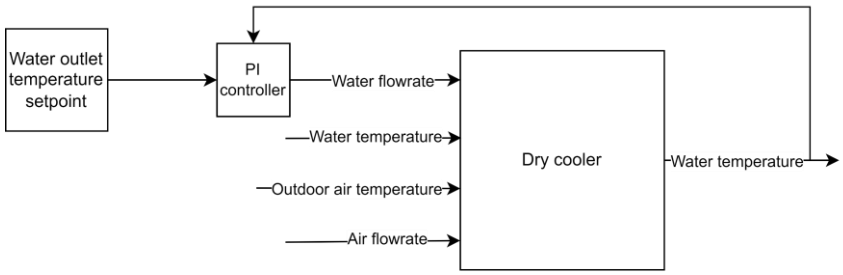

Figure 20 Display of the dry cooler model

4.3.8 Subsurface wells

Physics model

The physics model of the subsurface wells is modeled according to Rostampour et al. [22]. This is a relatively simple discrete first-order model of subsurface wells. The reason for choosing this model is that fact that it was the only model found which can be directly implemented into Simulink. All other models which could be found require complicated external programs. The equation used in the model can be found in Appendix II. The dynamic inputs are the injected water temperature and water flow rate, or the extracted water flow rate. The dynamic output is one average well temperature. The static input parameters are the natural aquifer temperature and the thermal loss factor. The subsurface model does not have an

individual control system, as the well flows are controlled on a central level, based on demand and generation.

4.3.9 Building (Hambase)

The building simulation model that has been selected is Hambase [23]. The reasons for selecting Hambase is that it does comply with all requirements (the correct dynamic inputs and outputs are possible) and that it is directly run from Matlab/Simulink. Therefore an external program + bridging program is not required, which reduces complexity and computational demand.

Hambase stands for Heat Air and Moisture model for Building And Systems Evaluation, and is a building simulation model developed within the Eindhoven University of Technology. It can be run in Matlab, but also directly in Simulink, which is the way it is used in this research. All building properties, like material layers, geometry of the building, windows, internal heat gains, etc. are defined in code form. When the building is defined, it can be connected to Simulink. The dynamic inputs into the Hambase model are the thermal power, the moisture flow, and fresh air supply flow rate provided to each room. The outputs are the air and radiant temperatures and the relative humidity in the rooms defined in the model.

Hambase does also provide an infiltration function, however, this does appear to increase the computational demand significantly. Therefore, the infiltration has been modeled separately in Simulink. This has been done in a similar way as is done in Vabi Elements, which relates the specific infiltration flow rate to the wind speed. With this relation and multiplying this with the shell area of each room, the infiltration flow to each room is calculated based on the actual wind speed.

4.4 Overall model

The parts above describe the different individual models. This section describes how all those individual models are connected together. This has been fully done according to the hydraulic layout shown in Figure 12. The figure corresponding to the explanation in this section can be found in Appendix IX.

Water flows

In the model, water flows are coordinated according to the hydraulic layout. There is a temperature control in both main CH and CW supplies, which are controlled based on a heating/cooling curve. This heating/cooling curve provides a relation between the desired water supply temperatures and the outdoor air temperature. After this, water flows to the different hydraulic groups, which are connected to the distributor. In some groups, it first passes through a temperature control based on heating/cooling curve, in other groups it goes straight to the consumers. After the water comes out of all individual consumers, it is mixed again with all other consumers connected to the same group. Part of this return water is recirculated back by the temperature control within the group, the remaining part of the return water flow mixes in the collector. Of this, some part of the water is again recirculated back by the main CH or CW supply temperature control, the remaining part of the water flows out of the building model, into the master flow control system. This is the main hydraulic circuit, in between the consumers, wells, and generators. Between the temperature controls

of the main CH/CW and the master flow control, the buffer vessel is situated, which is connected to the supply and the return sides.

In the master flow control and calculation system and temperature node calculation block, two things occur. First, the flows are controlled and calculated. More about this is explained in the next section of this report. The second thing that occurs in this block is the temperature node calculation. At many parts in the model, temperature changes. This for example happens in a heat exchanger, or when two flows of different temperatures mix. All points where a temperature change in the hydraulic circuit can happen are seen as a temperature node. At this temperature node, the resultant temperature is calculated during every moment in time. A total of 19 temperature nodes are distinguished in the main hydraulic layout, excluding the temperature nodes on the building consumer side, as they are calculated separately.

In the main model, there are four HXs. One between each generation circuit and the building circuit, and two between the subsurface circuit and the building circuits. As the flow rates are kept equal at both sides of each HX at all times, a constant temperature jump is assumed. This value has been assumed at 1K.

Power supplied to rooms
Most rooms in the model do have one or more heating and cooling devices present in them. The thermal power provided by those devices within each room is summed up, and fed into the Hambase model. Thermal power is also provided by the AHU. This is calculated based on the difference between the return air temperature (coming from the Hambase room temperature output) and the supplied air temperature (coming from the AHU model) and the mass flow rate of ventilation. Moisture flow from or to the rooms via ventilation air is calculated in a similar way.

4.5 Master control and strategy

With master control is meant the control of the overall system. There is made a differentiation between master control and strategy. The master control makes sure all the water flows in the directions it has to flow to at each moment in time, and has the correct temperatures (if physically possible). Master strategy does have an effect on where the water is desired at each moment. Master strategy is not active at most moments, but master control is active at all moments.

The starting points for the master control are the following:

- The building demand and control is seen as an individual functioning system. The goal is always to provide the main CH and CW circulation pumps with the water flow rate and temperature that is desired at any moment from the main system. The goal of the CH and CW circulation pumps themselves is to full fill the asked flow rate from all the consumers.
- Fulfilling the heat and cold demand is priority number one in the control system
- Heat and cold generation by the solar collectors and dry coolers are seen as individual functioning systems. If, at the given outdoor conditions and water inlet temperatures, the generation devices can generate heat/cold, they will do so, unless given a signal by the master strategy to be turned off.

- Direct heating and cooling, which means supplying heat/cold directly from the solar collectors and dry coolers to the building, does have priority over providing heating/cooling from the wells to the building. This means that generated heat/cold is always first supplied to the building, and when there is a surplus this is used to charge the wells.
- When there is a heat or cold generation surplus and the relevant buffer vessel is not full, the buffer vessel is first filled up before the wells start charging
- When the buffer vessel is not empty, and complete direct heating/cooling cannot be supplied, the buffer vessel is first fully discharged before the wells start discharging.
- If the direct heating/cooling is not sufficient to fulfill the demand water flow rate and the buffer vessel is empty, the relevant wells start discharging the required amount of flow to the building.

With these starting points in mind, flow control rules can be defined. To make the explanation more clear, in Figure 21 the hydraulic layout can be found, but this time with notations in it.

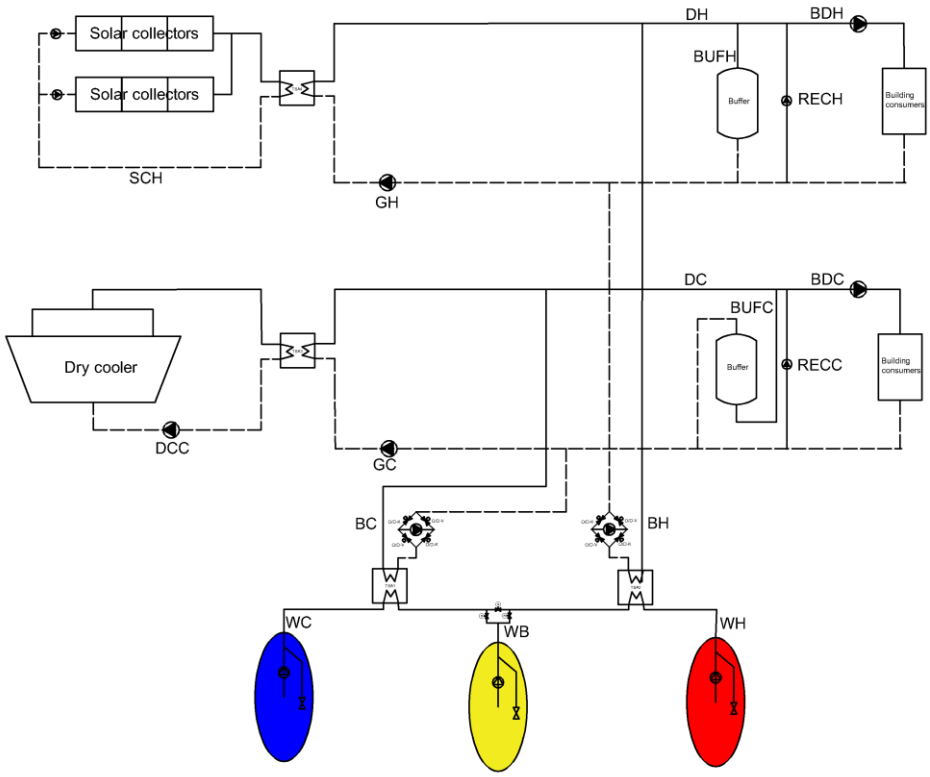

Figure 21 Basic hydraulic layout with notations

The notations indicate the flow at each point, and have the following meanings:

- SCH: Solar Collector Heat. The flow in the solar collector circuit. This flow is independently controlled from within the solar collector circuit.
- GH: Generation Heat. The flow at the other side of the solar collector HX. This flow is controlled so that it matches the flow rate at SCH.
- BDH: Building Demand Heat. The water flow to the building consumers. This flow is independently controlled, so that it matches the flow demand from the building consumers.

- RECH: Recirculation Heat. The recirculated flow from building return back to supply. This flow is independently controlled, so that the resultant temperature at BDH matches with the CH supply temperature setpoint, which is based on a heating curve.
- BUFH: Buffer Heat Flow. Volume flow through the buffer. This flow is controlled by the master control. Flow is determined by the flow differences between pumps.
- DH: Demand Heat. Combined water flow from solar collector and hot well to building. Is controlled by the master control.
- BH: Bridge flow: Flow through the bridge. This flow is controlled so that it matches the flow rate at WH.
- WH: Well Heat: Flow into or from hot well. This flow is controlled by the master control.
- DCC: Dry cooler Cold. The flow in the dry cooler circuit. This flow is independently controlled from within the dry cooler circuit.
- GC: Generation Cold. The flow at the other side of the dry cooler HX. This flow is controlled so that it matches the flow rate at DCC.
- BDC: Building Demand Cold. The water flow to the building consumers. This flow is independently controlled, so that it matches the flow demand from the building consumers.
- RECC: Recirculation Heat. The recirculated flow from building return back to supply. This flow is independently controlled, so that the resultant temperature at BDC matches with the CC supply temperature setpoint, which is based on a cooling curve.
- BUFC: Buffer Cold Flow. Volume flow through the buffer. This flow is controlled by the master control. Flow is determined by the flow differences between pumps.
- DC: Demand Cold. Combined water flow from dry cooler and cold well to building. Is controlled by the master control.
- BC: Bridge flow: Flow through the bridge. This flow is controlled so that it matches the flow rate at WC.
- WC: Well Cold: Flow into or from cold well. This flow is controlled by the master control.
- WB: Well Buffer: Flow into or from the buffer well. This flow is controlled by the master control.

From the description above can be seen that some flows are independently controlled on a level below the master control. This means that those flows are a given for the master control, they are an input. Based on the input of those independently controlled flows, the master control acts and controls the flows in such a way that the independently controlled flows can be matched. This is done according to multiple equations. To better understand the equations, it must be clear that all flows are always positive, with the exception of the well flows (WH, WC, WB), bridge flows (BH, BC), and buffer vessel flows (BUFH, BUFC). The well and bridge flows are positive when the relevant well is charging, and negative when the relevant well is discharging. The flow through the buffer vessel is positive when the buffer vessel is charging, and negative when discharging.

$$DH = BDH - RECH + BUFH \qquad 4$$

$$WH = BH \ \& \ GH = SCH \quad 5$$

$$BH = GH - DH \quad 6$$

$$DC = BDC - RECC + BUFC \quad 7$$

$$WC = BC \ \& \ GC = DCC \quad 8$$

$$BC = GC - DC \quad 9$$

$$WB = -WH - WC \quad 10$$

With these control rules, the required building demand flow can be met during normal operation, and if there is a generation surplus available, this is used to charge the wells (or the buffer vessel if it is not fully charged yet).

Pumps

All building consumers and generators have a limited pump capacity, according to realistic values. For the consumers, the pumping capacity for each consumer is applied according to the original design values. For the solar collectors and dry cooler, the pumping capacity is based on a selection. This means that all previously mentioned pumps do have a maximum capacity. The rate of change of the pumps is also limited so that the flow rate cannot jump from 0 to 100% instantly. Minimum flow rates for the pumps have not been considered.

The remaining pumps in the model are the well pumps and the bridge pumps. These pumps are directly controlled based on the flow difference between the generation and building demand pumps, according to the equations above. Those pumps have not been given a maximum flow limit, or a limit in rate of change. These pumps are ideally controlled, meaning that the flow output is instantly equal to the desired output, which comes from the equations above. However, this does not mean that these pump flow rates become unrealistically high or that the rate of change is instant, because these pump flow rates are dependent on the generation and building demand pumps, which all do have a limited capacity and rate of change limit. By controlling the pumps in this way, it is a little less realistic but much easier to control in the simulation. And overall it is expected that this does have a limited effect on the outcomes.

Strategy

The currently used strategy is modest and is done according to two rules. The first rule is that if the hot or cold well is full, the well is not charged anymore. This is accomplished by turning off the solar collector or dry cooler when the relevant well is full. The “well is full signal” is provided by a relay to prevent frequent switching between the full/not full signal. The charged state of the well is determined by assessing the water temperature and water volume in the well in reference to the weighted average building return water temperature. The second

strategy rule is that if the temperature in the hot well falls below a certain value (for now 30 °C is used), the well is not further discharged and only direct heating can occur.

4.6 Model adjusted to case parameters

The model parameters are adjusted to the case of the Mijnbouwstraat. For installations that already exist in the original design, those parameters are based on the available design documentation.

4.6.1 Building model (Hambase)

The Mijnbouwstraat case was implemented in Hambase. The input of the Hambase model is mainly based on the Vabi Elements model of the Mijnbouwstraat. This Vabi elements model was made during the design phase of the Mijnbouwstraat. This Vabi Elements model is also used to calibrate the Hambase Model.

Modeling

The Vabi Elements model incorporates almost all rooms of the Mijnbouwstraat design, which counts over 190 rooms. To reduce complexity, time intensity, and computational demand, the number of rooms in the Hambase model has been reduced by merging rooms. Three different room function types are distinguished. The first type is office and conference room, the second type is atrium, and the third type is technical or non-occupied room. The rooms have been merged per wing of the building; north wing, west wing, south wing, east wing, middle wing, and the two atria in the center. For each room, a room type has been assigned to it. This corresponds well with the original design, as there within each wing mostly every room has a similar function. By dividing the building in this way, a total of 16 rooms are created. Two additional rooms function as crawl space, which gives a total of 18 rooms in the Hambase model. Figure 22 projects the created rooms from the Hambase model on the ground floor on the floorplan. Each colored rectangle is one room in the Hambase model.

Figure 22 Display of the division of rooms on the ground floor (Source of floorplan is from original design)

On the first and second floors, a similar room division has been made. This leads to a total of 10 office/conference rooms, 2 atria, 4 technical/unoccupied rooms, and 2 crawl spaces.

The effect of merging rooms is expected to be limited, as the merged room mostly have the same function, and also do have the same orientations (south, west, etc.). The hallways are merged with the rooms. However, it is expected that this effect is also limited as in the original installation concept, air is supplied to the rooms, and extracted via the hallways. This means that the hallways also in the original design will have a temperature close to the rooms, as all ventilation air from the rooms passes through the hallways. The internal walls between the rooms which have been merged have been placed into the model, in order to not lose thermal mass.

The geometry and sizing of the building are based on the Vabi Elements model and the floor plans. However, there has been made some simplifications. Walls of each room have been made straight, meaning that notches in the external walls are not included. However, this has been compensated by making the straight wall a bit larger than the actual straight line, and therefore this effect is deemed small. All material layers (thicknesses, material properties) of the different construction components have been made identical to the constructions used in Vabi Elements. Also glazing is done with the same properties (HR++), and at the same locations as the Vabi elements model. For internal heat gains, the heat gain sum of all rooms which have been merged into the relevant room has been applied according to the Vabi Elements model (which uses standards for offices). For moisture production by persons, the number of designed persons in the rooms has been summed according to the original design and given a moisture production of 90 g/h per person [24]. Installation profiles and occupancy profiles have been made the same as in the Vabi elements model. The installations are active from 6:00 to 19:00. This means that during these hours the AHU is turned on and that the room temperature setpoints are according to day mode. The occupancy profile is from 8:00 to 18:00, which means that during these hours people are in the office. During weekends and nights, the installations are inactive (AHU off and night setpoints), and there is no occupancy. Infiltration to the building model has been implemented separately in Simulink in a similar way as is done in Vabi Elements.

Calibration of the Hambase model to Vabi Elements

The Vabi Elements model is the only reference available. Therefore, the Hambase model has been calibrated to the Vabi Elements model. This is done in two steps. In both steps, ventilation is disabled. The reason for doing this is that ventilation is a ‘man-made’ process, while the other forms of heat loss (heat loss through shell and infiltration) are natural. Because the AHU makes use of a modulating heat recovery, and specific and changing air supply temperature setpoints, the comparison between the two models would be more complex. Therefore, the calibration of the Hambase model with the Vabi Elements models is done with the ventilation disabled in both models. For both models, the heating and cooling power is set to unlimited, to get a better comparison.

The first step of the calibration is done by comparing the two models without infiltration. The calibration is done by multiplying the shell surface area in Hambase with a correction factor. With a correction factor of 1, all walls are in straight lines with a dimension equal to the 1-dimensional wall length, and not the 2-dimensional wall length, and therefore not accounting for any notches and elements like dormers. By adjusting the correction factor, the outdoor shell is made larger. The value of the correction factor is adjusted in such a way that the annual

heating and cooling demand of the Hambase model are close to Vabi elements model. The final calibrated value of the correction factor on the external shell area is 1.2.

The second calibration step is done with the previously calibrated model, and now with the infiltration active. This time, the adjusted parameter for the calibration is a correction factor on the infiltration leakage factor. Again, the aim of the calibration is to bring the annual heating and cooling demand of the Hambase model close to the Vabi elements model. The final calibrated value of the correction factor on the infiltration leakage factor is 0.62. Both calibrations are done using the NEN5060:2018 energy year climate file. This is a composed climate year that is representative for building energy consumption calculations in The Netherlands [25]. The results of the calibration can be found in Table 1. After the calibration, also a comparison between the Hambase model and the Vabi Elements model is made for the NEN5060:2018 1% year (which is an extreme year), which also can be found in the table.

Table 1 Calibration results of the Hambase model

	Heat or cold demand	*Vabi Elements*	*Hambase*	*Difference*
NEN5060 energy year				
Without infiltration	Heat	203,304 kWh	199,798 kWh	-1.72%
	Cold	313,913 kWh	334,798kWh	+6.65%
With infiltration	Heat	484,607 kWh	484,036 kWh	-0.12%
	Cold	237,058 kWh	206,464 kWh	-12.91%
NEN5060 1% year				
With infiltration	Heat	590,789 kWh	594,282kWh	+0.59%
	Cold	297,629 kWh	282,656 kWh	-5.03%

The heat demand shows small deviations for all scenarios. The cold demand shows larger deviations, but is still deemed to be within reasonable bounds. From the results in Table 1, it was concluded that calibration is successful based on these figures. However, also other metrics are compared to verify this in the figures below.

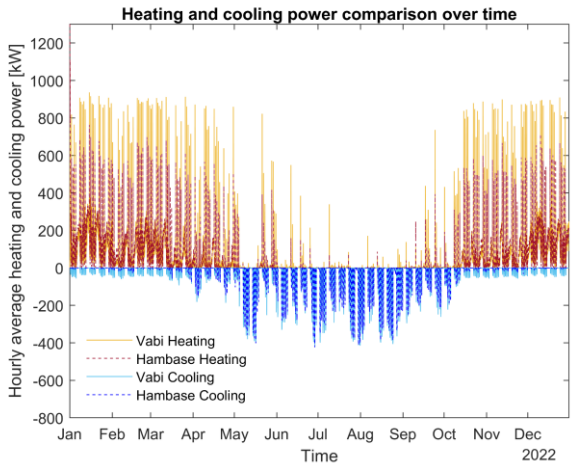

Figure 23 Comparison of the heating and cooling power over time

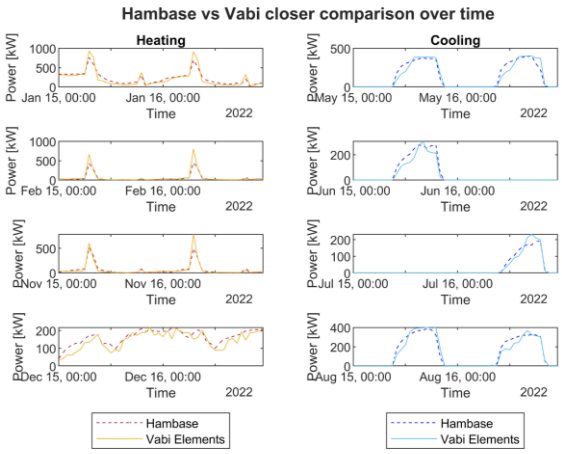

Figure 24 Zoomed-in view of comparison over time

Figure 23 and Figure 24 display the heating and cooling power comparison over time. The left figure shows this over a period of the whole year, and the right figure shows a zoomed-in version, in which each plot is of a period of two days. From both figures, it is visible that the Hambase model matches quite well with the Vabi elements model. The largest visible deviation is found in the left figure, where it seems that the Hambase heating power is structurally lower than the Vabi Elements heating power. However, when zooming in, these peaks only happen during the morning startup, when the thermostat switches from night to day setpoint. During a short period of time, the Vabi Elements model gives a higher power than the Hambase model. After this initial peak, the Hambase model and Vabi Elements model converge again. It is also visible on the right figure that the difference in the left figure seems more extreme than that is the case in reality.

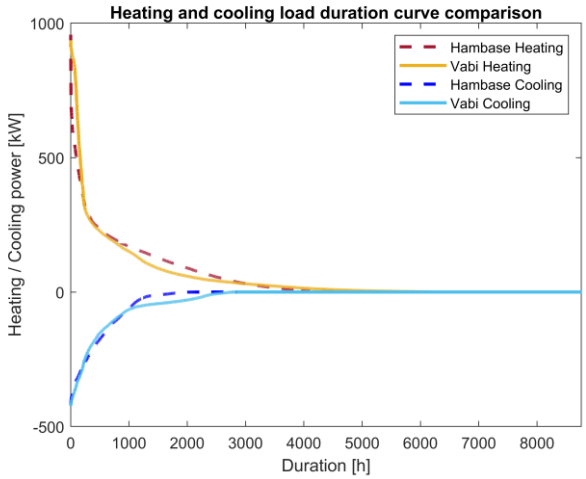

Figure 25 Comparison of load duration curves

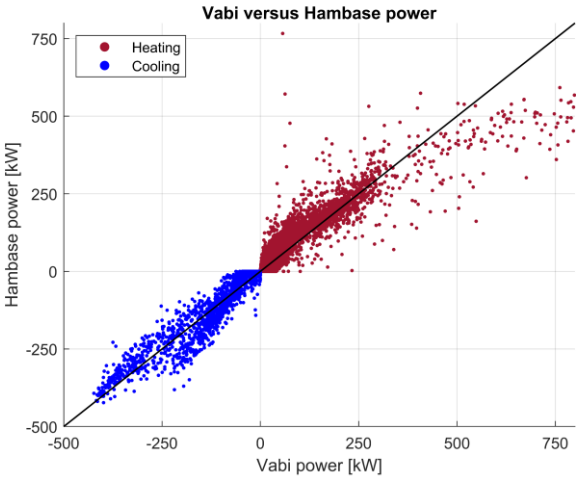

Figure 26 Comparison between Vabi power and Hambase power at the same moment in time

Figure 25 compares the load duration curves for both heating and cooling from Hambase with Vabi Elements. Both do match well. Figure 26 shows a point cloud with the comparison of heating and cooling power between Hambase and Vabi Elements at the same moment in time. This also matches well.

Based on all the comparisons of the Hambase model with the Vabi Elements model, it can be concluded that the Hambase model does line up with the Vabi Elements model, and therefore is deemed fit to further use during this research.

The final integral model (Hambase model connected to consumers) also includes heat loss by ventilation. The final model has a heat consumption of 561 MWh and a cold consumption of 150 MWh for a NEN5060 energy year. As some optimizations have been made to the model, and some adjustments based on the latest available design data, this is not one on one comparable anymore with the Vabi elements model. The final specific thermal energy consumptions are 44.5 MWh/m^2 for heating and 11.9 kWh/m^2 for cooling.

4.6.2 Consumers

The underfloor system, climate ceiling, radiator, and AHU models have been calibrated based on the original Mijnbouwstraat design. For each consumer, some required model parameters

were directly available in the design documents. Parameters that were unknown have been adjusted in such a way that the steady-state situations of the design point are according to the original design. All design points are a full-load situation. This means that all consumer models are calibrated based on the full load operating point, and the models comply at this operating point with the design.

4.6.3 Wells

The well model used during this research is relatively simple. A loss factor in the model determines the well thermal losses. Those losses are dependent on the temperature difference between the ground temperature and well temperature, and the volume of the well at a certain moment in time. The loss factor does have an abstract unit, where no applicable reference values can be found for. Therefore, the loss factor has been calibrated, based on assumed thermal recovery efficiencies of the wells. The assumed thermal recovery efficiency for each well has been obtained by reviewing literature.

Thermal recovery efficiency is defined according to [26]:

$$\eta_{th} = \frac{\int_{t=0}^{t_{end}} c_w * \dot{V}_{ext} * (T_{ext} - T_{amb})\, dt}{\int_{t=0}^{t_{end}} c_w * \dot{V}_{inj} * (T_{inj} - T_{amb})\, dt} \qquad 11$$

In which c_w is the specific heat of water, $\dot{V}_{ext}$ the extracted volume flow rate, $\dot{V}_{inj}$ the injected volume flow rate, T_{ext} the extracted temperature, T_{inj} the injected water temperature, and T_{amb} the natural groundwater temperature. This is 11.5°C according to Mijnbouwstraat ATES design documents.

It is hard to find a good estimation for the thermal recovery efficiencies that can be assumed during this research, as the values in the sources vary widely. Also, it cannot be made entirely clear from the sources why they vary so widely. The starting point of the search was that for the hot well, an average well temperature of 51°C is desired. The reasoning behind this is the fact that the maximum design temperature in the building is 50°C. Considering a temperature jump over the HX of 1K, an average hot well temperature of 51°C would lead to an average available building supply temperature of 50°C. For the hot well, 6 different sources have been consulted to come to a value for the thermal recovery efficiency which fall near the mentioned temperature range [27], [28], [29], [30], [31], [32]. Based on this, the thermal recovery efficiency of the hot well is assumed at 68%. When applying Equation 11, if with the desired average hot well temperature is 51.0°C, the required average injection temperature must be 69.6°C.

Preliminary simulations have shown that the buffer well temperature ranges from approximately 17°C to 25°C throughout the year. Based on [33], the buffer well thermal recovery efficiency is assumed to be 75%.

The building does use a relatively high CW supply temperature of 12°C. The temperature difference in the CW circuit is lower than in the CH circuit, mainly because of the closeness of the room temperature to the supply temperature. Therefore, it is more important for the CW supply temperature to not fall over the design temperature. Based on this, it is assumed that

the desired cold well temperature must be 10.5°C. After the HX this results in a supply temperature of 11.5°C, which gives some margin to the 12°C design setpoint. Based on [31],[34], the thermal recovery efficiency of the cold well is assumed at 80%. This gives a required injection temperature of 10.3°C. Due to the low temperature difference between the desired average well temperature and the natural groundwater temperature, the effective efficiency is high, and the risk that the desired supply temperature of 12°C cannot be met is limited.

4.6.4 Solar collectors

To determine the input for the model, it must be known how much roof space is available to place solar collectors on. The starting point of the solar collector setup is to generate as much heat as possible within the available roof space, neglecting economical aspects.

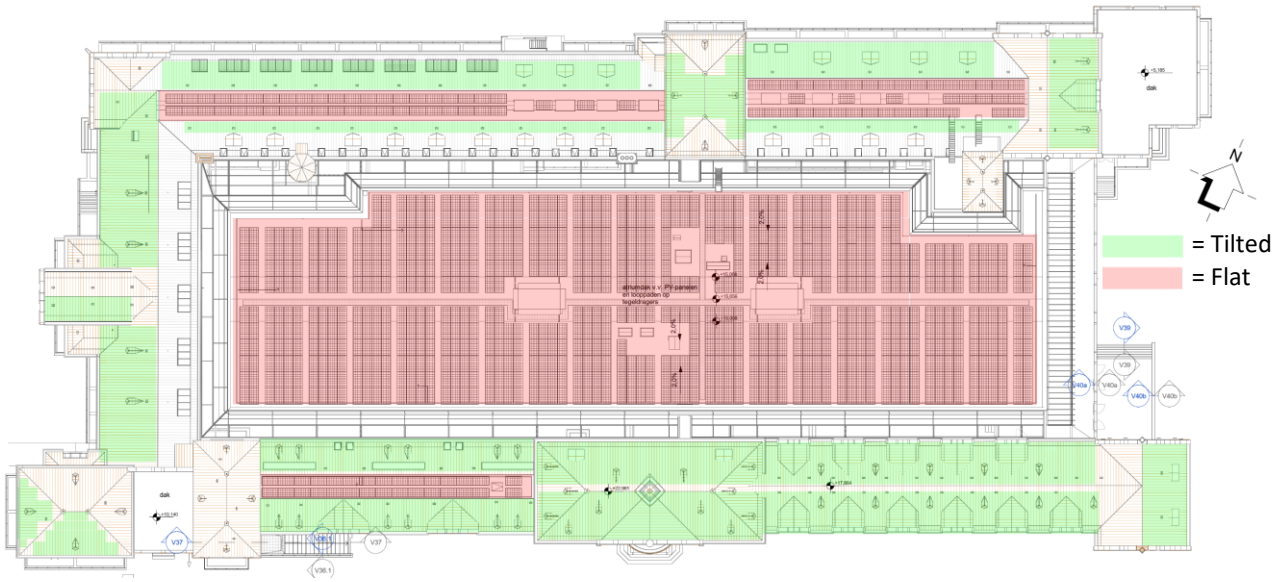

Figure 27 Overview of solar collector layout (Source of original drawing is design document of Mijnbouwstraat)

Figure 27 shows an indication of the solar collector layout. Solar collectors are placed on the marked red and green areas. However, not the whole marked areas are filled with solar collectors, because with the placement, obstacles, such as windows and architectural ornament are considered, reducing the available space for solar collectors, especially for the tilted roof parts. For the flat roof space on top of the atrium, it is assumed that 90% of the atrium roof can be filled with solar collectors, leaving 10% left for maintenance paths. On tilted roofs, the solar collectors have the orientation (azimuth and inclination) of the tilted roof it is placed on. For the flat roof parts, it was decided to use an east-west layout with 10° inclination. Per solar collector this leads to a lower yield than panels facing south However per available flat roof area, this leads to a higher yield. This is because if a south-facing layout would be used, a considerable amount of space must be left in between the solar collectors to prevent drawing shadows on each other. It has been confirmed by performing simulations that because of the extra required space between collectors, an east-west layout does have a higher yield than a south-facing layout for the same available roof space.

Orientations that are very close to each other have been merged in the simulation to reduce computational demand and complexity. The expected effects of this simplification are low. Table 2 shows the exact solar collector layout used in the model.

The applied solar collector during this research is the Remeha C250 collector. This is a glazed flat plate solar collector. There are two reasons why this particular solar collector has been selected. The first reason is that this is a high-performing solar collector, but also not the highest-performing available, to ensure representability. This is based on an analysis of the SPF database [35]. The second reason is that for this collector, all required information was available in the specifications sheet. The optic efficiency of this solar collector (η_0) is 81.0%, the linear heat loss factor (a_1) is 3.48 W/m^{2}K, and the quadratic heat loss factor (a_2) is 0.020 W/m^{2}K^2 [36].

Table 2 Overview of solar collector layout used in the simulation model

Roof	*Tilted/flat*	*Orientation [°]*	*Inclination [°]*	*SC area [m^2]*
Flat roofs West	Flat	240	10	1,045
Flat roofs East	Flat	60	10	1,045
Tilted South 1	Tilted	150	60	314
Tilted West	Tilted	240	57	332
Tilted North 1	Tilted	330	53	242
Tilted North 2	Tilted	330	60	137
Tilted South 2	Tilted	150	53	131
Tilted East	Tilted	60	60	118
Total				**3,364**

There was briefly looked into the option to use heat pipe vacuum tube solar collectors instead of flat plate solar collectors. The reason for this is the fact that some heat pipe vacuum tube solar collectors have a higher annual heat generation than flat plate solar collectors. For a south-facing orientation, the tested heat pipe vacuum tube solar collectors generated approximately 17% more heat. However, it was decided to not apply those during this research for a combination of reasons. The first reason is the fact that heat pipe vacuum tube collectors must have a minimum inclination of 25°to 30° [37], [38]. The reason behind this is the fact that a heat pipe system works fundamentally differently than a direct flow system as is used in the flat plate solar collector. The minimum required inclination of 25° would cause problems on the flat roof areas because there an east-west orientation with 10° inclination is applied. If the inclination would be increased to 25°, considerable shadow fall would be created, which would require more spacing between the collectors, creating a net lower yield for the same available roof space. Two heat pipe vacuum tube collectors could be found which indicate that they could be placed (almost) horizontally. However, for the first one, no performance data could be found [39]. Also, the type of aperture used in this solar collector showed a lower yield than flat plate solar collectors during simulations, when basing the performance data on collectors with similar type of aperture in the SPF database. The other heat pipe vacuum tube collector indicated relatively good performance figures, and uses a better aperture type [40]. However, it is not displayed how large the reduction in performance will be in this collector when it is installed almost horizontally versus when it is installed in a more tilted angle condition. Considering the way heat pipes work, it seems unlikely that the performance in horizontal position is equal to that in tilted position. Therefore, with this lack of information, this solar collector could not be used for this research. Another disadvantage of heat pipe vacuum tube solar collectors is the fact that these are more expensive than flat plate collectors by approximately 36% [41]. Also, flat plat collectors seem more robust than vacuum tube solar collectors.

For the above mentioned reasons, heat pipe vacuum tube solar collectors are not further investigated during this research. However, it may be wise to further investigate the potential and application of heat pipe vacuum tube solar collectors in a triplet system in later research. This is because it may also provide some additional benefits. Because the thermal losses are lower, the production during cold periods is expected to be higher, which can increase the share of directly supplied heating to the building, which can increase system efficiency. Also because of the increased generation relative to flat plate collectors, it might be worth to investigate applying heat pipe vacuum tube solar collectors on tilted roof parts (with an inclination of 25° and above).

4.6.5 Dry cooler

The dry cooler has been selected based on preliminary simulations. Assumed was the power at the operating conditions of a water inlet temperature of 25°C, outlet temperature of 8°C, and an outdoor temperature of 0°C. A 175 kW dry cooler was selected. From the Güntner selection tool website [42], a specific dry cooler was selected. This selection can be found in Appendix III. The simulations made clear that with a 175 kW dry cooler, there would be approximately 30% overcapacity for a NEN5060 energy year. However, when simulating the period 2016-2020, it appeared that the capacity of 175 kW was not enough. For that simulation period, it has been raised to 260 kW, which is also the final selected specification. This was done by scaling the selected dry cooler to the new size. Most, but not all required parameters for the models were present in the specification sheet. The unknown parameters have been fitted so it complies with the design operating condition. The dry cooler does have a footprint of approximately 8 m^2.

4.6.6 Other specifications

- The two buffer vessels each have a capacity of 5,000 L. This is higher than the 2,000 L vessels in the original doublet design, but still within reasonable size to fit inside a normal technical room without problems.
- The thermostat setpoints have been kept the same as the Mijnbouwstraat design. This is a heating setpoint of 21°C during the day and 19°C during the night for all usable rooms. The cooling setpoint is 24°C during the day. For office and conference rooms, the night cooling setpoint is 26°C, while for atria the night cooling setpoint is 28°C. The thermostats are air temperature controlled, which is closest to reality. The thermostat setpoints can be seen as conventional.

4.7 Incorporation of heat pump

When the available roof space for solar collectors is limited, there is a possibility that the total solar collector heat generation on an annual basis, while taking the losses in the system into account, is lower than the building heat demand. Also, there can be the situation that the solar collectors can generate enough heat for an average year, but not provide the robustness to generate enough heat for extreme weather periods. If these situations would arise, an additional heat source is required to make the system technically feasible and reliable. Later in this report, it will appear that indeed an additional heat source is required. For this research, a heat pump is used as this additional heat source. The reason for choosing a heat pump is the fact that it was deemed the most representative for most applications, as a heat pump is not dependent on available infrastructure (e.g. district heating network), and therefore can be applied in most buildings. Different implementations and types of heat pumps are possible

within the triplet system. The best possible solution is deemed to be a water-water heat pump that delivers only direct heat to the building, and not to the hot well. The argumentation behind this can be found in Appendix IV.

4.7.1 Incorporation in hydraulic layout

Figure 28 shows the heat pump within the hydraulic layout. The heat pump is controlled based on the heat demand, and will therefore only supply direct heating to the building. Therefore, the condenser is placed on the demand side of the hydraulic layout. The evaporator is placed on the generation side, because if there is no simultaneous cold demand when the heat pump is active, the cold generated in the evaporator is used to charge the cold well. On both the condenser and the evaporator there is a mixture control possibility. This is especially used during situations when the temperature difference between inlet and outlet is too high and must be reduced.

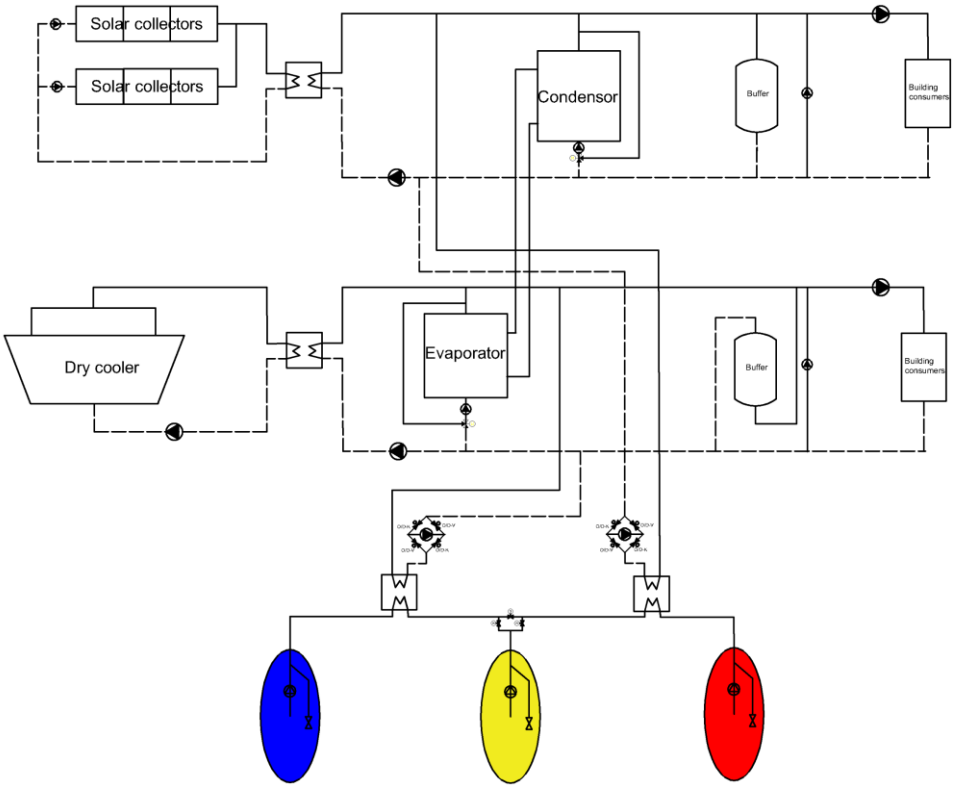

Figure 28 Hydraulic layout with water-water heat pump included

4.7.2 Heat pump model

The heat pump is incorporated into the simulation model. This is done in a simple yet useful way. First, the maximum theoretical possible COP at a particular moment is calculated using Equation 12 (derived from the Carnot efficiency equation).

$$COP_{theoretical} = \frac{T_{cond,out}}{T_{cond,out} - T_{evap,in}} \qquad 12$$

In which $T_{cond,out}$ is the condenser outlet temperature and $T_{evap,in}$ is the evaporator inlet temperature (both in Kelvin). The actual COP of the heat pump can be calculated by multiplying this theoretical COP with the system efficiency of the heat pump at that moment.

System efficiency data has been used from an earlier research [43], which also uses the above method. Partial load data of a specific heat pump (Trane RTWD 270HSE) from the manufacturer was used to create a relationship between system efficiency and partial load of the heat pump. The system efficiency ranges from 48% to 53%. By comparing datasheets of different heat pumps, this system efficiency range seems representative for most heat pumps. The COP resulting from this COP estimation modeling method has been compared to multiple heat pump data sheets for different available operating conditions. The results are close, mostly within a few percent for normal operating conditions that can occur in the system. Therefore, this method is deemed reliable enough for usage during this research.

The maximum available thermal power of a heat pump is dependent on multiple factors. For the same heat pump, the maximum thermal power changes with its operating conditions. After consulting heat pump manufacturers, the compressor work seems to be the most influencing factor in the maximum thermal power a heat pump can deliver at a certain moment. In reality it is more complex, but for the modeling, a constant maximum compressor electrical power is assumed, and the maximum available thermal power at a certain moment is the calculated COP value multiplied by this compressor electric power. This seems to be a logical approach, and is expected to be not too far off reality although this could not be tested.

The heat pump delivers the first level of heat demand to the building. If the heat pump runs at maximum capacity, first is looked at if direct heating from the solar collectors is available, then if the buffer if available (not empty), and then if indirect heating from the hot well is available.

The heat pump has been modeled with two flow-controlled pumps, which are controlled based on the heat/cold production and the actual dT. The evaporator has been given a mixture control. The reason for this is that the water temperature difference over the evaporator must be limited in order for the heat pump to function properly. It is assumed that this temperature difference can be a maximum of 7°C, based on a specification sheet found in which this is described [44], and after contact with a heat pump manufacturer. If the evaporator inlet temperature is higher than the outlet setpoint plus 7°C, the inlet temperature is reduced, so that the temperature difference is 7°C. This does have a negative effect on the energy consumption, as a lower evaporator inlet temperature results in a lower COP. Also, a minimum temperature difference over the evaporator of 3.5°C has been set. The reason for this is that if the temperature difference gets too low, the volume flows in the cold well and buffer well can be excessive. The minimum temperature difference of 3.5°C is maintained by lowering the evaporator outlet setpoint during moments the temperature difference would fall under 3.5°C. This occurs when the inlet temperature is low, mostly caused by an empty buffer well.

4.7.3 Dynamic power control

The situation can occur that the climate year deviates largely from a design year. For example, if there are multiple consecutive extremely cold years with also low heat generation, there is a risk that the hot well runs out of energy, which is unacceptable. Therefore, there must be an instrument that can prevent this from happening. For triplet systems with a heat pump present, the heat pump can be this instrument. If the hot well energy content deviates with a certain extent from the designed situation, the heat pump can be given the command to produce more or less energy than in the design situation. If the hot well energy content is

lower than desired, the heat pump has to produce a certain amount of extra heat in order to try to increase the energy level in the hot well. In the model, this is done by limiting the electrical heat pump power to a certain limit. This electrical limit has a relationship with the amount of heat that can be generated. For low electrical powers, this is in the range of 19 MWh_{th}/kW_{el} for a one-year period. As the electrical power increases, the heat generation per kW decreases. So, the required heat generation by the heat pump must first be estimated and then translated into an electrical power limit.

The adjustment of the heat pump power occurs two times a year. The first time is near the end of winter, in mid-February. The reason for doing this at the end of winter is the fact that then a better estimation can be made about if the winter was more or less extreme than an average winter. If a winter has a strict first half, but a mild second half, the total winter can end up average. But if the estimation was done during the middle of the winter, it would have been estimated as a strict winter, and then the heat pump power would have been turned up, which speaking afterward would have been unnecessary. By making the estimation more near the end of the winter, a better estimate can be made.

The second adjustment happens during the fall at the beginning of November. This is the moment after the hot well energy content certainly has reached its peak, and therefore the overall situation can best be estimated. This is because the energy extraction during last winter and the energy injection during last summer can now be combined into the estimation.

An indication of the adjustment process is displayed in Figure 29. During the first adjustment, the current hot well energy level is compared to the reference level at the same moment. If the deviation is higher than 50 MWh, the heat pump power is adjusted with a certain relationship between deviation and power setpoint. During the second adjustment, it is looked at the mean hot well energy level and at the peak energy level. The mean is calculated by taking the average between bottom and peak of the hot well content. This mean is then compared to the reference scenario and results in a certain deviation value. Then also the peak of the current situation is compared with the peak of the reference situation, which also results in a certain deviation. Then the average of those two deviations is taken. Based on this deviation, the heat pump's electrical power is adjusted during the second adjustment.

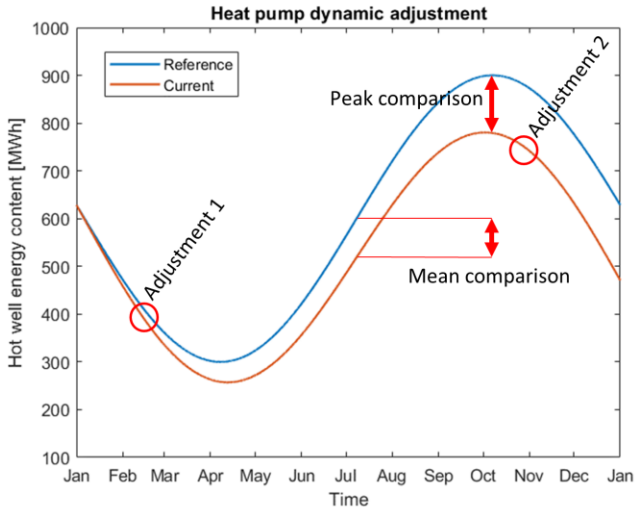

Figure 29 Indication of the heat pump dynamic power adjustment

This way of adjusting the heat generated by the heat pump is most likely not the most optimal and efficient way and certainly does have room for improvement. However, it is sufficient to fulfill the goals of this research.

4.8 Electric power and energy consumption calculation

In a triplet system, electric energy is consumed by pumps, dry cooler fan, and if applied, a heat pump. The electric power and consumption of those devices must be calculated in order to calculate the electric load and consumption of the triplet system. The dry cooler fan electric power and consumption is calculated based on the fan electric power specified in the dry cooler specification sheet, as the fan always runs at maximum speed (or is turned off). The heat pump electric power and consumption is calculated based on the supplied thermal heating power divided by the COP calculated in Equation 12. The electric power and consumption calculation method for the pumps is explained in the next section. Also, the electric power and consumption of the doublet system is calculated, explained in the section below that.

4.8.1 Pumps

There are multiple pumps in the system, as can be seen in the hydraulic layouts. For each pump, the electrical power is calculated during each moment in time and then integrated to calculate the energy consumption. The following steps have been done for each pump to model their power and energy consumption.

1. Determine the design flow rate and pressure drop in the system at the design flow rate. The assumed pressure drop per component can be found in Appendix V.
2. Determine the relationship between flow rate and pressure drop, using Equation 13 [45]:

$$dP = dP\ at\ design\ flow\ rate * \left(\frac{Flow\ rate}{Design\ flow\ rate}\right)^n \qquad 13$$

   With this equation, for different volume flow rates, the pressure drop in the system can be calculated. Exponent n is dependent on the part of the system the pump is placed in. Different components have different values of n. Appendix V shows the different values of n.
3. The previous step created a relationship between flow and pressure drop for each pump. The efficiency of a pump is not constant and is dependent on the occurring flow and pressure. Based on the data on the website of a large pump manufacturer [46], for each pump the relationship between flow, pressure, and pump efficiency has been fitted. This efficiency includes pump efficiency, motor efficiency, and frequency converter losses.
4. The volume flow passing through each pump comes from the main simulation model for each moment in time. With the previous steps, the flow rate can be converted into a pressure drop and a pump efficiency. It is assumed that the pressure drop in the system is equal to the pressure difference over the pump. With this information, the pump electrical power can be calculated by multiplying the pressure difference with the volume flow and dividing it by the pump efficiency at that moment.

In this way, the electrical power and consumption of each pump in the system is calculated individually.

4.8.2 Doublet

The energy consumption and the electrical power from the doublet system are calculated by applying a constant COP and EER value for heating and cooling. The values originate from a design SPF (Seasonal Performance Factor) calculation for the Mijnbouwstraat. The SCOP value for heating is 3.21 and the SEER value for cooling is 18.01. These values, and there with the energy consumption calculation for the doublet system include: water-water heat pumps, air-water heat pumps, well pumps, and bridge pumps consumption. In a separate simulation, the thermal heating and cooling powers are divided by the SCOP and SEER values to derive the electrical power. Integrating this leads to the electrical energy consumption. The same doublet simulation is also used to calculate the indoor comfort level for a doublet system. This is done by assuming the requested CH and CW temperatures according to the heating curve can always be met.

5 Results

The results are displayed and discussed in this chapter for multiple scenarios. The main focus is on the scenario with heat pump, which forms the basis scenario for the Mijnbouwstraat. As explained in the methodology, all simulated scenarios start in the operational phase (wells at nominal level), with the exception of the scenario where the startup phase is investigated.

5.1 Situation without heat pump

First, the situation for the Mijnbouwstraat is simulated without additional heat supply. This means the solar collector setup specified earlier is the only heat source. First is looked into if for a NEN5060 energy year, enough heat can be generated so that the triplet system (hot well) can sustain itself. The assessment method for this is monitoring the difference between the energy content of the hot well at the start of the year relative to the end of the year. If the energy content is equal or higher at the end of the year than at the beginning of the year, the triplet system is able to sustain itself. If the energy content is lower, the system cannot generate enough heat to sustain itself and therefore will run out of heat eventually. Figure 30 shows that the latter is the case. At the end of the year, there is a deficit of 14 MWh, meaning the system cannot sustain itself. The deficit is only 3% of the heating demand, but if there already is a deficit for an average year, it will be even higher for more extreme years. As there cannot be placed any more solar collectors, the conclusion is that a monovalent triplet system is not technically feasible, with the amount of heat generated by the solar collectors being the bottleneck.

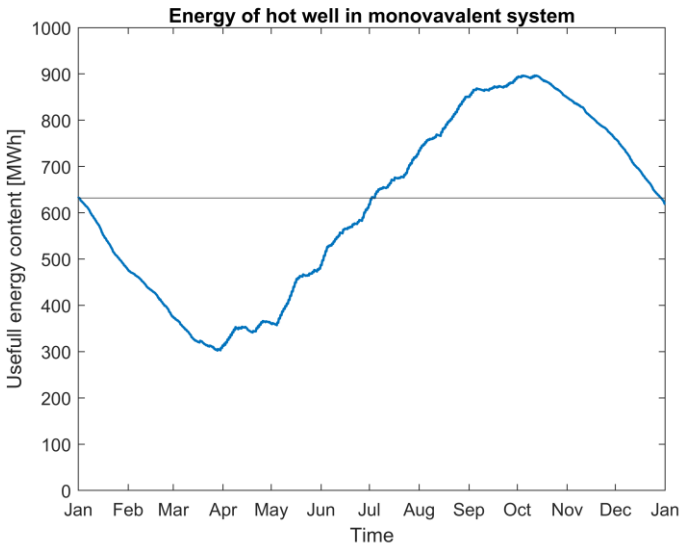

Figure 30 Hot well useful energy content for monovalent system

5.2 Situation with heat pump

As the monovalent system is not feasible for the Mijnbouwstraat, an additional heat source is required. The applied additional heat source is the water-water heat pump with its implementation as described earlier. The heat pump will generate the deficit in generated heat, with the result that the hot well energy content at the end of the year will be equal to the beginning of the year. The heat pump needs to generate 19 MWh to achieve this situation. This requires a heat pump with a thermal capacity of approximately 4 kW (0.77 kW electric), which is a small heat pump.

The design in this scenario acts as the reference situation for the other scenarios and is also the basis scenario to compare to the doublet system.

5.2.1 System dynamics

A triplet system works vastly different than doublet systems and conventional systems. There is no knowledge yet about the dynamics of the system. This for example includes where losses in the system are and the quantity of those losses at each point in the system. In the end, the losses in the system determine for a large part the feasibility of the system, so when better understanding the losses, also the feasibility can be assessed better. This part shows the dynamics for a NEN5060 energy year.

Losses heating side

Energy losses in the triplet system do have multiple causes. Figure 31 displays which losses occur on the heating side of the triplet and their quantities. The percentages shown are a fraction of the delivered heat to the building.

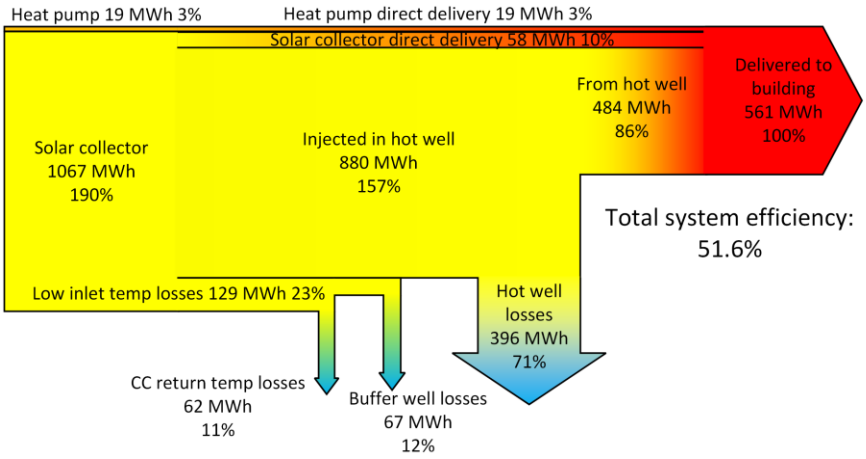

Figure 31 Sankey diagram of the heating side energy quantities

The heat pump generates 19.3 MWh. As all the energy from the condenser is always directly delivered to the building, the heat pump does not have any thermal heat losses. The solar collectors generate a total of 1,067 MWh. From this, 129 MWh is lost due to low inlet temperature losses. This occurs when the inlet temperature of the solar collector is lower than the weighted average return temperature of the CH. The solar collector must therefore achieve a higher temperature difference than that would be the case if no losses would have occurred elsewhere in the system. The low inlet temperature losses can be split into two components/causes. The first component is a lower inlet temperature caused by CW return water flowing into the solar collector, which gives a 62 MWh loss. This happens when there is heat generation and cold consumption at the same time, and is part of the functioning of a triplet concept. The other cause is the fact that CH and CW return waters are mixed in the buffer well, in combination with thermal losses from the buffer well to the ground. This accounts for a loss of 67 MWh. With the low inlet temperature loss extracted, 938 MWh of useful heat remains from the solar collector. 58 MWh of this is directly supplied to the CH circuit.

880 MWh is injected into the hot well. This is by far the largest loss factor in the system, as 396 MWh of useful energy is lost. The effective efficiency of the hot well is approximately 55%,

which means 45% of the energy injected into the well is lost. 484 MWh is extracted from the hot well and delivered to the building. The total system efficiency for the heating side is 51.6%. This is defined as heat delivered to the building as a fraction of the total gross generated heat.

Losses cooling side

Figure 32 displays which losses occur on the cooling side of the triplet and their quantities. The percentages shown are a fraction of the delivered cold to the building.

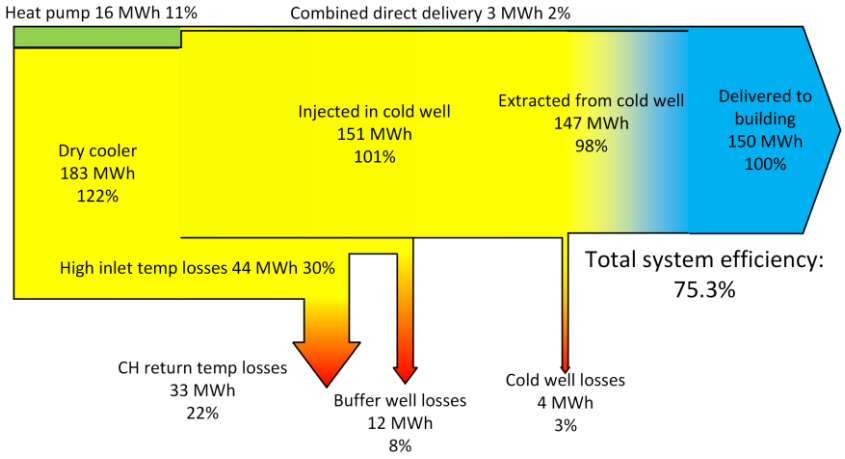

Figure 32 Sankey diagram of the cooling side energy quantities

The evaporator of the heat pump generates 16 MWh of cold. 2 MWh of cold is lost due to high inlet temperature losses, which gives a remaining 14 MWh of useful production. 3 MWh of this useful production is delivered directly to the building, while the other part is injected into the cold well. The dry cooler generates a total of 183 MWh. From this, 42 MWh is lost due to high inlet temperature losses, which gives (together with the heat pump) a loss of approximately 44 MWh. 33 MWh of this is caused by the CH return water let into the dry cooler and heat pump, and 12 MWh is caused by mixing in the buffer well. This then gives a useful cold generation by the dry cooler of 141 MWh. Less than 0.6 MWh is directly delivered to the building, while the remaining 140 MWh is injected into the cold well. The losses in the cold well are much lower than in the hot well, with a heat loss of 4 MWh. The remaining 147 MWh is extracted from the cold well, and delivered to the building. The effective efficiency of the cold well is approximately 97%. The total system efficiency for the cold side of the system is 75.3%. This means that the losses on the cold side are approximately only half the size of the hot side.

Delivery

Figure 33 displays the share of thermal energy directly delivered to the building, and the share that is being delivered indirectly to the building (with the intervention of the wells).

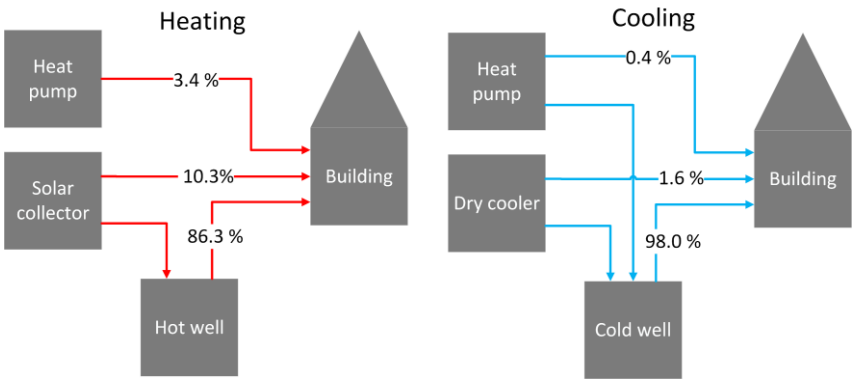

Figure 33 Diagram of direct and indirect delivery shares of heating and cooling side of triplet system

On the hot side, the heat pump produces 3.4% of the heat, and therefore also delivers 3.4% directly to the building. Of the useful solar collector production, only 6% is directly delivered to the building. This is 10.3% of the building demand. Of this 10.3%, 5.3% is not really being directly supplied to the building, but is used to charge the buffer vessel. Then after some time, when the solar collector generation falls below the heat demand, the buffer vessel is discharged again. The other 5% is actually directly supplied to the building, without interference of the buffer vessel. The largest part of the heat is being indirectly supplied with 86%, by discharging the hot well.

The cold side incorporates even less direct delivery than the hot side. Only 2% of the total energy is delivered directly to the building. Of this only 0.4% is actual direct delivery, as 1.6% first flows through the buffer vessel. 98% of the cold is indirect delivery by the cold well.

Occurrence of operational modes

When only considering the triplet system (without the functioning of the heat pump), 32 operational modes can occur. When also considering the heat pump, this number of operational modes approximately triples. Only the functioning of the triplet system itself without heat pump is considered in this analysis, to increase readability and simplicity. The graph in Figure 34 shows the occurrence of each operational mode in the period of one year. Appendix VI explains each operational mode.

Out of the 32 operational modes which can theoretically occur, only 23 actually occur. The most occurring operation mode is number 0. This is actually not really an operational mode, as this is the situation where all systems are turned off, meaning the building is free-floating (room temperatures are in between the heating and cooling setpoint). The second most occurring operational mode is mode 1. This is the situation with only heat demand, (no generations or cold demand). In this situation, the hot well is discharged to the building. The third most occurring is operational mode 7, which is only a cold demand, so discharging from the cold well. The fourth most occurring operational mode is mode 31. This is heat demand and cold generation at the same time while extracting water from the buffer well. The fifth most occurring operational mode is number 26, which is only heat generation. The sixth most occurring mode is mode 29, which is cold demand and heat generation at the same time.

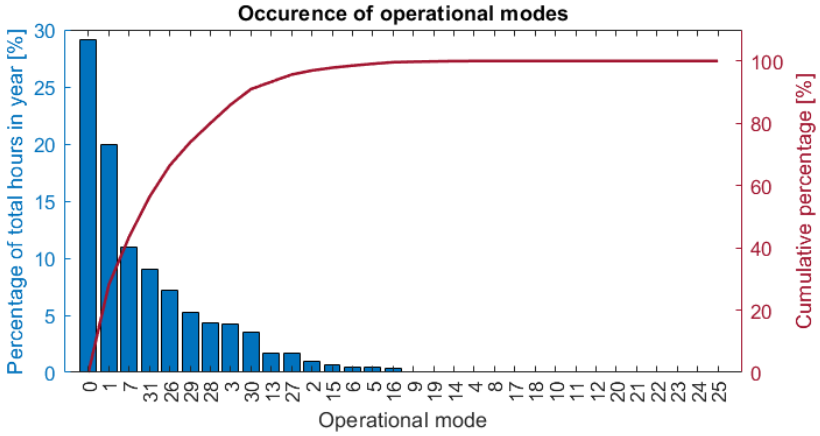

Figure 34 Occurrence of each operational mode

When excluding operational mode 0, 20% of the operational modes (6 modes) are responsible for 80% of the active triplet time. Those are all six relatively simple modes, with a maximum of two activities at the same time. The most complex modes (that include heat and cold generation and heat and cold demand all at the same time) do never actually occur during the year. 11 operation modes are active during more than 1% of the year. 6 modes are active between 0.1 and 1% of the year. 6 modes are active less than 0.1% of the year (but more than 0).

Solar collector generation

In the Mijnbouwstraat case, solar collectors are placed with eight different orientations. With an orientation is meant having a unique combination of inclination and azimuth. Due to this difference in orientation, the generation is not equal for every solar collector. Figure 35 shows the specific heat generation per solar collector orientation and its total heat generation. The building does have an approximate rotation of 30° to the west relative to the north. Meaning for example that collector names with an azimuth to the north are also actually rotated 30° to the west, but for readability the naming is only done to the four main wind directions.

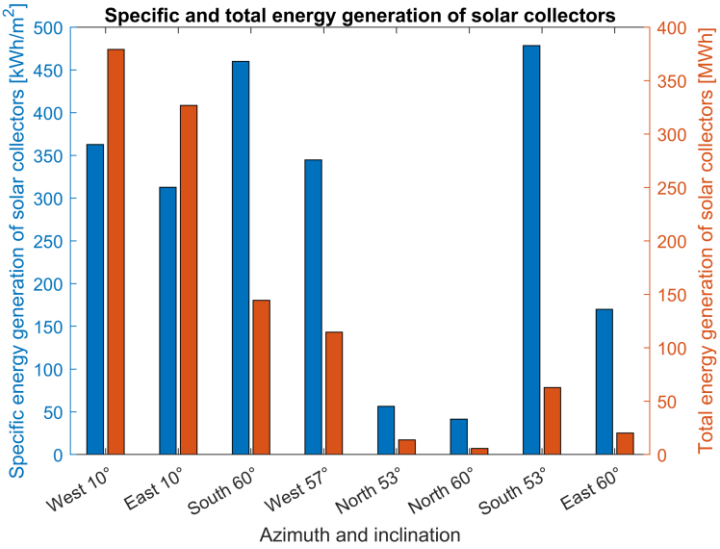

Figure 35 Overview of specific and total heat generation of the solar collectors per orientation

It is visible that the solar collectors orientated to the south have the highest specific production, as is expected. The west and east orientated collectors with an inclination of 10°

generate approximately 25% less. The collectors orientated to the north do have far less production. The collectors to the east with a 60° inclination generate approximately 45% less than the panels with the same azimuth with 10° inclination. These results show that it is important to choose appropriate orientations when no constraints are present. However, in this situation, and most likely most situations, this freedom is not present as there are constraints on the building roof layout and space availability.

Wells

The wells act differently than in a doublet system and do have different dynamics, such as pumped water volume and temperature variations throughout the year. Table 3 provides some statistics for each well, together with the following figures.

Table 3 ATES triplet well descriptive statistics

	Max / min temperature	*Pumped water volume out of the well*	*Min / max well volume*
Hot well	54.8 / 47.8 °C	18,279 m^3	13,613 / 29,865 m^3
Buffer well	26.4 / 18.1 °C	17,602 m^3	2,012 / 6,926 m^3
Cold well	10.5 / 10.4 °C	12,026 m^3	21,371 / 33,294 m^3

The buffer well plays an important role in the ATES triplet system. Figure 36 displays the share of the subsurface flow which flows via the buffer well.

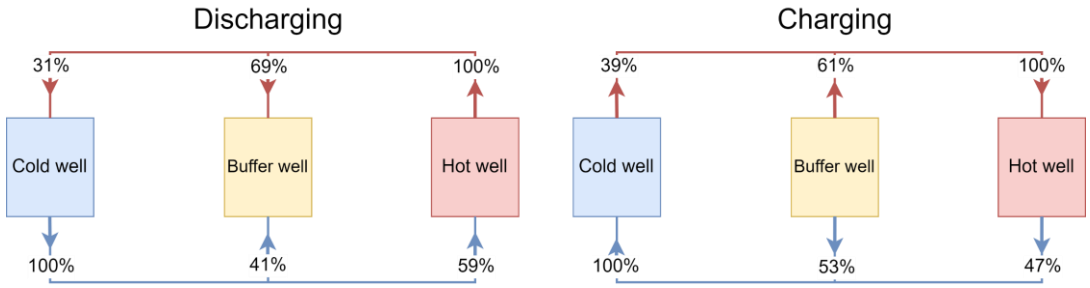

Figure 36 Display of subsurface flows via the buffer well

When discharging the hot well, 69% of the volume is injected into the buffer well, while 31% directly flows from the hot well to the cold well. When charging the hot well, 61% of the volume comes from the buffer well. The share of water volume that flows via the buffer well when discharging and charging the cold well is somewhat lower.

Hot well

It was decided to choose an average hot well energy content value that is approximately equal to one year of energy consumption in the building. In this way, there is a 50% margin for increased energy consumption, and the required energy input in the commissioning phase is limited to one year of energy (disregarding decrease in well efficiency during the commissioning phase). The hot well useful energy content and temperature over time are displayed in Figure 37. At the start of the year, the hot well is at an energy level of 630 MWh. As this is in the middle of the winter, there is almost no heat generation, and the well is discharged. The net discharging of the well lasts until the end of March. From the beginning of April, the energy injected into the well starts to become higher than the energy being extracted from the well, as heat generation increases and heat demand decreases. From this

moment on, the hot well starts growing in energy level. This growing phase lasts until mid-October, when the well reaches its peak energy content of 905 MWh. From this moment on, the level starts declining again. At the end of the year, the level is back at 630 MWh, as it was at the beginning of the year.

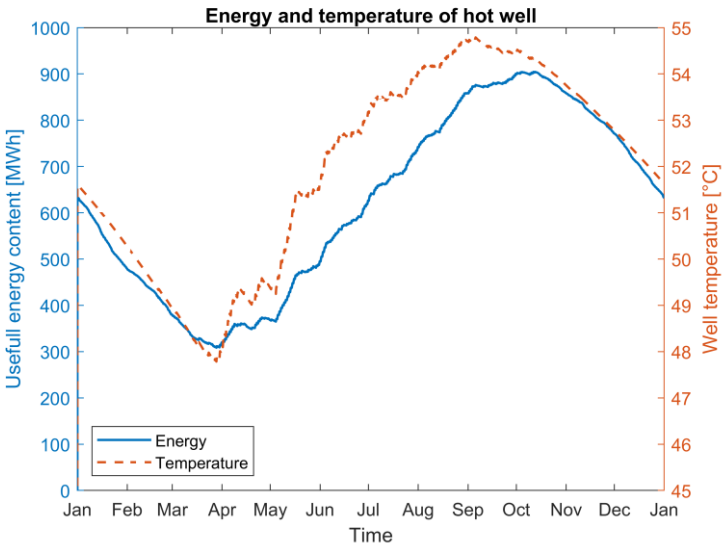

Figure 37 Energy content and temperature of the hot well throughout the year

The temperature variation follows a similar pattern as the energy content. The lowest point is reached at the same time as the energy level's lowest point, at a temperature of 47.8°C. At this moment, the well can deliver a supply temperature to the building of 46.8°C, which is lower than the design value of 50°C. The effects of this lowered supply temperature are discussed later. The temperature peak is reached at the beginning of September, at 54.8°C, which is one and half a month earlier than the peak of the energy content. The average temperature level is approximately 51°C, which is also the temperature that was aimed for. The total pumped volume out of the well is 18,279 m^3. The same amount is also injected during the year, as over one year the well is in balance.

Cold well

For the cold well, it was decided to go with a higher average well value relative to the cold demand. The reason for this is that it is easy to install an overcapacity in a dry cooler, as the costs and space requirements are limited. By creating a larger overcapacity in well content, multiyear extremes can be absorbed by the well, instead of required extra production by the heat pump. The well energy content has been limited to a value of 400 MWh. Above this value, the dry cooler turns off, until it falls below 390 MWh. However, the cold well can still grow above 400 MWh as the heat pump does not stop producing, as this is dependent on the hot side of the system. The cold well useful energy content and temperature over time are displayed in Figure 38. The well starts at a value of 330 MWh at the beginning of the year and starts growing until mid-February, when it reaches the 400 MWh limit. After that, the well slowly continues to grow because of the heat pump until the start of April, when it reaches a level of 402 MWh. From there on a slow decrease is visible, with a large decrease starting at the beginning of May when the cooling season starts. This large decrease lasts until the end of August. At mid-October, the well reaches its lowest point with 255 MWh. From then it starts increasing again, so at the end of the year it reaches a level of 330 MWh again.

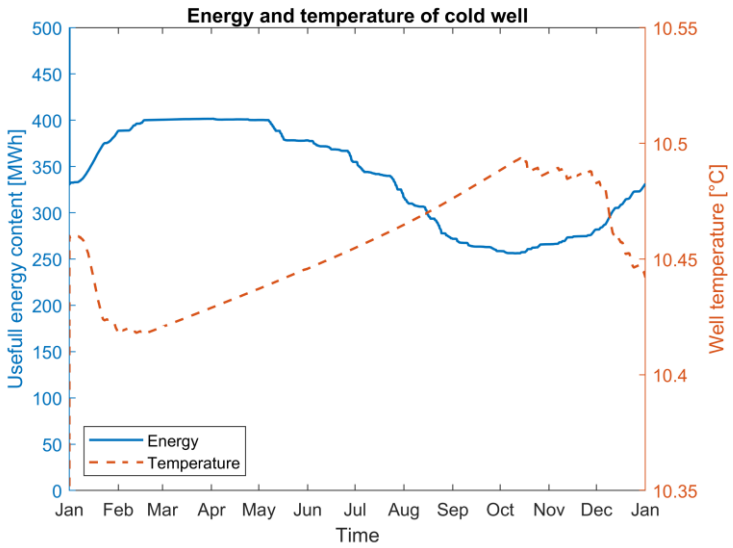

Figure 38 Energy content and temperature of the cold well throughout the year

The temperature variation over the year is very limited. It only varies between 10.4 and 10.5 °C throughout the year. The reason for this very limited variation is most likely due to the fact that the well temperature is very close to the natural groundwater temperature of 11.5°C. Annually, 12,026 m^3 is pumped in and out of the well. This is 81.8 m^3/MWh of extracted energy. This is 116% more than in the hot well, where only 37.8 m^3/MWh is required. The cause of this is the fact that the temperature difference on the hot side is larger than on the cold side, creating a lower energy density on the cold side.

Buffer well

In contrast to the previous two figures, Figure 39 does display the water volume instead of the energy content in the well. The reason for this is that the buffer well does not really contain any useful energy, as it is a mix of the return water of the CH and CW. Therefore the water volume and temperature are used to assess the buffer well. Until mid-February, the volume stays quite constant. The reason behind this is that the water extracted from the hot well caused by heat demand, and the water injected into the cold well caused by cold generation are approximately equal during this period. However, when at mid-February the dry cooler stops producing, the hot well extraction is larger than the cold well injection, causing the buffer well to grow. This lasts until the end of March. From here on, the well starts decreasing, caused by an overproduction of heat generation relative to the heat demand. During this period there is also cold demand, but as the cold demand is much smaller than the heat generation, it does not cause the well to grow until the end of July. During this time, there is a large cold demand from the building, which is greater than the flow from the heat generation, causing the buffer well to grow slightly. After that, the well volume level stays approximately level until the end of the year, when it reaches a level of 3,000 m^3 again.

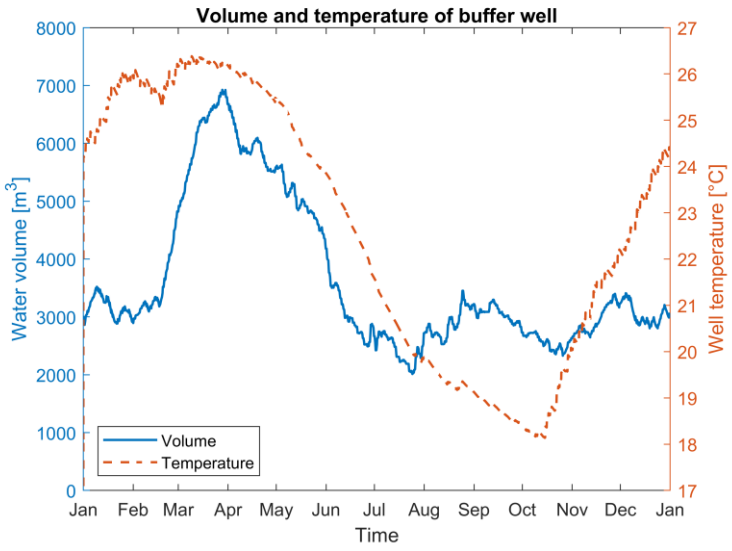

Figure 39 Volume content and temperature of the buffer well throughout the year

There is a large temperature variation in the well throughout the year. During the winter months, the temperature increases due to the injected CH return water, up until a maximum value of 26.4 °C. During the summer months, mostly CW return water is injected, causing the well temperature to drop to a minimum of 18.1°C. These temperatures are partly out of phase with the desired temperature for generation. This is because most heat is generated during summer when the buffer well temperature is on the cold side. Most cold is generated during winter, while the buffer well is on the warm side. This causes losses, which are described earlier in the report.

5.2.2 Energy and power

The electric energy consumption and electrical power are simulated for both the triplet system and the doublet system for a NEN5060 energy year.

Triplet electricity consumption

The electricity consumption of the different components in the triplet system are displayed in Figure 40.

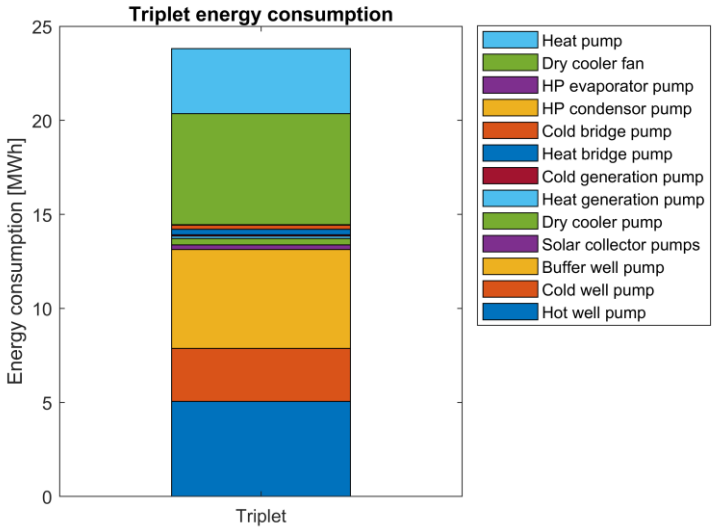

Figure 40 Electricity consumption of the triplet system for a NEN5060 energy year

The total annual energy consumption for the triplet is 23,810 kWh. The largest energy consumers are the three well pumps, the dry cooler fan, and the heat pump. The other pumps do have a relatively low energy consumption. Pumps are responsible for 60.7%, dry cooler fan for 24.8% and the heat pump for 14.5% of the total energy consumption. 12,144 kWh of the total goes toward the heating side of the system (51%). 11,665 kWh goes towards the cooling side (49%).

SPF

The Seasonal Performance Factor (SPF), Seasonal Coefficient of Performance (SCOP), and Seasonal Energy Efficiency Ratio (SEER) values of both the triplet and the doublet are displayed in Figure 41.

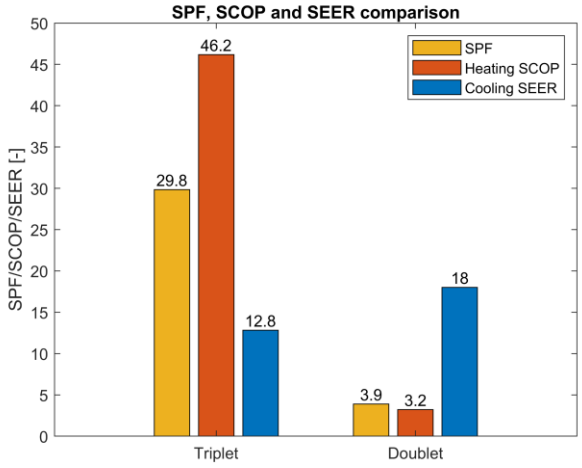

Figure 41 Performance comparison between triplet and doublet system for NEN5060 energy year

The SPF of the triplet energy plant is 29.83. This can be split up in a SCOP for heating of 46.2 and a SEER for cooling of 12.8. The SCOP for heating is significantly higher than the SEER for cooling. The first reason for this is the fact that the cooling system carries a lower temperature difference than the heating side, requiring a larger water movement per delivered quantity of energy (116% higher). The second reason is the fact that in the cooling system, a fan is responsible for the heat transfer from the air to the water in the dry cooler. In the heating system, the solar irradiation itself is directly responsible for the heat transfer to the water in the solar collector. Therefore, for heat generation, only the solar collector pump has to run, while for the dry cooler, the dry cooler pump and the fan have to run. The fan is relatively power intensive, and therefore consumes a significant amount of energy, reducing the cooling SEER.

Doublet electricity consumption and comparison

For the doublet system, the SPF is 3.88. The total energy consumption of the doublet energy plant is 183,040 kWh, meaning the triplet system saves 87.0% on electricity The SCOP for heating in the triplet is 1334% higher than in the doublet. However, the SEER for cooling in the triplet is 28.9% lower than in the triplet. The reason for this is the way cold is generated in the doublet versus the triplet. In a doublet, cold is generated by the evaporator of the heat pump, during moments the heat pump is in heating mode. The heat pump normally never functions in cooling mode. All the energy consumption by the heat pump is therefore attributed to the heating side, and not to the cooling side. Therefore, the cold generation in a doublet is ‘free’. In the triplet system from the case, only a small part of the cold is generated by the evaporator

of the heat pump, while the other much larger part is generated by the dry cooler, where all the energy is attributed to the cooling side, resulting in a lower SEER for cooling in the triplet system than in the doublet system.

Electrical power

Another advantage of a triplet system over a doublet system is the reduction of load on the electricity grid. This advantage is clearly visible in Figure 42. It is visible that the power drawn from the electricity grid is structurally much lower for the triplet system. This is also visible in the load duration curve. The peak electrical power for the doublet is 330 kW, while the peak power for the triplet is only 18.3 kW, which is a 94% reduction. From this can be concluded that the load on the electricity grid will be drastically reduced in this situation. For a NEN5060 1% year, the reduction in peak grid load is also 94%. Based on a rough estimation by an internal expert, the expected peak electrical power of the full building from the electricity grid in the original situation is 945 kW. This means on a full building level, the triplet reduces the peak by approximately 33% (assuming that the building peak is simultaneous with the doublet energy plant peak).

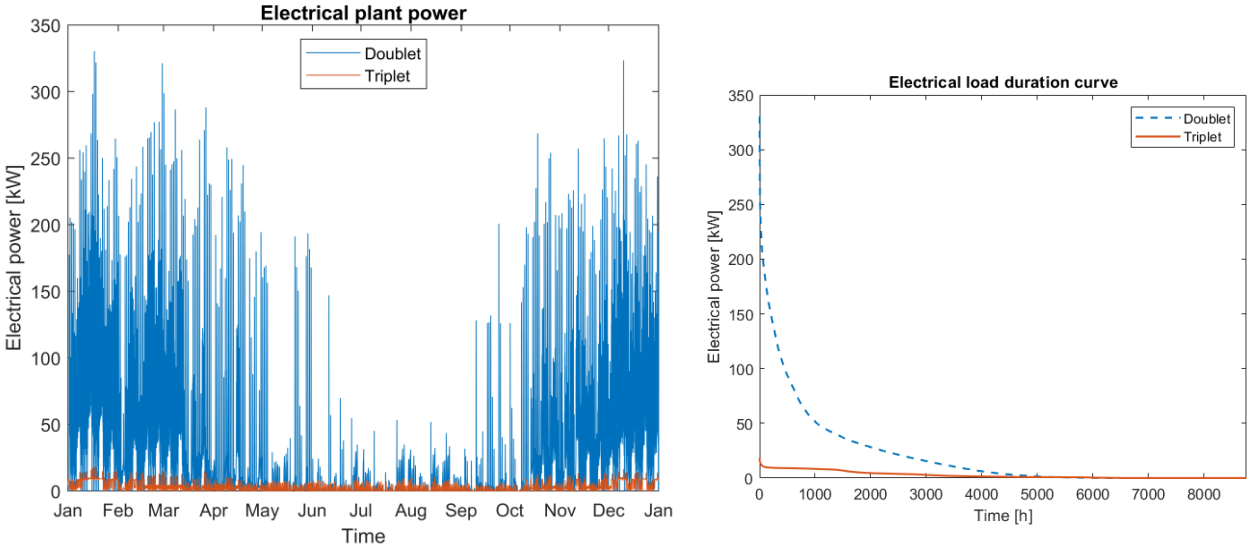

Figure 42 Electrical plant power over time (left) and Electrical power load duration curve (right) for NEN5060 energy year

5.2.3 Period 2016-2020

Next to the NEN5060 energy year, two real periods have been simulated using KNMI weather data. The first period are the years 1985 until 1989. Figure 43 displays the degree days for heating and cooling, and it shows the annual solar irradiation. It is visible that this period contains three consecutive cold years. Also, solar irradiation in these years is lower than in recent years. This combination will put strain on the hot well, and put the triplet to the ultimate test regarding reliability. The results from this simulation are used to determine the required heat pump capacity and discuss the reliability of the triplet system in the next section.

The second simulated period are the years 2016 until 2020, which will be discussed in this section. This is the most recent 5-year period with available climate data. The number of cooling degree days during this period is high, resulting in a relatively high cold demand.

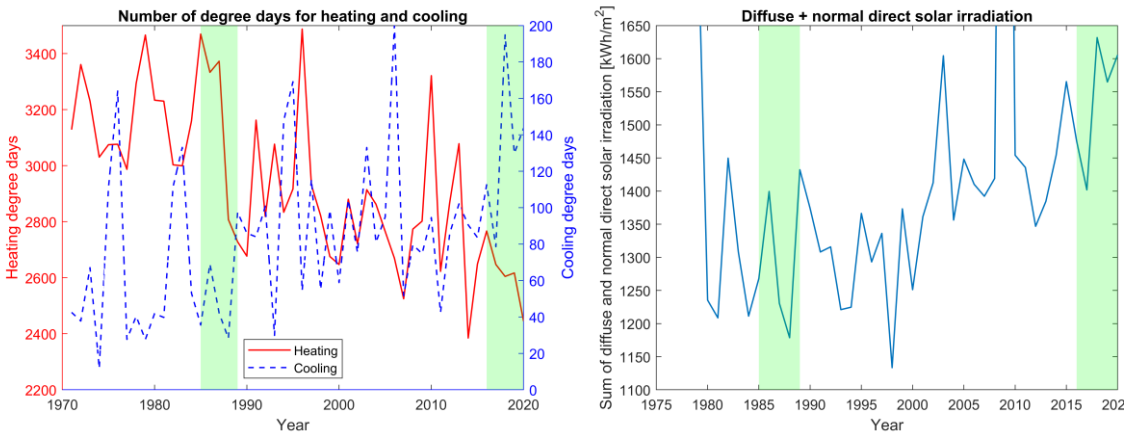

Figure 43 Heating and cooling degree days overview (left) and solar irradiation overview (right)

The average electrical energy consumption of the 2016-2020 period is 22,458 kWh per year. This is close to the calculated energy consumption for the NEN5060 energy year. The heating side of the system performs better than during the energy year. This is caused by the fact that heat demand is similar or lower than the energy year, but the solar collector heat generation is higher. This is visible in Figure 44, where the building heat consumption and heat generation by the solar collectors are compared to a NEN5060 energy year and 1% year. The average doublet scenario electricity consumption is 171,358 kWh per year. This means that the triplet system reduces energy consumption over this period by 86.9%.

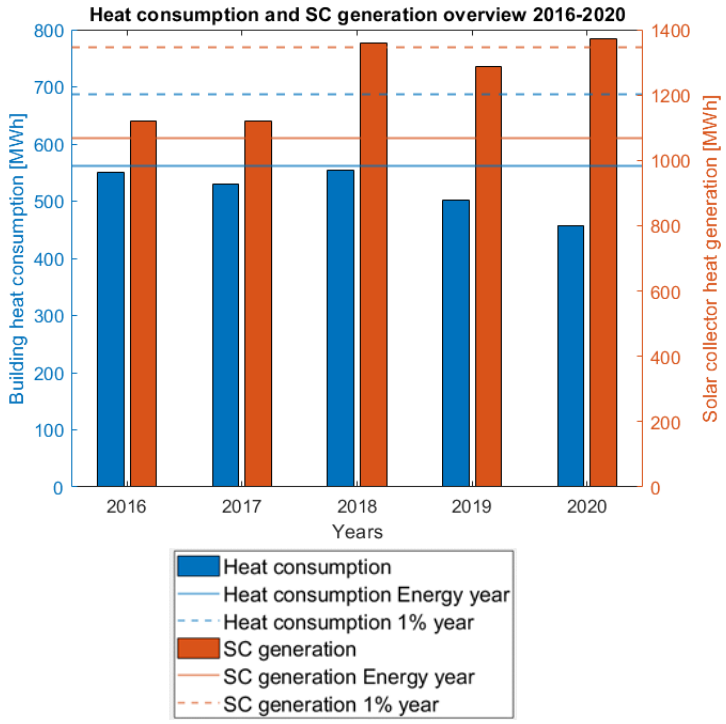

Figure 44 Overview of building heat consumption and solar collector heat generation during 2016-2020

The structural heat generation surplus causes the hot well energy content to rise, as can be seen in Figure 45. The heat pump already turns off in November 2016 and does not turn on during the remainder of the 5-year period.

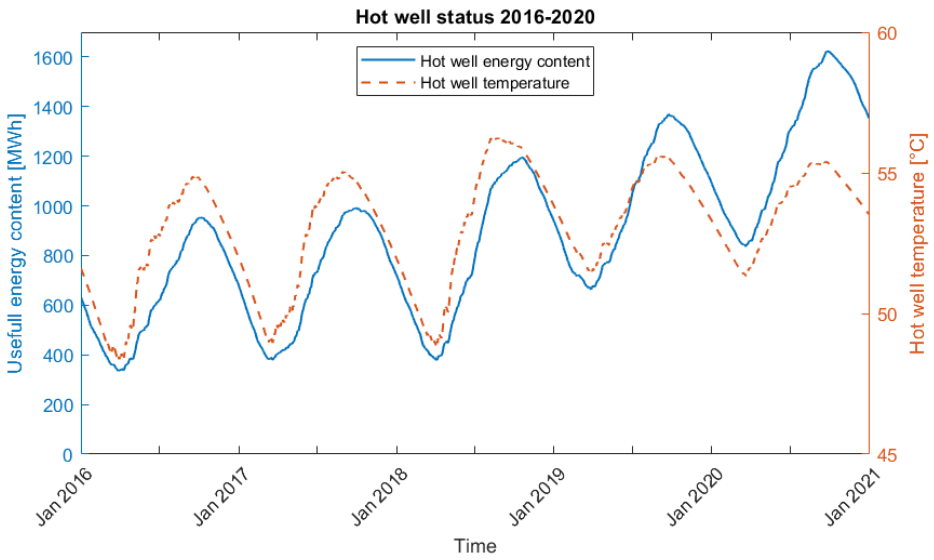

Figure 45 Hot well status during 2016-2020

The previous and all upcoming scenarios have been simulated using a 175 kW dry cooler, as this was based on the energy year simulation plus 30% extra margin. It was expected that this was enough, and gave no problems for all simulated scenarios. However, when simulating the period 2016-2020, it appeared that there is quite a large deficit in cold generation during some years. For the five-year period, it did not cause the cold well to run empty. However, considering a trend of warmer winters and warmer summers, it was deemed logical to increase the dry cooler power. This has been increased to a value of 260 kW and applied for the 2018-2020 part of the simulation period. All other simulated scenarios have been simulated using the initial dry cooler power value of 175kW, as those simulations were performed earlier. However, as for all scenarios each year the 400 MWh cold well maximum limit was reached, this will have no effect on the outcome, especially when controlling the dry cooler power efficiently. In the cost calculation, the value of 260 kW is used.

With a dry cooler capacity of 260 kW, the cold well energy content goes back to a desired pattern with no structural decrease in energy content, as can be seen in Figure 46. It has not been investigated how future-proof the dry cooler capacity is regarding climate change. However, considering the fact that the footprint of the dry cooler is small, and the fact that dry coolers are inexpensive, increasing the dry cooler power would have little effect on the financial and negative aspects of the technical feasibility.

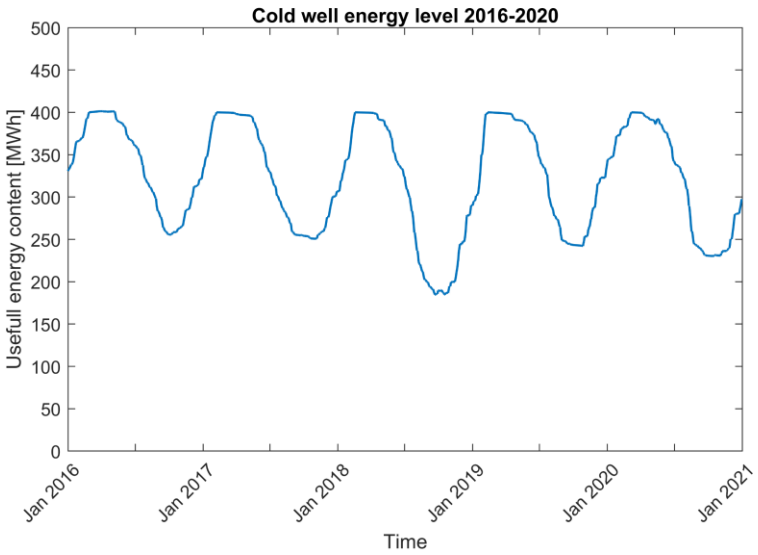

Figure 46 Cold well energy content during 2016-2020

5.2.4 Technical feasibility

In this section, multiple aspects regarding the technical feasibility of the triplet system are described.

Reliability

Not every year is a NEN5060 energy year. It is possible that multiple cold years consecutively occur, with high heat demand and low heat generation. It is important that the hot well never runs out of energy. From looking at the degree day numbers and the solar irradiation data, 1985-1989 seems to be the most challenging time period within the available climate data. It contains three consecutive cold years, with relatively low solar irradiation. This is also displayed in Figure 47, in comparison to the NEN5060 energy year and NEN5060 1% year. The heat consumption of the first three years is higher or equal to the NEN5060 1% year. The solar collector heat generation is in those first three years lower or almost equal to the NEN5060 energy year. This shows that this selected time perioded is quite extreme. The last two years of this period are more moderate.

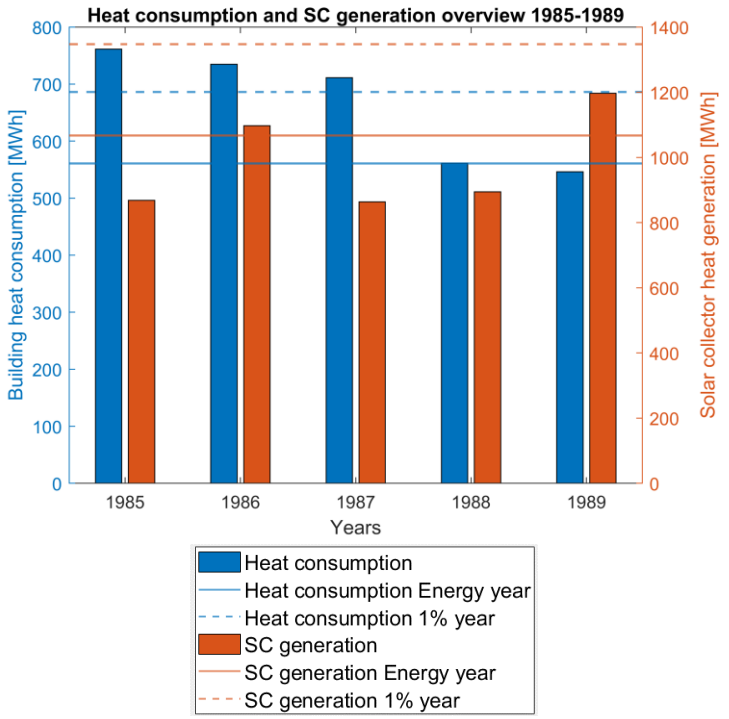

Figure 47 Overview of building heat consumption and solar collector heat generation during 1985-1985

If the heat pump power is kept the same as during the NEN5060 energy year, the hot well already runs out of heat in the winter of 1985-1986. Therefore, the dynamic heat pump power control is activated. Using an iterative process, the optimal relationship between hot well energy content deficit and heat pump power setpoint was found. The goal was to let the hot well energy level and temperature level not drop too low, and keep some margin left. The energy content of the hot well is displayed in Figure 48.

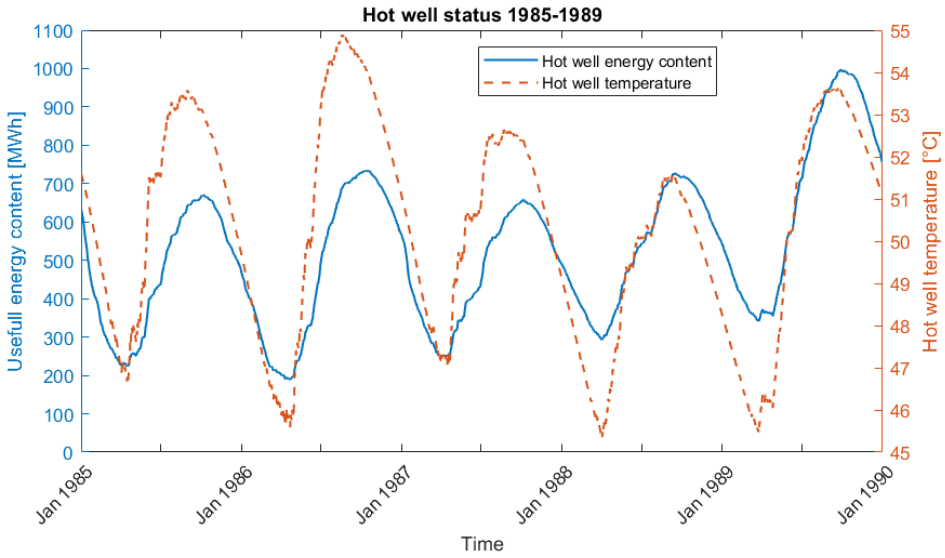

Figure 48 Hot well status during 1985-1989

The energy level reduction is mitigated by the heat pump stepping in. The lowest hot well level is 190 MWh, which is deemed as enough safety margin. The lowest temperature in the well is 45.3 °C. This is 2.5°C lower than during an energy year. However, as the main heat providers

are climate ceilings and underfloor heating, with relatively low supply temperatures, the effect of the temperature drop in the hot well is limited.

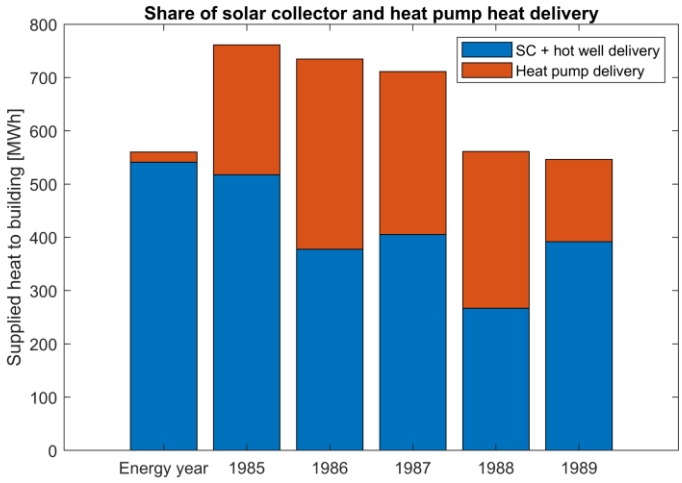

Figure 49 Share of heat pump generation during 1985-1989

During the period of 1985-1989, the heat pump has to generate much more heat than during the NEN5060 climate year, caused by lower generation and higher heat demand. This is displayed in Figure 49. In order to let the hot well energy content not run too low, the heat pump relieves the hot well by producing more heat. For each year in the five-year period, the heat pump generates more heat than during the energy year. However, in 1990, after the hot well is restored to normal levels after the cold consecutive five-year period, the heat pump turns off for the whole year, and the system fully depends on the hot well.

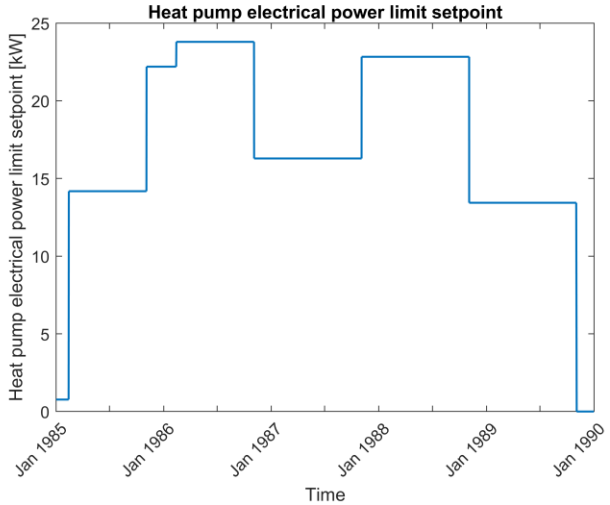

Figure 50 Heat pump dynamic electrical power limit setpoint during 1985-1989

Figure 50 displays the outcome of the dynamic heat pump power control, in terms of electrical power limit setpoint. The maximum selected electrical power value is 23.8 kW. Based on this the heat pump is selected, because this time period is regarded as worst case scenario the system has to sustain. To give some extra safety margin, an extra 20% in capacity is added, resulting in an electric power capacity of the heat pump of 29 kW. When looking at multiple water-water heat pump specification sheets, this translates to a nominal thermal heat design

power capacity of approximately 125 kW. As the original doublet Mijnbouwstraat design has a total installed heat pump capacity of 1,000 kW, the triplet only requires 12.5% of that.

It is not of much relevance for reliability, but as a cold period has been simulated, it may also be interesting to look at the electricity consumption during those years. For 1985-1989, the total electricity consumption of the triplet system is 326 MWh, while for a doublet system, this is 1,022 MWh. This means still a 68% reduction is accomplished, even during those cold years with relatively high heat pump generation share. The maximum occurring electrical grid load for the triplet is 45 kW (after removing a few very short-lasting extreme peaks), while the maximum occurring grid load of the doublet system is 331 kW. This means the maximum grid load is reduced by 86% during this period.

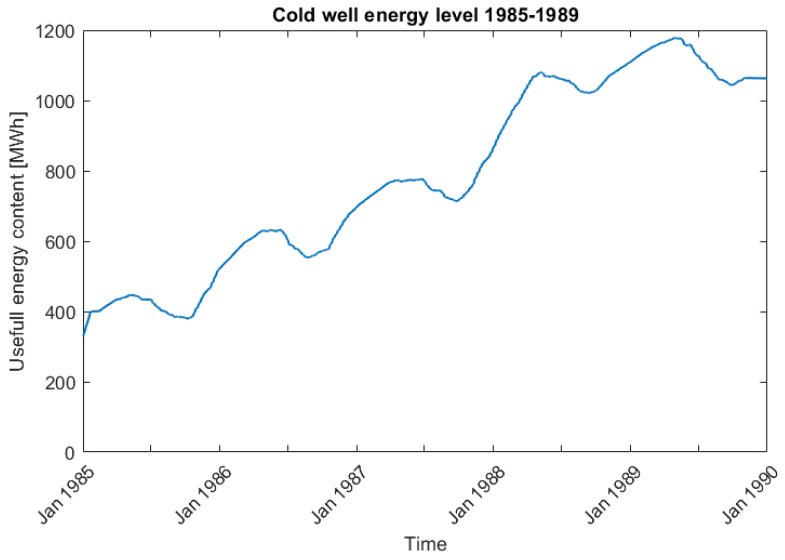

Figure 51 Cold well energy content during 1985-1989

Due to the vast increase in heat pump generation, and the fact that the heat demand in the building is systematically significantly higher than the cold demand, the cold well energy level increases significantly during the time period, as is visible in Figure 51. Almost all of this is caused by the cold production of the heat pump, as the dry cooler already turns off near the end of 1985. The maximum cold well volume is 92,100 m^3. The maximum volume during an energy year was 33,300 m^3. The increased cold well volume can potentially influence the other two wells in a negative way. This has not been investigated any further. However, if this problem would occur, the dry cooler can be used to regenerate water from the cold well to the buffer well during summer. This would lead to an increase in energy consumption, and also would require some hydraulic layout adjustments.

Thermal comfort

Thermal indoor comfort has been assessed using the ISSO 74 ATG method. In this method, the operational temperature range limits are dependent on the running mean outdoor temperature. For office and conference spaces class A/B is used, and for the atria class C is used for Beta buildings. More about this method is described in Appendix VII. The average over and under heating hours per room are determined both for the triplet system and for the doublet system for a NEN5060 energy year, a 1% year (very strict), and the periods 1985-1989 and 2016-2020, using the operative room temperatures. Moreover, also the deviations

between room air temperature and thermostat setpoint larger than 0.2°C were assessed during occupancy hours. The values are in hours. The results can be found in Table 4.

Table 4 Overview of average room over and under heating hours of the triplet versus doublet system

Year	Triplet ATG Overheating (hours)	Doublet ATG overheating(hours)	Difference to doublet	Triplet ATG underheating (hours)	Doublet ATG underheating (hours)	Difference to doublet	Triplet 0.2°C over cooling setpoint (hours)	Doublet 0.2°C over cooling setpoint (hours)	Difference to doublet	Triplet 0.2°C under heating setpoint (hours)	Doublet 0.2°C under heating setpoint (hours)	Difference to doublet
Energy year	25	25	0%	15	15	0%	74	74	0%	1	1	0%
1%	23	23	0%	19	19	0%	150	150	0%	2	2	0%
1985-1989	23	23	0%	16	16	0%	38	38	0%	2	2	0%
2017-2021	29	29	0%	12	12	0%	96	96	0%	0	0	0%

It is visible that for all simulated periods, there is almost no difference in ATG overheating and overheating hours, and also no difference in setpoint deviations (all differences round down to 0%) between triplet and doublet. For the triplet system, the CH supply temperature sometimes drops under the desired supply temperature according to the heating curve. The cause of this is that the hot well temperature varies, as can be seen in Figure 37. For the energy year, the minimum hot well temperature is 47.8°C, meaning only 46.8°C can be supplied. This is under the maximum design temperature (and upper limit of the heating curve) of 50°C. However, this does not cause any problems in the system. The reason for this is the fact that the main heat consumers are the climate ceiling and underfloor heating, which respectively have a maximum supply temperature of 45°C and 42°C. The consumers which have higher maximum supply temperatures are the radiators and the AHU heating coil. The radiators are barely active in the simulations, and therefore have no effect on this, also because they are not primarily designed for power delivery. The AHU heating coils are much more active, however, are designed with a large overcapacity, assuming an inactive heat recovery wheel. As the heat recovery wheel is active, the lower supply temperatures are more than enough for the heating coils to achieve their setpoints. Therefore, the varying temperatures do not have negative comfort effects.

Thermal power delivery

The current doublet design of the Mijnbouwstraat limits the ATES well flows at 85 m^3/h, due to subsurface constraints. The designed thermal power delivery to the building for heating is 1,000 kW (warm well plus heat pumps) and for cooling 600 kW (only cold well). Normally speaking, in a triplet, this power should be able to be delivered only by the wells. When assuming this situation, it can be calculated if this power delivery can be achieved with the triplet wells.

The hot well is designed to have an average temperature of 51°C. After passing the HX, this results in 50°C. The design CH return temperature is 40°C. This means if the well is at a temperature of 51°C, with a flow rate of 85 m^3/h it can deliver a thermal power of 989 kW, which is only slightly less than the required 1,000 kW. However, the hot well is not always at 51°. Figure 37 shows that during the energy year, the well temperature drops to 47.8°C. When assuming the return temperature of 40°, this would mean that with a flow rate of 85 m^3/h, only 672 kW can be delivered, which is lower than required. However, on the other side it shows that even for a strict year, with temperatures down to -18°C, this does not affect comfort, as the maximum hot well extraction flow only reaches 72.4 m^3/h. At that moment, approximately 1,000 kW is delivered. The well temperature at this moment is 48.2°C, while the building return temperature is 35.4°C, which is lower than the 40°C of the design. The reason for this seems to be the fact that the AHU heating coils are in partial mode at this moment, and therefore delivering a lower return temperature than designed for, and also the underfloor system structurally does have a design (and actual) return temperature below 40°C. This results in a lower return temperature, and therefore higher power delivery with equal flow. Therefore, as long as the hot well temperature is kept within a normal range, heating power delivery seems no issue for the triplet system. During the cold period of 1985-1989, at two short time periods (5 minutes) the flow rate goes slightly above 85 m^3/h. At those two moments, the flow is 87.1 m^3/h and 87.5 m^3/h. Considering that this only lasts 10 minutes in total and the fact that it is only a small amount over the limit, it would have a neglectable effect when the well pump would have been limited to 85 m^3/h. Therefore, it seems that the limit of 85 m^3/h can be maintained for the hot well with a triplet installation for the Mijnbouwstraat. Also, if other considerations would play a role, normally ATES wells with larger flow capacity can be designed to always guarantee a 1,000 kW delivery when desired. This can be done by creating wells with larger flow capacity (if permitted by subsurface conditions), or drilling extra wells, although this would increase investment costs.

The cold well is designed to have an average temperature of 10.5°C, which delivers 11.5°C to the building after the HX. The designed return temperature is 18°C. This means a power delivery of 643 kW at a flow rate of 85 m^3/h. This is higher than the requirement of 600 kW. As there are almost no cold well temperature fluctuations, the cold well will most likely always be at or below 10.5°C, and therefore can always supply at least 600 kW of cold to the building.

Control

Control in a triplet system is different than in a doublet system. It is expected to be more complex, but not too complex. Figure 34 showed that the most occurring operational modes are the more simple operational modes. The controls in the simulation are done in a slightly simplified way. However, it is expected that when implementing the system in reality, it can be controlled in a similar way. The starting point is to control the system based on flow differences. This can be achieved by placing volume flow sensors at the right places, and controlling the flow rate of pumps directly. When incorporating a buffer vessel of the right size, it is expected that the buffer vessel can absorb temporary flow inequalities without creating problems. This means the flow coordination between all pumps does not have to be perfect, and there is some room for control error, just as in a doublet system.

Theoretically, 32 different operational modes can occur in the triplet. When also counting in the functioning of the heat pump, the number of theoretical operational modes is expected

to be over 70. When not counting the heat pump, 17 modes are active for more than 8 hours per year as became clear from Figure 34. When for a longer time in one operational mode, control is expected to be easier than when switching operational modes frequently. Figure 52 shows the distribution of consecutive time in an operational mode. The bins are in intervals of 10 minutes. The x-axis shows the consecutive time in the same operational mode, and the y-axis counts the number of times this consecutive operational mode duration occurred. The first bin ranges from 0 to 10 minutes and has a count of 227. This means 227 times, the consecutive time of the same operation mode is between 0 and 10 minutes. The most occurring consecutive operational mode duration is between 30 and 40 minutes, which occurs 256 times. After that is a steep decline in the number of occurrences with increasing duration. The longest consecutive time of the same operational mode is 3570 minutes (60 hours). This is not visible in the figure, as it is limited to 1,000 minutes to increase readability. The median duration of the consecutive time of an operational mode is 75 minutes, while the average is 168 minutes, as can be seen in the boxplot.

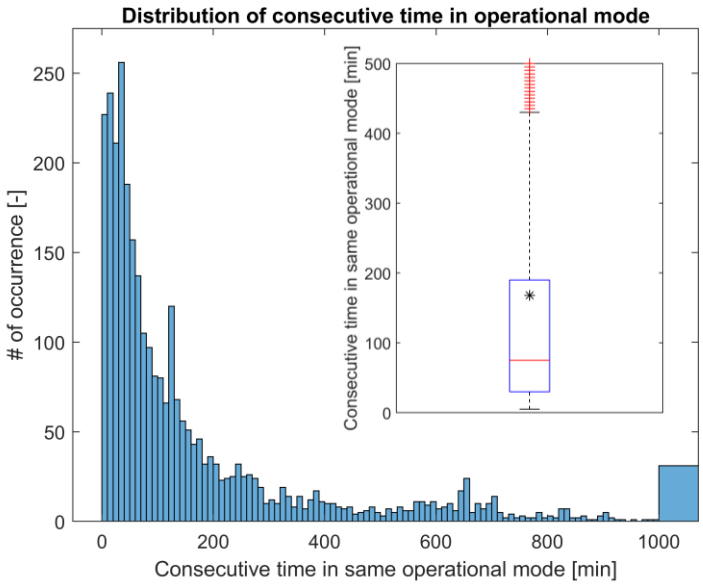

Figure 52 Operational mode duration distribution

Switching between operational modes with a duration of 10 minutes and lower can possibly be prevented by better and smarter usage of the buffer vessel than that now has been done in the simulation. It must be aimed to prevent frequent switching with such sort intervals, as it is expected to reduce system efficiency. One element that is not included in the simulation, but possibly can be a cause of frequent switching, are clouds. In the simulation, insolation data with one-hour interval is used. Between the hours, the data is interpolated. This means that in the simulation, the insolation progresses relatively gradually. However, in reality it is expected that during some moments this will happen less gradually, for example with changeable weather, when clouds come and go. This will cause the solar collector production to vary within a short time period and can cause frequent switching of operational modes. This issue has not been investigated during this research but is expected to occur in reality. Possibly smarter control and correct buffer sizing can mitigate this issue.

Strategy

With control is meant mostly the controlling between and within operational modes, with a timeframe of seconds to hours. A level above that is strategy. Strategy concerns the system over a longer timeframe, of months to years. In the model, there are two active strategy implementations. The first is the strategy that if the cold well has reached an energy content of 400 MWh, the dry cooler stops producing. This is to prevent the cold well from growing unnecessarily big. The second strategy is adjusting the heat pump production based on the current hot well level. The goal of that strategy is to ensure that the hot well does not run out of heat. If the hot well energy level is lower than the reference, the heat pump needs to start producing more heat. This strategy has been implemented in the model in a relatively simple way. It works, but most likely is not the most efficient way, and can be done in a more intelligent matter. When doing it in a more intelligent way, the required heat pump production may be estimated better, and therewith prevent unnecessary peaks on the electricity grid or underproduction which would decrease the hot well efficiency. It is possible that machine learning can play a role in achieving this intelligent heat pump strategy.

Startup

The startup phase of triplet systems can potentially form a problem. The reason for this is the fact that all three wells start at the natural ground water temperature of 11.5°C. Especially for the heating side this potentially can cause problems. To investigate the potential issues which can arise during the startup phase, a simulation of this startup period is performed. Consecutive NEN5060 energy years are used. By looking at the results of the other simulations, it was deemed that May 1st is the best time to start. This is because from then on, the hot well continuously grows, as the heat demand is low, and the heat generation starts to rise rapidly. For the whole startup period, the heat pump electrical power limit has been turned up to its maximum value of 29 kW_e (125 kW thermal design power).

From May 1st until the fall, there is almost no heat demand from the building. And the small heat demand that is present during some moments in the period can mostly be fulfilled by the heat pump. From the 4th of May, the hot well starts growing continuously, as is visible in Figure 53. In mid-October, the peak for that year is reached with a value of 494 MWh. This is approximately 400 MWh lower than in a normal operational year (after the system has already passed the startup phase), where the peak is around 900 MWh. Over the winter, the hot well content drops, to start gaining again from the beginning of April. In the second year, a peak of 729 MWh is reached. On the 28th of January in the third year, the hot well reaches the condition it would be in during a normal operational year, meaning the end of the startup phase. Due to the fact that the buffer well also starts at the natural ground water temperature, and remains during most of the startup phase, more useful energy is lost during the startup phase than during the normal operational phase. In the normal operational phase, the useful generated energy to gross generated energy ratio by the solar collector is 91%. During the startup phase, this is reduced to 83%.

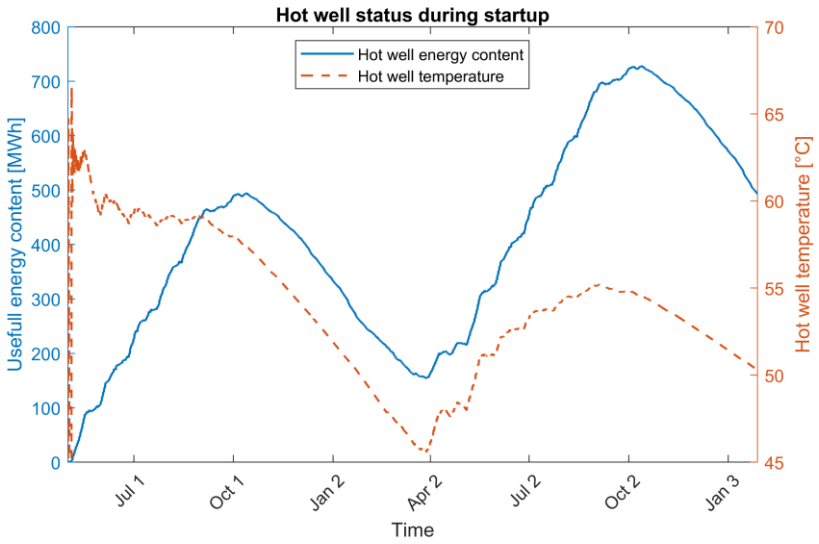

Figure 53 Hot well status during the startup period

Before the start of the first winter, the hot well has reached a sufficient temperature and energy content. No decrease in thermal comfort was noted in the simulation.

The startup period starts when also the cooling season starts. The cold well is empty at the start of the startup period and will stay mostly empty until mid-October, as is visible in Figure 54. However, when the cold well is empty, it does not mean it cannot provide cooling to the building. This is because it has the natural groundwater temperature of 11.5°C. The building requires a CW supply temperature of 12°C. With a cold well temperature of 11.5°C, this results in a CW supply temperature of 12.5°C. This is a little higher than what is desired, however does not affect the comfort in the building. The reason for this is the fact that the main cold consumers are the climate ceilings and the underfloor cooling system. Those require higher supply temperatures (15°C and 17°C). The AHU cooling coil requires a supply temperature of 12°C. But because it has a large overcapacity, this also does not form a problem. After the summer ends, the heat pump and the dry cooler start generating cold, and from then on the cold well energy content rises. The cold well temperature drops, and in the second summer, the desired CW supply temperature of 12°C can always be supplied.

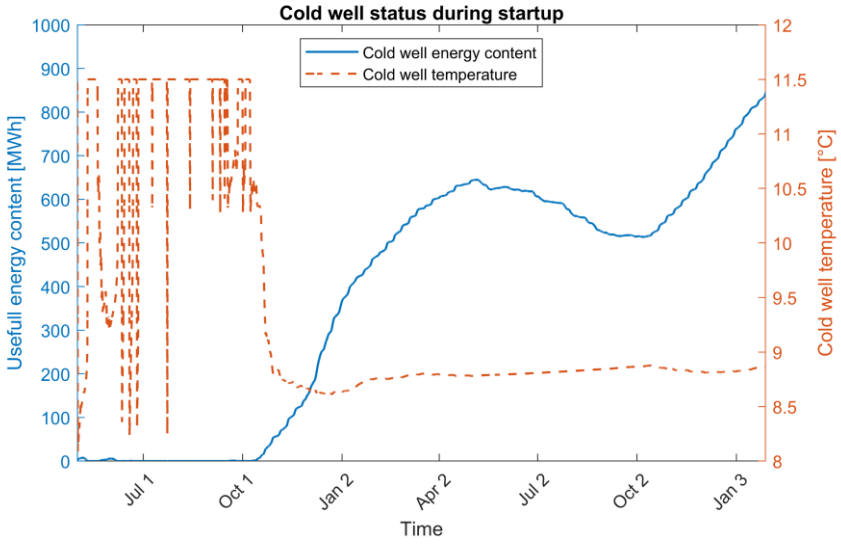

Figure 54 Cold well status during the startup period

The simulation shows that the startup phase lasts from May 1st in year 1, to January 28th in year 3 (approximately 20 months). The performed simulation shows that there is no reduction in comfort during the startup phase and that the startup can occur with just the equipment which is already present in the design, without the requirement of an additional heat source during the startup phase. However, there are some factors that can decrease the startup performance relative to the situation displayed in the simulation:

- The used well model during this research is a relatively simple well model. In reality, during the first years when commissioning an ATES system (startup period), the well thermal recovery efficiency is reduced [3]. This results in higher heat losses in the hot well during the startup phase. When this is considered, this can possibly result in the fact that the hot well runs out of energy after the first winter and/or that the temperature is not high enough.

- The simulation uses a NEN5060 energy year. However, it is also possible that the weather during the startup phase is less favorable. Especially when the first summer is cold / not sunny and the first winter is cold, this can potentially cause the hot well to run out of energy during the first winter.

- The simulation uses the optimal starting point at the beginning of May. When designing and planning the construction of a building or renovation, the aimed commissioning date can be set at May. However, construction delays are common. When in the original planning the commissioning date is in May, but due to delays the actual commissioning date is in October, a problem arises. The hot well will then be empty at the start of the winter, resulting in the fact that almost no heat can be delivered to the building, drastically decreasing comfort. This situation would not be acceptable.

Considering those factors, it is possible that the startup phase is more problematic than displayed in this simulation. This would then require a temporary additional heat source during the startup phase, especially when starting up near the heating season.

The calculated extra required electrical energy consumption during the startup phase relative to a normal operational period is 105,200 kWh. Considering the above-mentioned uncertainties regarding the startup phase, the cost calculation will use an extra required energy of 150,000 kWh during the startup phase.

5.3 Scenario with lower hot well efficiency

For this scenario, the hot well thermal recovery efficiency has been reduced from 68% down to 58%. The simulation done is for a NEN5060 energy year. As no more heat can be generated by the solar collectors, as the roof is fully filled, more heat needs to be generated by the heat pump in order to compensate for the increased hot well losses due to the lower well efficiency.

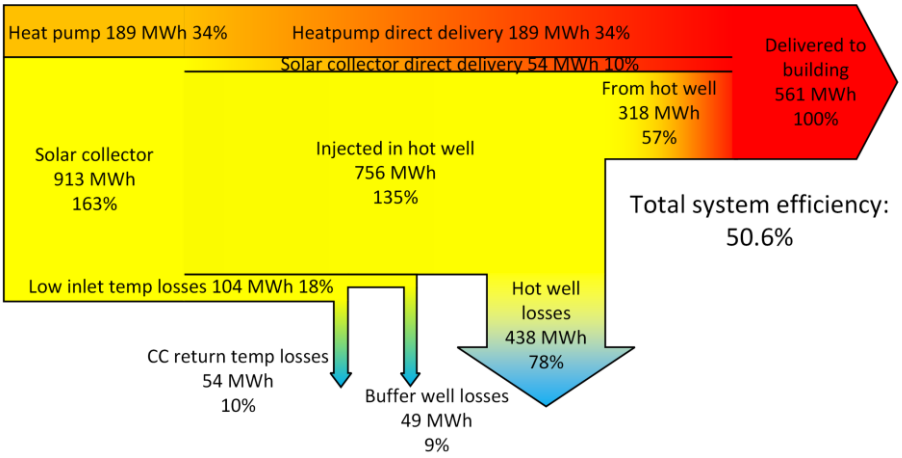

Figure 55 Sankey energy diagram of the hot side energy quantities for the lower hot well efficiency scenario

When looking at Figure 55, a few things can be noticed when comparing it to the same diagram for the basis scenario in Figure 31. The first thing is that the solar collectors now generate 913 MWh, while for the basis scenario they generated 1,067 MWh, which is a 14.4% reduction. The solar collector layout was kept the same. The cause of the lowered solar collector generation in this scenario is the fact that, because of the lower hot well efficiency, the solar collector must produce water of 81.6°C instead of 71.6°C to reach an average well temperature of 51°C. This higher outlet temperature results in a higher temperature of the solar collector surface, and therefore also higher thermal losses to the environment, explaining the lower heat generation by the solar collectors.

The heat pump generation is about nine times higher than in the reference situation. Next to the 189 MWh in heat it generates, it also generates 154 MWh of cold. Because of the increased cold production of the heat pump, the dry cooler production decreases to 24 MWh. Direct delivery from the solar collector reduces by 8%, most likely due to the increased outlet temperature. The relative hot well losses are larger. The heat delivery from the well is smaller, because of the larger well losses, and the reduction in heat generation from the solar collectors. Hot well effective efficiency is approximately 42%. In the basis scenario this was 55%, so this is a large reduction. The total heating system efficiency only reduces from 51.6% to 50.6%. The reason for the only small reduction is the fact that now more energy is generated and directly delivered by the heat pump, which has no heat losses.

5.3.1 Energy

The total electrical energy consumption is 48,240 kWh. This is a 103% increase from the reference situation. It is, however, still a 74% reduction relative to the doublet situation. The SPF is 14.7, which is approximately half of the reference situation. The SCOP for heating reduces from 46.2 to 13.6. The SEER for cooling rises from 12.8 to 21.6. This last fact is caused by the increased cold production of the heat pump. The peak electrical power of the energy plant is 24.5 kW.

5.4 Quadruplet

In the reference situation, part of the energy generated by the solar collectors is wasted because of the low water inlet temperatures caused by the CW return water flow, and buffer well mixing and losses. Those losses are coherent to the triplet concept. This form of heat loss can partly be eliminated by replacing the triplet concept for a quadruplet concept. In a quadruplet concept, there is not one buffer well, but two. The hot well is connected to one buffer well, and the cold well is connected to one buffer well. By doing this, the hot and cold sides of the system are not connected anymore. This would remove heat loss from CW return water in the solar collector, and the losses caused by the buffer well mixing. The buffer well thermal losses will still be present, and possibly increase. The quadruplet system has been simulated for a NEN5060 energy year. The adjusted hydraulic layout for the quadruplet system can be found in Figure 56.

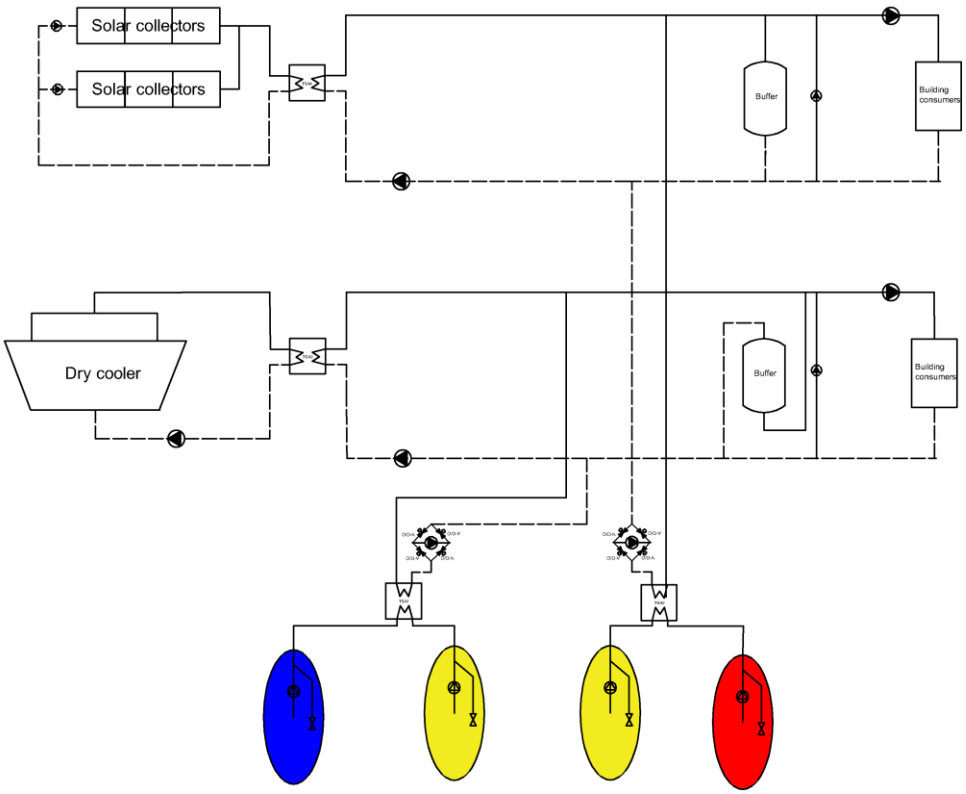

Figure 56 Hydraulic layout of quadruplet system

The losses of the hot and cold sides of the quadruplet system are displayed in Figure 57 and Figure 58.

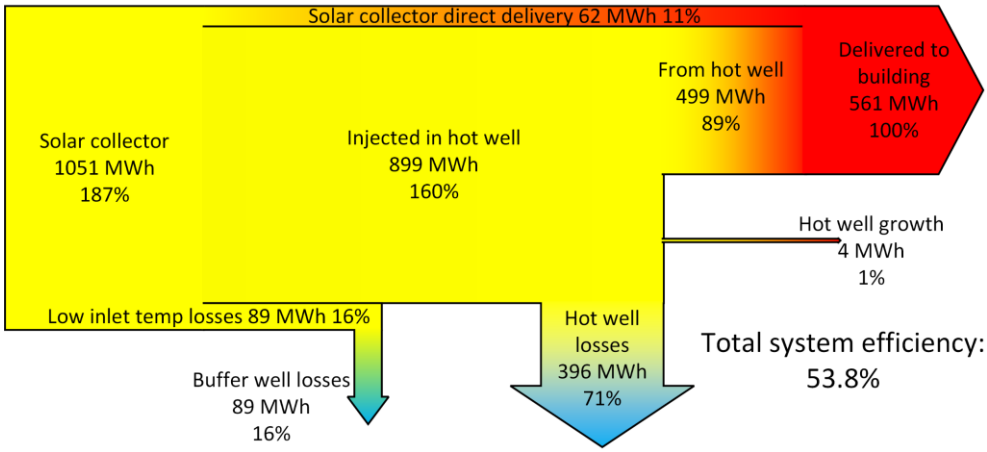

Figure 57 Sankey energy diagram for the hot side energy quantities for quadruplet concept

It is visible that the low inlet temperature losses are reduced from 129 MWh to 89 MWh. The reduction of those losses was the goal of this concept, and it succeeded. Due to the lower losses, more energy can be injected and also extracted from the hot well. Because of this, the heat generation by only the solar collectors is sufficient, and therefore the heat pump can be deactivated. There is a small heat overproduction, causing the hot well to grow with 4 MWh. The total system efficiency is increased to 53.8%, compared to 51.6% for the reference situation.

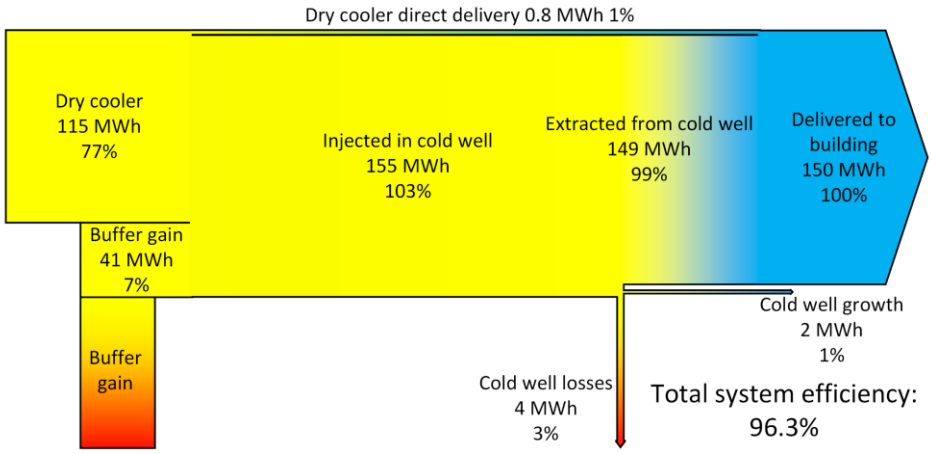

Figure 58 Sankey energy diagram for the cold side energy quantities for quadruplet concept

The Sankey diagram for the cold side now looks quite different than in the basis scenario in Figure 32. The reason for this is the fact that there are no losses anymore due to high CH return temperature, and the fact that the buffer well now actually gains energy. This is because the buffer well does have thermal heat loss to the ground. However, this thermal heat loss is positive, because it reduces the buffer well temperature, which is a gain of cold energy. The dry cooler has to produce 115 MWh, which is the gross energy production. The net cold production however is higher than the gross production due to the buffer well temperature drop, gaining an additional 41 MWh of useful cold. The total system efficiency is now 96.3%, due to the cold gain in the buffer well, compared to 75.3% in the basis scenario.

5.4.1 Energy

The electrical consumption is 22,589 kWh. This is a 5% reduction from the triplet situation, and an 87.7% reduction relative to the doublet. The electrical load peaks on the grid are slightly higher, with a peak of 21.7 kW. This is due to the fact that the water temperature difference while loading the cold well dropped due to the temperature reduction in the buffer well, causing an increase in water flow rate when the dry cooler is active, and hence a larger electrical power consumption by the pumps at those moments. Also the fact that there are now two well pumps present adds to this.

The SPF of the system is 31.4. The SCOP for the heating side is 53.9. This is an increase relative to the reference triplet situation. The SEER for the cooling side is 12.3. This actually is a slight drop from the reference situation. This seems counterintuitive, as from the Sankey diagram came clear that, due to the temperature drop in the buffer, less energy needs to be produced with the dry cooler than that is actually consumed in the building. This lowers the energy consumption of the dry cooler fan. However, due to the lower temperature difference during cold well charging, the electricity consumption of the pumps (especially the buffer well pumps) increases more than the reduction in fan energy consumption. The result of this is that the SEER slightly decreases instead of increases. The removal of the cold production from the heat pump also plays a role in this.

The addition of the fourth well requires additional hardware, but actually makes the system control and dynamics simpler, and easier to predict. The reason behind this is the fact that the hot and cold sides of the system are not connected anymore. However, the creation of the fourth well would also result in higher investment costs and maintenance costs.

5.5 Only solar collectors

The reference situation showed that the solar collectors alone cannot generate enough heat for the hot well to sustain itself and therefore heat production by the heat pump is required. As the roof was already filled with solar collectors, there was no more space for extra solar collectors left. In this scenario, this available roof space constraint is ignored. To increase representability, only an east-west orientation with an inclination of 10° is used for solar collector placement instead of all different kinds of orientations. Two sub-scenarios have been simulated. First, the required number of solar collectors for a NEN5060 energy year to sustain itself. Secondly, the required amount of solar collector area required to sustain itself during the period of 1985-1989.

Energy year

For the energy year, approximately 3,175 m^2 of solar collectors are required. This is less than the 3,364 m^2 which is present on the roof in the reference case. However, in the reference case, different orientations are used, with for example 379 m^2 orientated to the north with very low yield. Therefore, the weighted average performance of the solar collectors of the reference case is slightly lower than that is the case with all solar collectors orientated east-west. The electrical energy consumption in this situation is 21,270 kWh, which is a 10.7% reduction from the reference situation. The system SPF rises from 29.8 to 33.4. The SCOP for heating rises from 46.2 to 61.5, caused by the removal of the heat pump production. The SEER for cooling slightly lowers from 12.8 to 12.3, also caused by the removal of the heat pump.

Cold period

Also, the period 1985-1989 has been simulated. If only 3,175 m^2 of solar collectors is placed, the hot well quickly runs out of heat in the winter of 1986, which is undesirable. This is no surprise, as we saw a similar result for the basis scenario for this time period. To prevent this from happening, more solar collector area is required. Through an iterative process, it was looked into how many solar collectors must be placed in order to let the hot well not run empty or too low during this time period, and also let the temperature in this hot well not drop too much, as is visible in Figure 59. It appears that approximately 4,500 m^2 is required.

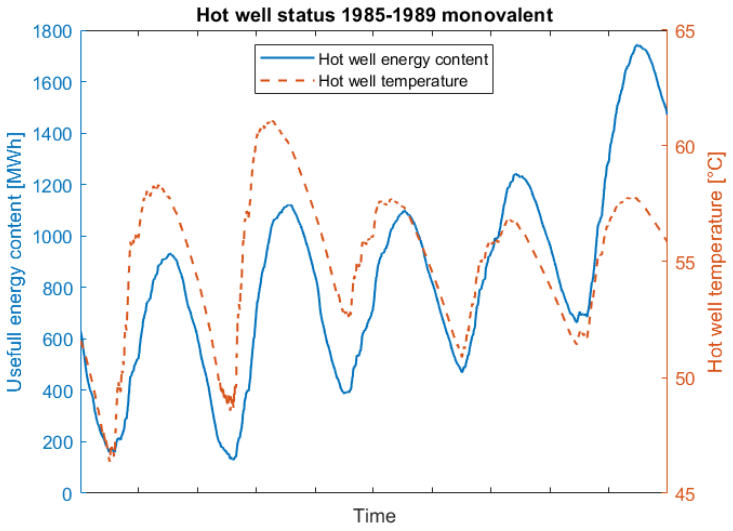

Figure 59 Hot well status for monovalent system during 1985-1989

This means the required solar collector area to guarantee robustness (assuming this is proved with the 1985-1989 period) is approximately 42% higher than that is required to sustain an average year.

5.5.1 Technical possibilities

As first described, this scenario is not technically possible for the Mijnbouwstraat case, as there is not enough roof space available. However, it is possible to widen the view while still using the Mijnbouwstraat as a basis. The middle part of the roof is flat, as this is on top of the new atria. The outer parts of the roof are all part of the old building and do have tilted roofs. Because of those tilted roofs, the available roof space for solar collectors is reduced. However, what would happen for the Mijnbouwstraat with the available roof space if it is assumed that the whole roof would be a flat roof? If it is assumed with a flat roof with the size of the main outline of the building, this gives a flat roof space of approximately 5,500 m^2. As 4,500 m^2 is required to guarantee robustness, it seems that a monovalent triplet system would be possible if the Mijnbouwstraat would have a fully flat roof.

An attempt can be made to generalize this outcome for application in other buildings. The Mijnbouwstraat does have a design heat demand of 561 MWh in the simulation (for a NEN5060 energy year). The exact heat losses are dependent on the dynamics of the system, which are for example dependent on the ratio between heat and cold demand (buffer well mixture losses and low return temperature losses), and the hot well efficiency. But the same

ratio and efficiency is assumed as for the Mijnbouwstraat, this leads to the simple conclusion that 8.04 m^2 of solar collector area is required for each MWh of design heat demand.

If the required solar collector area is calculated for the scenario with an assumed 58% hot well efficiency (by extrapolating with the gained knowledge), this would require roughly 6,700 m^2 (caused by increased losses in the hot well, and the decrease in heat generation because of higher outlet temperature). As the assumed flat roof on the Mijnbouwstraat is only approximately 5,500 m^2, this would not fit on the roof.

Three factors must be taken into consideration when generalizing the results. The first factor is the fact that the Mijnbouwstraat does have a relatively low heat demand. The second factor is the fact that assuming a flat roof on the Mijnbouwstraat possibly creates a higher roof to usable surface area ratio than average buildings, due to the fact that the atria are only one floor. The third factor is that uncertainties and safety factors must be considered. This for example is to account for possible deviations in simulated performance versus real performance and decrease in performance as the system ages. This would result in higher required solar collector areas than now calculated for a monovalent system.

The results show that if the Mijnbouwstraat would have a flat roof, a monovalent system would be possible with a hot well efficiency of 68%, but not with a hot well efficiency of 58%. It is realistically possible that hot well efficiency indeed is 58% instead of 68%. When then also taking into consideration that the Mijnbouwstraat is a relatively positive case, and the fact that uncertainties must be considered, it is suspected that the technical feasibility for a monovalent triplet system is unlikely for many buildings.

5.6 Financial feasibility

A Total Cost of Ownership (TCO) calculation has been made for both the triplet and doublet system for comparison. This has been done for the simulated scenario, but also for a more business case optimized scenario, which is explained later. The TCO calculation consists of direct construction costs, depreciation, reinvestment cost, maintenance costs, and energy costs. Subsidies have not been considered for both the triplet and doublet. The TCO is calculated over a period of 30 years. The reason for choosing a 30-year period is that 30 years is the expected lifetime of an ATES system [47]. Also, most other components have an expected lifetime near that range, as can be seen in Table 11 of Appendix VIII. It is therefore logical that after 30 years the heating and cooling system is renewed, and therefore is the cutoff point for the TCO calculation.

Three energy cost levels have been used, as energy costs play an important role in the payback time, but are quite unpredictable. The values used are a low scenario of 0.13 €/kWh, middle scenario of 0.23 €/kWh, and a high scenario of 0.33 €/kWh. Also, three different energy consumptions by the triplet system have been assumed, to accommodate for uncertainty in the energy consumption calculation of the triplet system. The first scenario is where the energy consumption is equal to the outcome of the NEN5060 energy year simulation for the basis scenario (triplet with heat pump), plus the required extra energy during startup. The second scenario uses the same value plus 30% to accommodate for uncertainties plus the required extra energy during startup. The third scenario uses the energy consumption of the scenario with reduced hot well efficiency during a NEN5060 energy year plus 30% plus the

extra energy required during startup. It is assumed that the required extra energy is equal to that of the basis scenario for the calculation. Also, it is assumed that the direct construction costs for the reduced hot well efficiency scenario are equal to the basis scenario. The assumptions made for the TCO calculation can be found in Appendix VIII. The TCO is expressed in net current value. An annual inflation of 2% and a discount rate of 3% have been assumed. The doublet is used as a reference scenario, also calculated for the NEN5060 energy year.

5.6.1 Basis scenario

First, the direct construction costs distribution of the triplet system in comparison to the doublet system is investigated. Direct construction costs are similar to the investment cost, but in direct construction costs, fewer components are considered. In the direct construction costs, components such as main contractor profit and risk surcharges, insurances, and design costs are not taken into account. What is considered are all hardware materials, installation costs, material surcharges, and third-party surcharges. The comparison in direct construction costs is displayed in Figure 60.

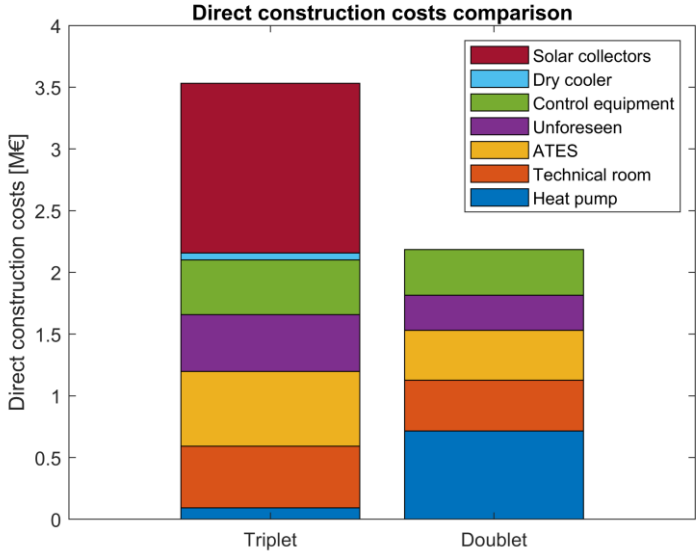

Figure 60 Comparison of direct construction costs of triplet and doublet

The direct construction costs of the triplet are with a total of €3.5 million higher than the doublet, which has a total of €2.2 million. This means that the initial direct construction costs of the triplet are approximately 59% higher than the doublet. The heat pump costs in the triplet are lower. However, the increase in costs of the ATES, technical room, dry cooler, control equipment, and especially the solar collectors make this decrease undone.

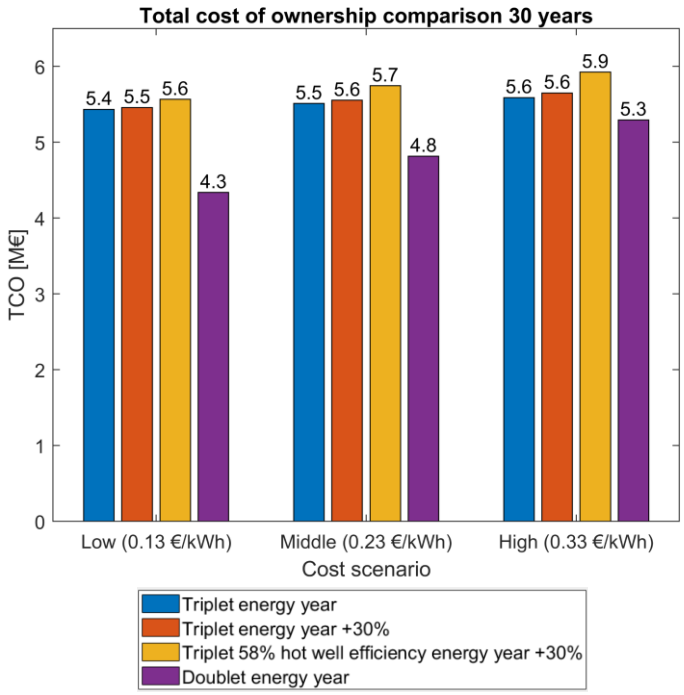

Figure 61 Total cost of ownership over 30 years comparison

Figure 61 displays the total cost of ownership over the 30-year period for the three different electricity cost levels. It is visible that for all cost levels, the doublet always does have a lower TCO than the three different triplet scenarios. The most realistic is the probably middle cost level. It is visible that there is a difference between the doublet TCO and the triplet TCO of €0.7 to € 0.9 million. This means that for the middle cost level, the TCO of a triplet is approximately 17% higher than a doublet.

5.6.2 Business case optimized scenario

The solar collectors make up a large share of the total investment costs. The goal of the solar collector layout in the basis scenario was to generate as much heat as possible. This was accomplished by placing as many solar collectors as possible. However, this does not seem to be the most economical solution, because this layout includes 379 m^2 of solar collectors oriented to the north, with much lower yield than the other orientations. The north-facing collectors are 11.3% of the total collector area, but only generate 1.8% of the heat. From an economical perspective it makes sense to remove the north-facing collectors, with only a limited effect on the energy consumption. No separate simulation has been run with this scenario. Results are interpolated based on the gained data extracted from the other simulations.

The increased energy consumption is calculated to be approximately 1,900 kWh for the basis scenario, and 1,300 kWh for the lower hot well efficiency scenario. This is relatively high, looking at the small reduction in solar collector generation, but this is caused by the fact that the heat pump is responsible for the marginal heat generation. The direct construction costs of this business case optimized scenario drop by €160,100.-.

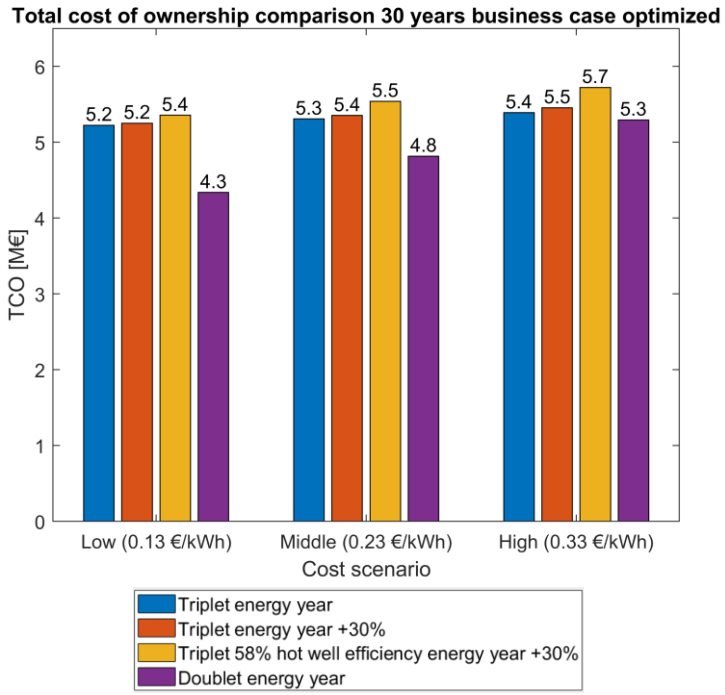

Figure 62 Total cost of ownership over 30 years comparison for the more business case optimized scenario

The total cost of ownership for this more business case optimized scenario shows improved results in Figure 62. For the high cost level, the TCO of the triplet now is close to the doublet system. For the middle cost scenario, the difference between triplet and doublet TCO reduces to between €0.5 and €0.7 million. If the triplet energy year +30% scenario is taken, the TCO for the middle cost scenario is 11.2% higher than the doublet. Considering the benefits of the triplet regarding CO_2 emission reduction and electricity grid relief, this difference in TCO seems limited and the increased TCO might be worth it. For the low-cost scenario, the gap between doublet and triplet TCO is larger, with an approximate 21% difference.

Figure 63 displays the division of the TCO for the business case optimized +30% and the doublet for the middle cost scenario. The items in the TCO are direct construction costs (consisting of the initial direct construction cost and the reinvested direct construction cost minus the residual cost), maintenance costs, and energy costs. It is visible that the energy costs of the triplet are much lower than for the triplet with a reduction of €865k (79%) over the 30-year period. However, for both systems, the energy costs are only a limited share of the total TCO. The maintenance costs of the triplet are €257k (21%) higher, and the direct construction costs are €1.2M 46% higher. Therefore, the energy savings cannot make up for the higher direct construction costs and maintenance costs. It is visible that even if the triplet would use no energy at all, the TCO of the triplet still would be higher.

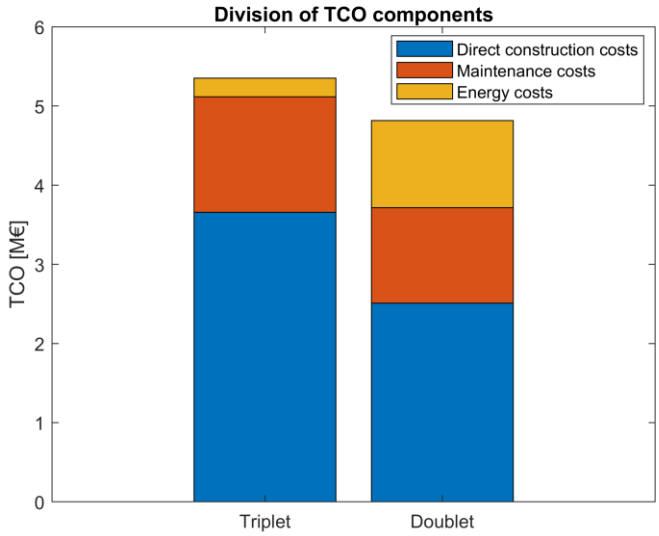

Figure 63 Division of TCO components for the business case optimized triplet +30% scenario and doublet for middle cost scenario

Most likely is it possible to further improve the business case as that has been done now by removing more solar collectors. This can further increase the financial performance of the triplet, but would also increase energy consumption, CO_2 emissions, and electricity grid loads. The hot well efficiency does only seem to have a limited effect on the TCO results. For the high electricity cost level, the TCO of the triplet can come close to a doublet. Potential financial benefits coming from reduced electricity grid loads, decrease in greenhouse gas emissions, compliance with government climate objectives which would not have been possible with doublet systems, and potential subsidies have not been considered but likely can increase the financial performance of a triplet system.

5.7 CO_2 emission reduction

Both a doublet and triplet system exclusively use electric energy. The triplet system reduces electricity consumption by approximately 83% relative to the doublet over a period of 30 years (considering the more business case optimized scenario energy consumption plus 30%, including extra required energy during startup). When the electricity generation source is the same for a triplet as for the doublet, the CO_2 emission reduction is the same percentage per year. The absolute CO_2 emission reduction however is dependent on the specific CO_2 emission of the electricity source. If the building owner only buys green energy, there will be no CO_2 emission reduction at all, because it would be 0 for both the triplet and doublet. It is therefore important to select a representative specific CO_2 emission factor. There is an ongoing downtrend in electricity CO_2 emission factor, caused by the increased implementation of sustainable generation [48]. To accommodate for representability and the fact that there is a decreasing trend, electricity generation CO_2 emission predictions by the Dutch Environmental Assessment Agency (PBL) are used. They predict the emission factor for 2025 and 2030 [49]. They calculated it using two different methods leading to two different results. This is an average (integral method) and a marginal method (reference park method). For electricity consumption reductions, the marginal method is advised [50]. However, the values for both methods will be used.

The goal for the Dutch government is to be almost CO_2 emission neutral in 2050 [51]. It is assumed that electricity production will be fully emission-free in 2050, and the emission factor from 2030 to 2050 is linearly interpolated to be 0 in 2050. This then leads to the emission factor over the period of 30 years, starting in 2025, displayed in Figure 64. Also included is a CO_2 emission factor prediction made by Royal HaskoningDHV. In that prediction, it is not assumed that the emission will be 0 in 2050, and uses average emission data (not marginal). All three scenarios are rough estimations, however, it is deemed fairer for comparison than just using the current CO_2 emission factors for the whole period.

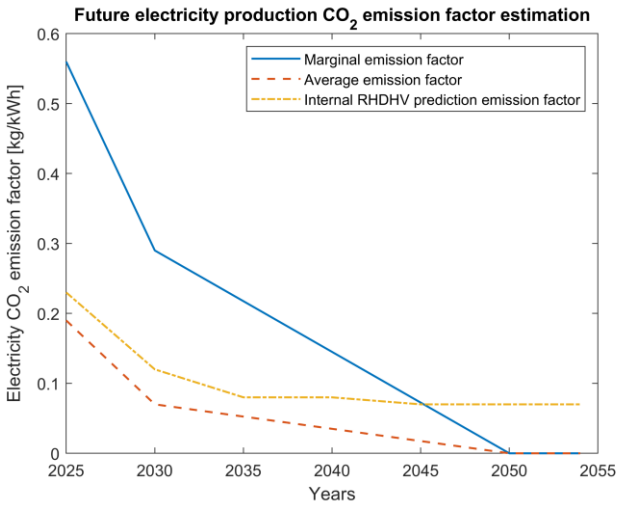

Figure 64 Assumed electricity production emission factors

For the same four scenarios as in the TCO business case optimized scenario calculation, the CO_2 emissions for the period of 2025 until 2054 are calculated (30 years) and displayed in Figure 65.

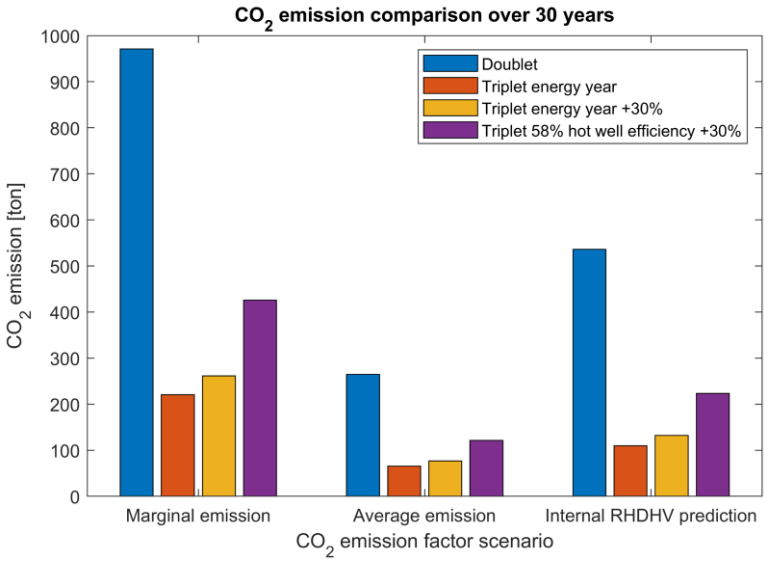

Figure 65 CO_2 emissions over a 30-year period comparison

For the marginal emission factor scenario, the CO_2 emission reduction relative to the doublet equals 545 to 751 tons, depending on the triplet scenario. This are reductions of 56% to 77%. For the average emission factor scenario, the CO_2 emission reductions are 143 to 199 tons

(54% to 75%). For the internal RHDHV predictions, the emission savings are 313.1 to 426 tons (58% to 80%).

Taking the different emission scenarios and triplet scenarios into account, the expected absolute CO_2 emission reduction ranges from 143 to 751 tons, and the relative CO_2 emission reduction ranges from 54% to 80%. Embedded greenhouse gas emissions are not taken into account, but can possibly shift the results.

5.8 Conflict with PV panels

(Almost) the whole roof is filled with solar collectors for the purpose of the triplet system. In the original design of the Mijnbouwstraat, PV panels are placed on the roof with a total area of approximately 1,500 m^2. The estimated annual electrical energy generation of these panels is approximately 240 MWh (based on internal design documents). When implementing the triplet system, this means that the PV panels need to be removed, and therefore also removing the 240 MWh of electricity generation. The triplet results have shown that (assuming the business case optimized basis triplet scenario + 30%) the triplet can save approximately 150 MWh of electricity per year. However, this means that with the triplet in place, an extra 90 MWh of electrical energy needs to be extracted from the electricity grid. As generated electrical energy generated by PV panels is regarded to have no CO_2 emission, implementing a triplet instead of a doublet would actually result in a higher CO_2 emission (unless it uses green electricity). This is contrary to the sustainable goal of the triplet system. Considering the three different CO_2 emission scenarios, the triplet would lead to an increase in CO_2 emissions with 130 to 477 tons over 30 years. Also, for the cost calculation was assumed that there would be a net electricity consumption decrease. However, in this case it would result in a net electricity consumption increase with the implementation of the triplet. This will significantly negatively affect the TCO of the triplet system, and there with the financial feasibility.

Next to the increase in electrical grid consumption and increase in CO_2 emissions, there are also consequences for the compliance of set sustainability goals for the building. The initial goal before the start of the design was to make the building Paris Proof. When this goal was set, the Paris Proof total net energy consumption level was 50 kWh/m^2. However, the Paris Proof value has been raised in the meanwhile to 70 kWh/m^2. However, the design goal for the Mijnbouwstraat is still set at 50 kWh/m^2. In the early phase of the design, a Paris Proof calculation was made. This calculation includes energy consumption for heating, cooling, ventilation, CH and CW circulation pumps, domestic hot water, lighting, and devices. When adjusting the calculation with the latest heat and cold consumptions, this comes to a total energy consumption of 867.4 MWh (68.8 kWh/m^2). When also adjusting for the latest PV panel layout, which generates 240 MWh (19.0 kWh/m^2), the net energy consumption then comes to 49.8 kWh/m^2, which is within the goal of 50 kWh/m^2. When then implementing the triplet system, the energy consumption lowers to 718 MWh (57.0 kWh/m^2). But because there is now no electrical generation anymore, the net specific energy consumption raises to 57.0 kWh/m^2, which is above the goal of 50 kWh/m^2, and an increase to the doublet situation. Although, it is below the Paris Proof level. The significant reduction in electricity grid load will keep existing.

A potential solution to increase this performance is to apply PVT collectors. PVT collectors can both generate heat and electricity with the same panel. By evaluating different PVT collectors from [52], [53], most glazed PVT collectors have similar thermal performance figures. n_0=0.53, a_1=4.57 W/m^{2}K, and a_2=0.014 W/m^{2}K^2 seem representative of a large share of PVT collectors. By performing a separate simulation (only the solar collector model, not connected to the building and other installations), it was found that the thermal heat generation of PVT collectors is 65% less than that of solar collectors (370 MWh instead of 1063 MWh). This is caused by the lower optical efficiency and higher heat loss factor of PVT collectors relative to solar collectors. A performance estimation can be made about what would happen if all solar collectors are replaced by PVT collectors based on the data in Figure 31. It is then assumed that the system dynamics and the hot well efficiency stay equal. This leads to an electrical energy consumption of 112 MWh when all solar collectors are replaced by PVT collectors (including 30% safety factor). This means now only 71 MWh (39%) is saved relative to the doublet situation. This is a more rough estimate, as it deviates further from the original situation but is still expected to be within reasonable error. Where the heat pump in the original situation delivers 5% of the heat to the building, in this situation it has to deliver 63% of the heat. This decreases the benefits of the triplet system significantly. Based on [54], [55] and the fact that the water outlet temperature of the panel will be relatively high, it is assumed that the electrical generation of PVT collectors is 14% less than the PV panels (therefore 200 Wp/m^2 and 0.8 kWh/Wp (based on internal design documents) times 0.86 is assumed). The electrical annual generation will then be 411 MWh. This would give a lower electricity consumption from the grid than in the doublet situation by approximately 242 MWh.

However, this is not a totally fair comparison, because for the doublet situation, only part of the roof is filled with PV panels. If for the doublet situation it is assumed that the same roof area is filled with PV panels as is filled with PVT collectors for the triplet situation, it would reduce the electricity consumption from the grid by 238 MWh relative to the original doublet situation. This almost leaves no difference in triplet and doublet net energy consumption.

Considering those two situations, the triplet with PVT collectors is still more energy efficient than the doublet system. However, important advantages for the triplet are highly reduced with the introduction of the PVT collectors, as 63% of the heat now must be generated by the heat pump. This causes another issue, which is that the heat pump now produces much more cold than what is required. This would cause the cold well to expand year over year. If no cold is then generated back into the buffer well, the cold well can start to negatively influence the buffer and hot wells. For the energy consumption calculation, it is assumed that this cold is regenerated back into the buffer well using the dry cooler. Considering the significant heat pump share, this scenario seems not feasible.

There can also be a scenario where not all solar collectors are replaced with PVT collectors, but only a part of them, so that the electricity generation is equal to that of the original doublet situation. Considering the lower electrical yield by PVT collectors relative to PV panels, 1744 m^2 of PVT collectors must be placed to generate 240 MWh of electrical energy. This would lead to an estimated decrease in heat generation by the PVT collectors of 383 MWh. This increases the energy consumption of the triplet to 71 MWh (including 30% safety margin). The heat share that must be delivered by the heat pump raises to 38%. The net consumption from the grid relative to the original doublet situation reduces by 112 MWh. The CO_2 emission

relative to the doublet reduces with 133 (average) to 510 (marginal) tons over a 30-year period. On a whole building level, this is a 15% to 16% reduction. The net energy consumption of the building becomes 40.9 kWh/m^2, which is an 18% decrease. In this situation, there is no overproduction of cold by the heat pump, so no regeneration is required. The expected peak load on the grid is approximately 30 kW. This is a 91% reduction from the doublet energy plant.

For this scenario, a new TCO calculation can be made. It is expected that the heat pump capacity raises from 125 kW to 175 kW, and is adjusted in the direct construction costs calculation. Part of the original solar collectors must be replaced by PVT collectors, which will cost more than solar collectors. However, it is assumed that the increase in PVT collector price is compensated by the cost saving of the PV panel removal. Therefore, no price adjustments are made for the PVT collectors. Only the middle electricity cost scenario has been calculated. Over a period of 30 years, the original business case optimized TCO difference between triplet and doublet for the middle cost scenario is €537k in advantage for the doublet, which is +11.2%. For the scenario with PVT, this leads to a difference of €833k in advantage of the doublet, which is +17.3%.

Table 5 provides an overview of the different mentioned PVT scenarios. It also includes a partially covered PVT scenario with a well efficiency of 58% instead of 68%. It is visible that in that situation, the heat pump share is over 50%. Also over 60 MWh of cold must be regenerated annually.

Table 5 Overview of different PVT scenarios

	Energy consumption energy plant	*Electrical generation*	*Heat pump share*	*Net specific building consumption*	*Energy plant grid load peak*	*TCO difference relative to original doublet*	*CO_2 emissions relative to doublet on building level*
	MWh_e	MWh_e	%	kWh_e/m^2	kW_e	%	%
Original doublet	183	240	100%	49.8	330	-	-
Doublet full PV panels	183	478	100%	30.9	330		
Triplet 68% efficiency only SC	33	0	5%	57.0	19	> +41%	+17%*
Triplet 68% efficiency full PVT	112	411	63%	30.6			
Triplet 68% efficiency partial PVT	71	240	38%	40.9	30	+17.3%	-15%*
Triplet 58% efficiency partial PVT	97	240	56%	43.0	40	+20.6%	-11%*

*Zero when made use of green energy from electricity grid

To summarize, in the situation of the Mijnbouwstraat where PV panels are placed on the roof, implementing a triplet system with only solar collectors would result in a net decrease in

consumed electricity from the grid. Attached to this are higher CO_2 emissions and an increase in energy bill. The TCO calculation was calculated with a reduction in energy bill, not taking the PV panel removal into account. With an increased energy bill for the triplet, the TCO calculation results in a significantly more negative performance for the triplet system. This is because from a financial standpoint, the higher investment costs of the triplet must be compensated by the reduction in operational costs. But if next to the investment costs the operational costs are also higher, the difference in TCO between the doublet and triplet will keep growing for each year. This is unfeasible. When partially applying PVT collectors so that the electrical generation is equal to the original situation, there will be a decrease in net consumption from the grid relative to the doublet situation. However, the share in heat pump delivery will be 38%, or even 56% when a lower hot well efficiency is assumed. This decreases the advantages of electricity grid peak power reduction, CO_2 emission, and energy consumption. The energy savings relative to the doublet are lower, reducing financial feasibility. It is likely the conflict between triplet and PV panels would occur for most buildings, as it will be a big challenge to comply with regulations without electrical generation. When the heating share from the hot well decreases, the hot well volume will be smaller. This would lead to a lower hot well efficiency, but has not been considered.

5.9 Feasibility with monumental status into account

By looking at the other results, it can already be expected that when the monumental status of the Mijnbouwstraat is considered, an ATES triplet system is not feasible. This is because all solar collectors which would be visible from the streets must be removed. This means that of the 2,985 m^2 solar collectors, 764 m^2 must be removed. This leaves over 2221 m^2 of solar collectors. Of this, 1,744 m^2 must be converted to PVT collectors, as was shown in the previous section. Assuming constant system dynamics and well efficiencies to the original situation, only 386 MWh of heat is generated by the solar collectors and PVT collectors. This has as result that approximately 62% of the heat must be generated by the heat pump. The energy consumption will rise to approximately 109 MWh (including 30% safety factor). There will be a large imbalance in cold generation (by the heat pump) and cold consumption, which would require regeneration. There will be an energy saving of 74 MWh per year relative to the doublet, which is only 40%. The expected energy plant electric peak is roughly 45 kW, which is still a large decrease relative to a doublet (-86%). The difference in TCO to the doublet is expected to be €711k (+14.8%).

Considering the only small decrease in energy consumption, the fact that the majority of the heat comes from the heat pump, a 15% difference in TCO, required cold regeneration, and the fact there is a good possibility that the hot well efficiency is lower than is now assumed, resulting in higher energy consumption, an ATES triplet system is deemed unfeasible for the Mijnbouwstraat when the monumental status is taken into account, as is the case in reality.

6 Discussion, conclusions and future research

This chapter presents the discussion, conclusions, and recommendations for future work.

6.1 Discussion

- This research uses a relatively simple model for the subsurface wells. This is done in the consideration that no better usable and integral model was available at the moment, that the focus of this research is more on the building and generation side, and the fact that a detailed subsurface model is under development. As the used model is a simplified model, it also gives simplified results, and most likely with a higher deviation from reality. Therefore, it for example is possible that in reality, temperature deviations in the hot well can be larger. If this is the case, this would mean that the well temperature can drop below a desirable temperature, which can cause problems in heat power delivery to the building. Also, for this research, the well efficiencies are assumed at a certain level, based on literature, while in reality, this is a function of the specific subsurface conditions and the way the well is used. It is also possible that the relationship between well thermal recovery efficiency and the effective efficiency in reality is somewhat different than the simple well model does make appear. This is due to the fact that it makes use of one weighted average well temperature within a bubble. It therefore does not consider the temperature change of the water outside the bubble. In reality, it is possible that due to the energy losses from within the bubble to outside the bubble, it creates some useful energy outside of the bubble instead of the assumption in the simple model that all energy lost to outside the bubble is wasted energy. Also, when selecting the thermal recovery efficiency for the hot well, the size of the ATES wells were not taken into consideration to increase representability. However, smaller ATES wells do have lower thermal recovery efficiencies. An advanced triplet subsurface model is currently under development in the NWO-funded ATES triplet project. This model will be able to closer estimate the well dynamics, such as temperature deviations and thermal recovery efficiency, which will lead to a more accurate model.

- There often is a performance gap between simulation and reality [56], [57]. This can have many causes. The created simulation model in this research tries to model reality as well as possible, but has not been validated. The individual models are calibrated based on the available design information. However, the design information is on the full load point of the component. Partial load information was not available and therefore the models are not adjusted and compared for partial load situations. As the system operates in partial load for the majority of the time, partial load performance can have an impact on the total system performance. However, by looking at the results, the expected impact on the final conclusions is limited.

  Also, other parts of the system can perform differently than is now simulated. This especially can cause problems if the different uncertainties in the simulation all fall the wrong way. For example, if the heat demand is higher than simulated and the solar collector heat generation is lower than simulated, then the heat generation by the heat pump is increased from both sides. Those uncertainties are the reason that in the TCO calculation and the CO_2 emission calculation, scenarios with a +30% safety factor are considered.

- In this research is assumed that the dry cooler is not bound to noise restraints, and can operate whenever it is desired. However, in reality, the noise created by the dry cooler can form a problem, in the form of noise pollution. When this is the case, the fan speed must be reduced at certain moments (for example at night), to decrease the sound pressure level. Attached to this fan speed reduction is a cooling power reduction. If noise pollution is a big problem for a certain situation, which causes fan speed reduction during a large share of the time, a higher dry cooler capacity must be selected. However, considering the relatively low costs and footprint of a dry cooler, a required increase in dry cooler capacity most likely does have little effect on the overall feasibility.

- When it appeared that the solar collectors alone cannot generate enough heat to sustain itself, an additional heat source was introduced in the form of a heat pump. The reason for choosing a heat pump was that it was deemed the most widely applicable solution for most buildings. However, it is also possible to use a different additional heat source. For example, the Mijnbouwstraat will have a connection to potentially connect the building with the to-be-built geothermic heat supply on the TU Delft campus. This geothermic connection would be a good replacement for the heat pump in a triplet system. For other situations, where a connection to a district heating network is available, that could also be a good solution. It is also possible that these alternatives can function as the main heat source instead of solar collectors in combination with an ATES triplet system.

- Subsidies have not been considered in the TCO calculation because there is too much uncertainty. There are multiple reasons for this uncertainty. The first reason is the fact that a triplet system does not yet exists, and therefore is unclear in what subsidy category it exactly would fall. Another reason for uncertainty is that subsidies change very regularly. Subsidies are applicable for a doublet (heat pump and PV panels). It is therefore logical that also subsidies would be available for a triplet system (at least for the solar collectors and/or PVT panels). The exact impact of subsidies on the financial performance of the triplet is difficult to predict. Considering the advantages of a triplet over a doublet, in principal it would be logical for the government to grant higher subsidies for a triplet system than for a doublet system. If this indeed would be the case, the TCO difference between doublet and triplet would decrease.

The results of this research can be used to gain insight into the functioning and feasibility of an ATES triplet system. Before an ATES triplet system can be implemented in practice, further extensive research is required. The simulation model that is created during this research will partly be used in the ongoing NWO-funded ATES triplet project. This project will look further into the feasibility and functioning of ATES triplet systems.

6.2 Conclusions

An ATES triplet system is technically feasible for a building like the Mijnbouwstraat when not taking the monumental status into account. A monovalent system is not technically feasible because of the structural deficit in heat generation by the solar collectors. Also, for the reliability of heat supply, an additional heat source is required. With a 125 kW heat pump in place, the system is expected to be able to sustain through consecutive extreme weather periods without running out of heat. By doing this, the reliability of heat supply by the triplet system is not in doubt. Technical feasibility for the cooling side is much easier to reach, as the footprint of a dry cooler is small, and the costs are low. The triplet system does not lead to a decrease in building user comfort relative to a doublet system. The simulation results show that thermal power delivery is no problem. All peak power can come from the wells with similar flow capacity as used in the doublet. Temperatures in the hot well do not drop too low to cause a decrease in comfort in the simulation. However, due to the usage of a relatively simple subsurface model, it is possible that this can be different in reality, and must be further investigated. During the startup of the system, it is possible that an extra temporary heat source is required to guarantee sufficient heat delivery to the building.

The dynamics of a triplet system are vastly different than in a doublet system. It is expected that the control of the system is more complex than in a doublet system, but feasible. Relative to the energy plant consumption of a doublet, the triplet with all solar collectors achieves significant savings. Depending on the hot well thermal recovery efficiency, these savings range from 65% to 82%, taking the 30% safety factor for the triplet into account in the more business case optimized scenario. The peak load on the electricity grid is reduced by approximately 94%, relative to the energy plant of the doublet. On a full building level, this is a 33% reduction.

For none of the calculated scenarios can the triplet system financially outperform a doublet system over a period of 30 years. The investment costs of the triplet system are much higher than the doublet, and the results indicate that this cannot be recouped by the energy savings. Despite the lower financial performance, the difference in total cost of ownership of the triplet relative to the doublet is limited. For the middle electricity price scenario, the difference in TCO is 11% higher than the doublet, which is a limited amount. Most likely, the business case for the triplet system can be improved, resulting in a closer match to the doublet. Considering the large benefits of the triplet system over the doublet system, it is possible that the increase in TCO is worth it to implement a triplet system. Subsidies can possibly (partially) close the gap.

The case of the Mijnbouwstraat most likely is a positive case. The reason for this is the relatively low heat and cold demand and the fact that it has three usable floor levels. It is likely that many buildings have a higher thermal demand than the Mijnbouwstraat building. When the specific heating demand is higher, this would lead to a higher required heat generation by the heat pump, reducing the advantage over a doublet quickly with increased demand. Also, an increase in cold demand would lead to a lower overall SPF, due to the fact that the SEER for the cooling side is much lower than the SCOP for the heating side (with low heat pump share). Also, buildings with more than three usable floors will have worse performance, as the roof area to usable floor area ratio decreases, increasing the heat pump share. Therefore, it is expected that for many buildings, the performance of a triplet will be lower than for the

Mijnbouwstraat case. This decreases the advantages and increases the gap in TCO to a doublet, reducing the feasibility.

A monovalent system is expected to be not feasible for many buildings. It may be technically feasible for some situations, but as a significant amount of extra solar collectors is required to guarantee system reliability, it most likely is not financially feasible, as those extra solar collectors are barely used. It is therefore expected to be more advantageous to try to cover the average heat demand with the solar collectors, and extreme weather years with the heat pump or other additional heat sources.

The simulation shows that a quadruplet configuration performs better than a triplet system, although the difference is limited. Due to the limited increase in performance, it is likely that the financial performance of the system is lower than the triplet, because of the required extra ATES well.

For buildings with PV panels in place, like the Mijnbouwstraat building, this can cause a conflict with the triplet system. The triplet system requires most of the roof, if not all roof, to be filled with solar collectors, which leaves no place left for PV panels. The reduction in energy consumption by the triplet system is lower than the generated energy by the PV panels when they would be left in place (at least for the Mijnbouwstraat case). This causes a net increase in electricity consumption and CO_2 emission relative to a doublet situation when a triplet system is implemented with only solar collectors. The only leftover advantage of the triplet in this case would be the reduced grid load, while all other advantages are wiped out, and would further decrease the financial performance. PVT collectors can be an option, but significantly reduce heat generation relative to solar collectors (-65%). This causes the required heat generation by the heat pump to increase significantly (5% to 38%), which causes a large increase in energy consumption (33 MWh to 71 MWh) when compensating for the lost electricity generation by partly placing PVT collectors. The energy consumption is still less than the doublet, but the difference is decreased (82% to 61%). When a lower hot well efficiency is assumed, the heat pump share even increases to over 56%. The advantage of CO_2 emission reduction is smaller, and the difference in TCO rises from 11% to 17%. The advantage of electricity grid load reduction also becomes smaller, but the reduction is still significant. This can potentially play an important role in reducing grid congestion, which in regards can be a key element in accelerating the energy transition.

An ATES triplet system is technically feasible and can be reliable when an additional heat source is included. Financial performance is worse than a doublet system and is expected to be for most situations, not considering potential subsidies. Energetically, it is expected that a triplet system will always perform better than a doublet system. When there is a conflict with PV panels, a triplet system will have decreased performance, reducing its advantages over a doublet system, and have decreased financial performance. This makes the business case worse, and the decision to implement a triplet system over a doublet system less attractive.

No conclusive statement can be made about the feasibility of an ATES triplet system, as this is dependent on many factors. For example how a building owner would weigh the increase in TCO relative to the achieved energy consumption, CO_2, and grid load reductions. Or what the effect is of the collector placement on the building's appearance. Also what the actual hot well

efficiency will be will play an important role. The subsidy intensity also will a role in this, as this can improve financial performance. Current regulations would now prevent a triplet system from being implemented, but this can possibly change in the future.

6.3 Recommendations for future research

- As is already in the planning, it is recommended to connect the simulation model to a more advanced subsurface model. This will give better insight into the actual well efficiencies and temperature dynamics and therefore can give a more complete answer regarding the feasibility of an ATES triplet system.

- Lowering the required CH supply temperature can possibly cause an increase in system performance. By lowering the required CH supply temperature, the hot well temperature can also drop, likely resulting in lower hot well losses. The consumers in the building must be fit for this lower supply temperature, otherwise it can give problems in thermal power delivery. The simple subsurface model used during this research was not fit to investigate this, but the subsurface model under development will be.

- It was discussed that heat pipe vacuum tube solar collectors have been considered, but not further investigated in this research due to a combination of reasons. One of those reasons was that heat pipe vacuum tube solar collectors normally cannot be placed with an inclination less than 25°. Two heat pipe vacuum tube solar collectors could be found where it is claimed that they could operate in (almost) horizontal positions. However, as nothing was stated about the decrease in efficiency when indeed placing it in a horizontal position, this was too uncertain to use in this research. However, it might be worth it to further investigate the application of heat pipe vacuum tube solar collectors, as they potentially can increase the performance of the triplet system.

  Also, there can be looked into better performing PVT collectors. Most found PVT collectors all had very similar thermal performance figures. The applied PVT collector in this research was based on those figures. One PVT collector could be found with much higher performance. However, it looks like a ‘too good to be true’ situation. The reason for thinking that is that next to the much higher optical efficiency than other PVT collectors, it also has a high electrical efficiency and the lowest indicated price of all PVT collectors. Therefore, it was not further looked into this collector. However, it may be worth it to investigate higher performing PVT collectors, as this can improve the triplet performance.

  Also, it can be investigated if optimizations in solar collector layout are possible. On flat roof parts, an east-west layout was selected, to generate the most heat per available roof area, and to prevent shadow fall from collector on collector. Most heat is generated during the summer months, when the angle of the sun is the highest. It can be investigated if the system would benefit from a more ‘aggressive’ solar collector layout, in which shadow fall when the sun angle is low is taken for granted, in return for a more optimal solar collector orientation (facing south with larger inclination). This could potentially result in a higher heat generation within the available roof area. This could not be investigated during this research, as shadow fall is not included in the used simulation model.

- Direct heat and cold delivery to the building is preferred over indirect delivery, as with direct delivery the energy losses are lower, especially for the hot side of the system. However, due to the phase difference between heat demand and heat generation, the direct heating share is limited. The buffer vessel helps to improve this, but is not suitable to store large amounts, and loses energy over time. It is possible that the performance of the system can be improved by introducing an additional short-term (days/weeks) energy storage, where losses are time-independent. It is recommended to investigate the possibilities to combine the triplet system with other forms of energy storage in order to improve system efficiency and/or costs. A possible option for this can for example be heat storage in salt hydrates.

- The effect of change in building usage has not been investigated in this research, but can have effects on the feasibility of a triplet system. Changing thermostat setpoints, occupancy rate, and building function can impact the thermal demand, which in regards can have an effect on the functioning of the system and reliability of the system. It is recommended to investigate the effects of changing building usage on the feasibility of a triplet system.

- This research focuses on only one case. Based on the outcome of this case, in relation to the fact that this case is deemed a more positive case than many buildings, some statements are made about the expected feasibility for other buildings, but with caution. The best way to investigate the overall feasibility of a triplet system is to investigate a wide range of buildings. The conflict with PV panels is here important to consider. It might not be necessary to create dynamic simulations for all those buildings. When knowing the available roof area, heat demand, cold demand, and considering the system dynamics learned from this research, a rough estimate can already be made.

- Control in a triplet system is expected to be more complex than in a doublet system. This for example is caused by the large number of possible operational modes, and the extra buffer well. The control in this research is done in a more simplified way than that can be applied in reality. It is recommended to further investigate the control possibilities of triplet systems, and what effect the control has on the system performance and efficiency. Also is recommended to investigate a smarter way to estimate and control the required heat generation share of the heat pump.

- The current regulatory restriction of a maximum ATES injection temperature of 25°C would prevent the implementation of a triplet system. It is recommended to investigate the chance that this regulatory restriction can be removed in the future, to make triplet systems possible.

References

[1] Netbeheer Nederland, “Netcapaciteit - Netbeheer Nederland.” https://www.netbeheernederland.nl/dossiers/netcapaciteit-60 (accessed Mar. 06, 2023).

[2] M. Bloemendal and A. Van Wijk, “Verwarming en koeling zonder warmtepomp met WKO-triplet,” 2017. https://www.h2owaternetwerk.nl/vakartikelen/verwarming-en-koeling-zonder-warmtepomp-met-wko-triplet (accessed Mar. 02, 2023).

[3] J. J. Pape, “Feasibility study of an ATES triplet,” 2017.

[4] RVO, “Ondiepe bodemenergie - open systemen,” 2021. https://www.rvo.nl/onderwerpen/bodemenergie-aardwarmte/open-systemen (accessed Mar. 01, 2023).

[5] ISSO, “ISSO-publicatie 39 Energiecentrale met warmte en koude opslag (WKO),” 2014.

[6] Monumentaal, “Royal HaskoningDHV omarmt faculteitsgebouw - MONUMENTAAL magazine,” 2022. https://www.monumentaal.com/royal-haskoningdhv-omarmt-faculteitsgebouw/ (accessed Mar. 24, 2023).

[7] Dutch Green Building Council, “Paris Proof met het deltaplan duurzame renovatie,” 2018.

[8] C. H. P. Hoogervorst, “DE ENERGIENEUTRALE WIJK IN NEDERLAND,” 2009.

[9] Atho, “Vloerverwarming - ATHO Centrale Verwarming.” https://www.atho.nl/vloerverwarming (accessed Nov. 16, 2022).

[10] ISSO, “ISSO publicatie 49 Kwaliteitseisen vloer-en wandverwarming en vloer- en wandkoeling,” 2004.

[11] IES, “Heat Emitter Radiant Fraction.” https://help.iesve.com/ve2021/table_13_heat_emitter_radiant_fraction.htm# (accessed Nov. 16, 2022).

[12] Dantuma Wegkamp, “Stralingsverwarming is de toekomst,” 2015. https://dantumawegkamp.nl/kennisbank/stralingsverwarming-is-de-toekomst (accessed Nov. 16, 2022).

[13] Christopher L. Conroy and Stanley A. Mumma, “Ceiling Radiant Cooling Panels as a Viable Distributed Parallel Sensible Cooling Technology Integrated with Dedicated Outdoor Air Systems,” *ASHRAE Trans*, 2001.

[14] J. A. Duffie and W. A. Beckman, “Solar engineering of thermal processes,” 1991.

[15] M. Embaye, R. K. Al-Dadah, and S. Mahmoud, “Effect of flow pulsation on energy consumption of a radiator in a centrally heated building,” *International Journal of Low-Carbon Technologies*, vol. 11, no. 1, pp. 119–129, Apr. 2014, doi: 10.1093/ijlct/ctu024.

[16] Engie, “Op welk cijfer zet je je thermostaatkraan voor welke temperatuur?,” 2020. https://www.engie.be/nl/blog/verwarming/thermostaatkraan-cijfers-en-temperaturen/ (accessed Nov. 16, 2022).

[17] M. Soleimani, “Analysis of the Thermal Performance of Hydronic Radiators and Building Envelop: Developing Experimental (Step Response) and Theoretical Models and Using Simulink to Investigate Different Control Strategies,” *Civil Engineering Research Journal*, vol. 2, no. 4, Oct. 2017, doi: 10.19080/cerj.2017.02.555595.

[18] X. Baoping, F. Lin, and D. Hongfa, “SIMULATION ON HYDRAULIC HEATING SYSTEM OF BUILDING UNDER THE CONTROL OF THERMOSTAT RADIATOR VALVES,” 2007.

[19] R. P. Kramer, “Clever climate control for culture: energy efficient indoor climate control strategies for museums respecting collection preservation and thermal comfort of visitors,” 2017.

[20] J. Buzás, I. Farkas, A. Biró, and R. Németh, “Modelling and Simulation of a Solar Thermal System,” *IFAC Proceedings Volumes*, vol. 30, no. 5, pp. 143–147, May 1997, doi: 10.1016/s1474-6670(17)44423-5.

[21] M. Grahovac, P. Tzscheutschler, M. Grahovac, and P. Liedl, “Simplified Solar Collector Model: Hourly Simulation of Solar Boundary Condition for Multi-Energy Optimization,” 2010. [Online]. Available: https://www.researchgate.net/publication/277202650

[22] V. Rostampour Samarin, M. Bloemendal, M. Jaxa-Rozen, and T. Keviczky, “A control-oriented model for combined building climate comfort and aquifer thermal energy storage system,” 2016.

[23] de M. H. Wit, “Hambase : heat, air and moisturmodel for building and systems evaluatione ,” 2006. Accessed: Mar. 23, 2023. [Online]. Available: www.tue.nl/taverne

[24] M. Wit de, “Hambase Part II Input and Output.” 2013.

[25] NEN, “NEN5060+A1 Hygrothermische eigenschappen van gebouwen - Referentieklimaatgegevens,” 2018.

[26] M. Abuasbeh, J. Acuña, A. Lazzarotto, and B. Palm, “Long term performance monitoring and KPIs’ evaluation of Aquifer Thermal Energy Storage system in Esker formation: Case study in Stockholm,” *Geothermics*, vol. 96, Nov. 2021, doi: 10.1016/J.GEOTHERMICS.2021.102166.

[27] L. Gao, J. Zhao, Q. An, X. Liu, and Y. Du, “Thermal performance of medium-to-high-temperature aquifer thermal energy storage systems,” *Appl Therm Eng*, vol. 146, pp. 898–909, Jan. 2019, doi: 10.1016/J.APPLTHERMALENG.2018.09.104.

[28] B. Sanner, F. Kabus, P. Seibt, and J. Bartels, “Underground Thermal Energy Storage for the German Parliament in Berlin, System Concept and Operational Experiences,” *Proceedings World Geothermal Congress*, pp. 24–29, 2005.

[29] L. Paci, L. Pasquinelli, and I. Fabricius, “Overview of High Temperature Aquifer Thermal Energy Storage (HT-ATES): challenges and strengths,” *Conference: CERE - Discussion Meeting*, 2016, Accessed: Feb. 07, 2023. [Online]. Available: https://www.researchgate.net/publication/304024115_Overview_of_High_Temperature_Aquifer_Thermal_Energy_Storage_HT-ATES_challenges_and_strengths?channel=doi&linkId=5763ca0208aecb4f6fee101b&showFulltext=true

[30] L. Gao, J. Zhao, Q. An, J. Wang, and X. Liu, “A review on system performance studies of aquifer thermal energy storage,” *Energy Procedia*, vol. 142, pp. 3537–3545, Dec. 2017, doi: 10.1016/J.EGYPRO.2017.12.242.

[31] W. Sommer, J. Valstar, P. van Gaans, T. Grotenhuis, and H. Rijnaarts, “The impact of aquifer heterogeneity on the performance of aquifer thermal energy storage,” *Water Resour Res*, vol. 49, no. 12, pp. 8128–8138, Dec. 2013, doi: 10.1002/2013WR013677.

[32] R. M. Zeghici, G. H. P. Oude Essink, N. Hartog, and W. Sommer, “Integrated assessment of variable density–viscosity groundwater flow for a high temperature mono-well aquifer thermal energy storage (HT-ATES) system in a geothermal reservoir,” *Geothermics*, vol. 55, pp. 58–68, May 2015, doi: 10.1016/J.GEOTHERMICS.2014.12.006.

[33] S. Ganguly, M. S. Mohan Kumar, A. Date, and A. Akbarzadeh, “Numerical investigation of temperature distribution and thermal performance while charging-discharging thermal energy in aquifer,” *Appl Therm Eng*, vol. 115, pp. 756–773, Mar. 2017, doi: 10.1016/J.APPLTHERMALENG.2017.01.009.

[34] M. Bakr, N. van Oostrom, and W. Sommer, “Efficiency of and interference among multiple Aquifer Thermal Energy Storage systems; A Dutch case study,” *Renew Energy*, vol. 60, pp. 53–62, Dec. 2013, doi: 10.1016/J.RENENE.2013.04.004.

[35] SPF, “Collectors | SPF-Testing Rapperswil.” https://www.spftesting.info/data/1.kollektoren/?l=en (accessed Feb. 08, 2023).

[36] Remeha, “Remeha Solar Pro.” Remeha, 2019.

[37] Gasworks.ie, “ Solar Vacuum Tubes .” https://www.gasworks.ie/services/solar-thermal-vacuum-tubes/ (accessed Feb. 08, 2023).

[38] Alternative energy tutorials, “Evacuated Tube Collector for Solar Hot Water System.” https://www.alternative-energy-tutorials.com/solar-hot-water/evacuated-tube-collector.html (accessed Feb. 08, 2023).

[39] Resolar, “TC Heatpipe - Resolar.” https://www.resolar.nl/tc-heatpipe/#page-content (accessed Mar. 14, 2023).

[40] Viessmann, “Vitosol 300-TM: buiscollector | Viessmann NL.” https://www.viessmann.nl/nl/producten/zonnecollectoren/vitosol-300-tm.html#Produktdetails (accessed Mar. 14, 2023).

[41] Zonneboiler-advies.nl, “Zonnecollector kopen: Soorten, Werking, Prijs & Rendement.” https://www.zonneboiler-advies.nl/zonnecollector (accessed Feb. 22, 2023).

[42] Güntner, “myGüntner Drycooler.” https://www.myguentner.com/#/mygpc (accessed Mar. 23, 2023).

[43] R. Wasman, “Optimalisatie van WKO-systemen door het verbeteren van de retourtemperatuur vanuit luchtbehandelingskasten,” 2020.

[44] Carrier, “61WG/30WG/30WGA-A selectiegegevens.” 2020.

[45] ISSO, “ISSO-publicatie 95 Procesengineering voor klimaatinstallaties,” 2016.

[46] Grundfos, “Dimensioneringspagina | Grundfos.” https://product-selection.grundfos.com/nl/size-page?qcid=2061728082 (accessed Mar. 30, 2023).

[47] Expertise Centrum Warmte, “Bodemenergie en WKO,” 2022. https://www.expertisecentrumwarmte.nl/themas/technische+oplossingen/techniekfactsheets+energiebronnen/bodemenergie+en+wko/default.aspx (accessed Feb. 22, 2023).

[48] CBS, “Rendementen en CO2-emissie van elektriciteitsproductie in Nederland, update 2020,” 2020. https://www.cbs.nl/nl-nl/achtergrond/2022/05/rendementen-en-co2-emissie-van-elektriciteitsproductie-in-nederland-update-2020 (accessed Mar. 06, 2023).

[49] P. Planbureau voor de Leefomgeving, “Klimaat- en Energieverkenning 2022,” 2022, Accessed: Feb. 22, 2023. [Online]. Available: www.pbl.nl/kev
[50] Agentschap NL, “Berekening van de CO2-emissies, het primair fossiel energiegebruik en het rendement van elektriciteit in Nederland,” 2012.
[51] “Klimaatakkoord,” 2019.
[52] B. Perers, S. Furbo, and J. Dragsted, “O1 PVT Technology Research - Best practices report,” 2021.
[53] Econo, “Hoe moet je collector rendement en opbrengst interpreteren ?” https://www.econo.nl/wetenswaardig-hoe-moet-je-collector-rendement-en-opbrengst-interpreteren (accessed Feb. 27, 2023).
[54] W. Van Helden, B. Roossien, and J. Mimpen, “Maximalisering zonne-energie per vierkante meter met PVT,” *VV+*, 2013.
[55] J. H. Kim and J. T. Kim, “Comparison of electrical and thermal performances of glazed and unglazed PVT collectors,” *International Journal of Photoenergy*, vol. 2012, 2012, doi: 10.1155/2012/957847.
[56] C. van Dronkelaar, M. Dowson, C. Spataru, and D. Mumovic, “A Review of the Regulatory Energy Performance Gap and Its Underlying Causes in Non-domestic Buildings,” *Front Mech Eng*, vol. 1, p. 17, Jan. 2016, doi: 10.3389/FMECH.2015.00017/BIBTEX.
[57] P. De Wilde and R. Jones, “The building energy performance gap: up close and personal”.
[58] ISSO, “ISSO-publicatie 74 Thermische behaaglijkheid,” 2014.
[59] Vabi, “Beperkt opwekkingsvermogen belastingduurkromme,” 2016. https://www.vabi.nl/nieuws/beperkt-opwekkingsvermogen-vabi-elements-gebouwsimulatie/ (accessed Mar. 27, 2023).
[60] Homedeal, “Zonnecollector [Prijzen, mogelijkheden & tips].” https://www.homedeal.nl/zonnepanelen/zonnecollector/ (accessed Feb. 22, 2023).
[61] Solar-nu.nl, “HRSolar HPC-2,5 zonneboiler collector (2,5 m2).” https://www.solar-nu-webshop.nl/webshop/zonnecollector--zonneboiler/zonnecollector-vlakkeplaat/detail/254/hrsolar-hpc-25-zonneboiler-collector-25-m2.html (accessed Feb. 22, 2023).
[62] Solar Garant, “OEG Vlakkeplaat collector 4Plus harpabsorptie 2.53m2.” https://solargarant.nl/oeg-vlakkeplaat-collector-oeg-4plus-harpabsorptie/ (accessed Feb. 22, 2023).
[63] Remeha, “C250 V, C250 H.” https://products.remeha.be/site/index/catalog/type/cons/language/nl/web_code/remeha_c250_h_v (accessed Feb. 22, 2023).
[64] Techniekwebshop.nl, “Remeha Solar Pro - collector / C250V.” https://www.techniekwebshop.nl/remeha-solar-pro-collector-c250v-zonne-voor-verticale-montage-zonnecollector-verkoop-per-1-x-1-stuk-7203644-3661238660410-9020323.html (accessed Feb. 22, 2023).
[65] DTP, “Factsheet: WKO en warmtepompen.” https://www.dynamictidalpower.eu/resources/Documenten/wko-RVO.pdf (accessed Feb. 22, 2023).
[66] Wasco, “Flamco SideFlow Clean 5.0L - Wasco.” https://www.wasco.nl/artikel/3671660 (accessed Mar. 30, 2023).

[67] Ubel, “Ubel | SpiroVent - Superior - S400 - Vacuümontgasser - Ontgassers.” https://ubel.nl/assortiment/1916/spirovent-superior-vacu%E2%88%9A%C2%BAmontgasser-spirovent-superior (accessed Mar. 30, 2023).

[68] General Services Administration, “HONEYCOMB SOLAR THERMAL COLLECTOR,” *GPG-027*, 2016, Accessed: Feb. 22, 2023. [Online]. Available: www.gsa.gov/gpg

[69] Klima Gaucin, “Solar thermal energy.” http://klimagaucin.com/en/about-us/solar-thermal-energy/ (accessed Feb. 22, 2023).

[70] Cooling Tower Systems, “Cooling Tower Life Expentancy,” 2021. https://www.coolingtowersystems.com/blogs/cts-news/cooling-tower-life-expentancy (accessed Feb. 22, 2023).

[71] Mining.com, “Refurbishment Extends Cooling Tower Life By 20 Years,” 2014. https://www.mining.com/web/refurbishment-extends-cooling-tower-life-by-20-years/ (accessed Feb. 22, 2023).

[72] Daikin, “De levensduur van de warmtepomp.” https://www.daikin.be/nl_be/warmtepompen/informatie/levensduur.html (accessed Feb. 22, 2023).

[73] Warmtepomp-info.nl, “Warmtepomp Carrier: info + prijzen.” https://www.warmtepomp-info.nl/warmtepomp-carrier/ (accessed Feb. 22, 2023).

[74] NIBE, “Warmtepomp levensduur: hoelang zit je warm met warmtepomp?” https://aardgasvrij.nibenl.eu/werking/warmtepomp-levensduur (accessed Feb. 22, 2023).

[75] B. Schiebler, F. Giovannetti, and S. Fischer, “Reduction of maintenance costs for solar thermal systems with overheating prevention,” 2018. https://task54.iea-shc.org/Data/Sites/1/publications/B03-Info-Sheet--Reduction-of-Maintenance-Costs-by-Preventing-Overheating.pdf (accessed Feb. 22, 2023).

Appendix

Appendix I | Deviations in the model relative to the real building

AHUs In the original design, there are three AHUs. AHU North of 35,850 m^3/h, AHU South of 28,400 m^3/h, and AHU South-East of 5,500 m^3/h. The reason for using one smaller AHU are mainly practical reasons, like ductwork space and technical room space, and not power or energy related reasons. To save extra modeling work, complexity, and computational demand, AHU South and South-East are combined into one AHU. As combining the two AHUs results in a design flow rate very similar to the North AHU, the two remaining AHUs will be kept the same specification. It is expected that the simplifications mentioned above will have little effect on the results.

FCUs In some special rooms in the original design, fan coil units (FCUs) are used. The reason for using these are mainly practical reasons. In the model, FCUs are not modeled. It is assumed that these rooms also use the climate ceiling and radiator setup like the other rooms. It is expected that this simplification has little effect on the results.

Reheaters In the original design, there are reheaters present in the ducts to the atria. Those reheaters most likely are present to reduce the time constant of the heating system in the atria, because they respond faster than the underfloor heating. To save modeling work, complexity, and computational demand, the reheaters in the atria are not modeled. It is expected that this can have some influence on the outcome, but that this is very limited. Reason for expecting this is that the underfloor heating alone can provide enough heating power in almost all cases, but only is slower responding, which results in a longer time required to get to the heating temperature setpoint. However, as the comfort requirement in the atria is lower than in offices, and that the night heating setpoint is already near the required minimum comfort temperature, the effect on comfort will be small.

Underfloor cooling In the original design, there is a flow control on the cooling side of the underfloor system HX to control the supply temperature of the water on the other side of the HX. In the model, this has been changed to a temperature control instead of flow control. The reason for this is that by doing it in this way, no complex HX model has to be modeled, but a simple constant temperature jump can be assumed. It is expected that this deviation has little influence on the results.

MER/SER In the original design, there are some MER/SER rooms with cooling by FCUs. In the Vabi Elements model, this has not been included. The installed capacity for this is 14 kW. Relative to the total installed cooling capacity (approximately 800 kW), this is low. Also, the cooling demand for this system throughout the year is unknown. Therefore, the MER/SER room cooling has not been modeled. The effect of this deviation is most likely small, but cannot be said with full certainty.

Groups In the original design, there are two climate ceiling groups and two radiator groups. This is mostly done for practical reasons. In the model, this has been simplified to one group for each. It is expected that this deviation has no little to no effect on the results.

CO_2 control The original design does incorporate VAV control for most rooms based on CO_2 concentration. This is also incorporated in the original Vabi Elements model. However, the

effect of the CO_2 control is considered to be small, at least in the models. There are two reasons for this. The first reason is that the occupancy is kept constant during the day in the simulations. Therefore, the CO_2 concentration will also be kept fairly constant, and with that also the flow rate. In reality, the occupancy will vary throughout the day, especially for meeting rooms. However, the data is not available to model those variations. The second reason is the fact that is it not an all-air system. The ventilation system's primary function is to supply fresh air, and not transport energy. Of course, some energy is transported by the air, as the air temperature does have to be within a certain setpoint. However, considering that there is a modulated heat recovery wheel, the influence on the total energy demand by removing CO_2 control is expected to be limited. Considering those arguments and in addition the additional modeling work and complexity, CO_2 control is not included in the model. The expected influence of this decision on the results is limited.

Appendix II | Equations used in simulation model

Underfloor model
Source: [8]

$$R_x = \frac{d_x \ln\left(\frac{d_x}{\pi\delta}\right)}{2\pi\lambda_b * (\pi\delta l)} \quad 14$$

$$C_{pipe,1}\frac{dT_{pipe,1}}{dt} = \frac{T_{finishing\ layer} - T_{pipe,1,avg}}{2R_x} + \dot{m}c_p(T_{in} - T_{pipe,1}) \quad 15$$

$$C_{pipe,2}\frac{dT_{pipe,2}}{dt} = \frac{T_{finishing\ layer} - T_{pipe,2,avg}}{2R_x} + \dot{m}c_p(T_{pipe,1} - T_{pipe,2}) \quad 16$$

$$C_{surf,top}\frac{dT_{surf,top}}{dt} = \frac{T_{top\ layer} - T_{surf,top}}{R_1} + \frac{T_{above} - T_{surf,top}}{R_{top}} \quad 17$$

$$C_{top\ layer}\frac{dT_{top\ layer}}{dt} = \frac{T_{surf,top} - T_{top\ layer}}{R_1} + \frac{T_{finishing\ layer} - T_{top\ layer}}{R_2} \quad 18$$

$$C_{finishing\ layer}\frac{dT_{finishing\ layer}}{dt} = \frac{T_{top\ layer} - T_{finishing\ layer}}{R_2} + \frac{T_{pipe,1,avg} + T_{pipe,2,avg} - 2T_{finisnging\ layer}}{2R_x} + \frac{T_{ins} - T_{finishing\ layer}}{R_3} \quad 19$$

$$C_{insulation}\frac{dT_{insulation}}{dt} = \frac{T_{finishing\ layer} - T_{insulation}}{R_3} + \frac{T_{concrete} - T_{insulation}}{R_4} \quad 20$$

$$C_{concrete}\frac{dT_{concrete}}{dt} = \frac{T_{insulation} - T_{concrete}}{R_4} + \frac{T_{surf,bot} - T_{concrete}}{R_2} \quad 21$$

$$C_{surf,bot}\frac{dT_{surf,bot}}{dt} = \frac{T_{concrete} - T_{surf,bt}}{R_5} + \frac{T_{under} - T_{surf,bot}}{R_{bot}} \quad 22$$

In which R_x is the replacement resistance of the heat flow from the water to the construction, $\dot{m}$ is the mass flow rate of water, d_x is the pipe distance, δ is the pipe diameter, $\lambda_b$is the heat conductivity of the finishing layer, l is the pipe length, C is the heat capacity of the material layer, R is the heat resistance of the different layers. R_{top} is the heat transfer resistance between the floor surface and the room, T are the temperatures, of which T_{in} is the water inlet temperature, and $T_{pipe,2}$ is the return temperature. Temperatures are in °C, dimensions in m, heat conductivity in W/mK, resistance in K/W, heat capacity in J/K, and mass flows in kg/s.

Climate ceiling

Source: [13]

$$\mu = \sqrt{\frac{U_0}{k\delta}} \quad 23$$

$$F = \frac{\tanh\left(\frac{\mu(w - D)}{2}\right)}{\frac{\mu(w - D)}{2}} \quad 24$$

$$F' = \frac{D + (w - D)F}{w} \quad 25$$

$$\frac{T_{out} - T_{room}}{T_{in} - T_{room}} = e^{\frac{-UAF'}{\dot{m}c_p}} \quad 26$$

$$F_R = \frac{\dot{m}c_p(T_{out} - T_{in})}{-AU_0(T_{in} - T_{room})} \quad 27$$

$$T_{p,mean} = T_{in} + \frac{\dot{m}c_p(T_{out} - T_{in})}{AF_RU_0} \quad 28$$

In which U_0 is the heat transfer coefficient from the plate to the room, k is the plate thermal conductivity, δ is the fin thickness, w is the pipe distance, D is the tube diameter, A is the plate area, $\dot{m}$ is the mass flow rate of water, and T are the different temperatures. Based on this formula set, the thermal power provided to the room and the return temperature can be calculated. Temperatures are in °C, heat transfer coefficient is in W/m^{2}k, dimensions are in m, heat conductivity is in W/mK and the mass flow rate is in kg/s.

Radiator

Source: [15]

$$(M_{rad}c_{rad} + M_wc_w)\frac{dT_{w,m}}{dt} = \dot{m}_wc_w\Delta T - U_0 * A * LMDT \quad 29$$

$$dT_{w,m} = \frac{T_{w,in} + T_{w,out}}{2} \quad 30$$

$$LMDT = \frac{T_{w,in} - T_{w,out}}{\ln\left(\frac{T_{w,in} - T_{room}}{T_{w,out} - T_{room}}\right)} \quad 31$$

$$\dot{Q}_w = \dot{m}_w c_w \Delta T \quad 32$$

$$\dot{Q}_{rad} = U_0 * A * LMDT \quad 33$$

In which M is the mass of the water content and of the metal, U_0 is the heat transfer coefficient of the radiator to the room, $\dot{m}$ is the mass flow rate of water, A is the radiator surface in contact with the room, LMDT is the logarithmic mean temperature difference and T are the different temperatures. Temperatures are in °C, heat transfer coefficient is in W/m²K, dimensions are in m, mass flow rate is in kg/s, and specific heat capacity is in J/kgK.

Solar collector

$$\rho V c_p \frac{dT_{out}}{dt} = A * I\left(n_0 - a_1\frac{T_c - T_{outdoor}}{I} - a_2\frac{(T_c - T_{outdoor})^2}{I}\right) - \dot{m}c_p(T_{out} - T_{in}) \quad 34$$

In which V is the water volume inside of the solar collector, A is the aperture area , I is the effective solar irradiance on the aperture area, n_0 the optical efficiency, $a_1$the linear heat loss coefficient, a_2 the quadratic heat loss coefficient, $\dot{m}$ is the mass flow rate of water, $T_{outdoor}$ the outdoor air temperature, and T_c the solar collector temperature. When there is a mass flow, the average temperature between the inlet and outlet water is used for T_c. When there is no mass flow, the outlet temperature is used for T_c, which is then the same as the stagnant water temperature. Temperatures are in °C, irradiance is in W/m², mass flow rate is in kg/s, volume is in m³, and specific heat capacity is in J/kgK.

Subsurface model

Source: [22]

$$T_{aq+1} = \frac{V_{aq} * T_{aq}}{V_{aq} + V_{in}} + \frac{V_{in} * T_{in}}{V_{aq} + V_{in}} - \frac{\alpha(T_{aq} - T_{amb})}{V_{aq} + V_{in}} \quad 35$$

In which T_{aq+1} is the aquifer temperature at the calculated time step, T_{aq} is the aquifer temperature at the previous time step, $V_{aq}$is the aquifer volume at the previous time step, V_{in} is the injected or extracted water volume at the previous time step, T_{in} is the injected water temperature at the previous time step, T_{amb} is the aquifer's natural temperature, and α is the thermal loss factor. Temperatures are in °C and volumes are in m³.

Appendix III | Dry cooler selection

Güntner

Date: 19.1.2023

Drycooler / GFHC FD 050.1/23-53-0041715M

Capacity:	175,00 kW [1]	**Medium:**	Ethyleen glycol 34 Vol. % [2]
Opp. reserve:	-3,70 %	**Intredetemp.:**	25,00 °C
Luchtdebiet:	39 930,00 m³/h	**Uittredetemp.:**	8,00 °C
Luchtsnelheid:	2,50 m/s		
Lucht intrede:	0,00 °C 40 %	**Drukverlies:**	0.50 bar
Hoogte:	0,00 m	**Volumestroom:**	9.61 m³/h
Lucht uittrede:	12,70 °C 17 %		
K-Waarde:	29.58 W/(m²·K)	**Massastroom:**	10191 kg/h
Ventilatoren (AC): (VT03150U)	6 Aantal 3~400V 50HzΔ/(Y)		
Motorgegevens:		**Geluidsdrukniveau:**	53,00 dB(A) in 10,00 m [4]
Toerental:	1390 min-1 / (1180 min-1)	**Geluidsvermogen:**	84,00 dB(A)
Capaciteit(el.):	0.72 kW	**ErP:**	Compliant [5]
Stroomopname:	1,41 A [3]		
totale el. opgenomen vermogen:	4,36 kW	**energie efficiency klasse:**	E
Omkasting:	Staal verzinkt, RAL 7035	**Pijpen:**	Koper [6]
W.W. oppervlak:	575,50 m²	**Lamellen:**	Aluminium [6]
Pijpinhoud:	62.7 l	**Aansl. per apparaat:**	
Lam. afstand:	2,10 mm	**Intrede:**	42.0 * 1.60 mm
Ledig gewicht:	420 kg [8]	**Uittrede:**	42.0 * 1.60 mm
Max. bedrijfsdruk:	10,00 bar	**PED classification:**	Art. 4, par. 3 [7]
		Passeringen:	8
Afmetingen: [8]			
Length:	2784 mm	**Verzamelaar:**	42.0 * 1.60 mm
Width:	1696 mm	**Verdeelpijp:**	42.0 * 1.60 mm
Height:	919 mm [8]	**Circuits:**	1N
No. legs:	4	**Strangen:**	24

Figure 66 Display of selection data of the 175 kW dry cooler from Güntner selection tool

Appendix IV | Heat pump type argumentation

By analyzing the system, 3 different main heat pump implementation concepts could be found. The concepts are the following:

1. Using the heat pump to charge the hot well during the year
2. Using the heat pump for direct heat supply to the building when the hot well is empty
3. Using the heat pump over the year for direct heat supply to the building

In concept 1, the heat pump works in a similar way as the solar collectors do. It charges the hot well, and during moments of building demand, it delivers directly to the building. The difference with the solar collectors is that the heat pump is not or less dependent on the outdoor conditions (dependent on heat pump type), and therefore can generate heat at a relatively constant level throughout the year.

In concept 2, the heat pump only becomes active when the hot well is empty. The solar collectors will charge the hot well, but because the heat generation by the solar collectors is not enough, it is expected that the hot well will be empty at some moment in the year. When the hot well cannot supply heat anymore, the heat pump will activate and supply heat directly to the building. At the design stage, it is unknown when the hot well (which time of the year) will be empty, as this is dependent on the occurred weather. Therefore, the heat pump in this concept must be designed to supply the maximum peak load to the building. When it is compared to the current doublet design, the combined installed heat pump thermal heating capacity is 1,000 kW. For the triplet with a concept 2 heat pump, this would then require a similar heat pump setup as in the original doublet design.

In concept 3, the heat pump is used to directly supply heat to the building. The heat pump will supply a base load to the building, with a maximum dependent on the heat pump limit. The remaining required heat is then delivered by the hot well and the solar collector, just as with the monovalent system. By providing this baseload heat delivery to the building, part of the heat demand is fulfilled by the heat pump, relieving the hot well.

The three heat pump concepts are judged based on 3 criteria. This will be used to select the best concept, which will be used further in this research. The three criteria are energy efficiency, load on the electricity grid, and required heat pump capacity.

Energy efficiency

As concept 1 is used to charge the well, the required condenser outlet temperature must be approximately 70°C, similar to the solar collector. This is relatively high for a heat pump and will result in a significantly lower COP than for direct heating, which only requires 50°C in concepts 2 and 3. Also, in concept 1 a large part of the heat generated by the heat pump is lost because of the low hot well efficiency, which requires more heat generation than in concept 3. Therefore, it is expected that concept 3 will have a higher energy efficiency than concept 1. The COP of concept 2 is expected to be more similar to concept 3. However, it is expected that in concept 2 more heat must be generated by the heat pump than in concept 3. The reason for this is that the heat pump is only activated when the hot well is empty. When the hot well is empty, the heat losses which occur during the charging of the hot well are

higher than normal. This then requires a larger heating share to be generated by the heat pump. Therefore, it is expected that concept 3 is the most energy efficient concept.

Load on grid
Concepts 1 and 3 generate heat throughout the year. Concept 1 can generate at a constant level thought out the year. Concept 3 adapts to the building load. But, as it is expected that the installed heat pump capacity for concept 3 is lower than for concept 1 (because of well losses in concept 1), the load on the grid will be similar between those two concepts. Concept 2 will have a significant load on the grid because it must supply full heating power to the building when the hot well is empty. Therefore this can give a peak to the electricity grid similar to a doublet system. Therefore it is expected that concepts 1 and 3 give a lower load on the electricity grid than concept 2.

Installed capacity
Installed capacity can be translated to investment costs, and therefore is used as a criterion. It is clear that concept 2 requires the largest power, as it must be able to provide peak heating demand when the well is empty. The required generated useful heat for concepts 1 and 3 will be similar. But because concept 1 must generate more heat to generate the same amount of useful heat as in concept 3, it is expected that the heat pump in concept 3 requires the least amount of installed capacity.

Concept 3 is expected to be the most energy efficient and have the lowest required installed capacity. The load on the grid is expected to be similar to concept 1. Based on these arguments, concept 3 seems to be the best concept for a heat pump implementation in an ATES triplet system.

Water-water or air-water heat pump
Within concept 3, a choice can be made between a water-water or an air-water heat pump.
To determine the best option out of those two, a simple calculation is made. The starting point of this calculation is that both heat pumps must generate 25 MWh of useful heat on an annual basis for a NEN5060 energy year. The 25 MWh is an estimate of the required generation to get the hot well in balance (same energy level at the start and the end of the year) from an early simulation. For the water-water heat pump, the assumed buffer well temperature is 19°C throughout the whole year. The heat pump system efficiency is assumed to be 50%. The condenser outlet temperature is kept constant at 50°C. With this, the COP is then constant though out the year at 5.05. The heat pump is active the whole year. It is assumed that the maximum heat pump capacity is determined by the electric connection value. Based on this, the required electric connection value of the heat pump is 1.1 kW. The annual electricity consumption is 5 MWh. The annual generated cold by the condenser is 20 MWh.

For the air-water heat pump, the evaporator inlet temperature is dependent on the outdoor air temperature, and therefore also the COP is dependent on the outdoor temperature. To prevent too low COP values, it is assumed that the heat pump is not active during December, January, and February, which are the coldest months. The condenser outlet temperature is assumed to be 50°C. Based on these assumptions, the required electric connection capacity is 2.8 kW. The annual electric energy consumption is 6.4 MWh.

Based on the energy consumption and the required heat pump capacity, the water-water heat pump performs better. Also other considerations can be made. The water-water heat pump generates 20 MWh of cold, which can be used to charge the cold well. This then requires a lower dry cooler capacity. As the annual cold demand is approximately 150 MWh, there is more than enough margin to prevent the cold well from growing, and the dry cooler still will be required, which can control the energy content in the cold well. Another advantage of the water-water heat pump relative to the air-water heat pump is that it does not provide any external noise. The air-water heat pump does have a fan on the outside, which produces noise, which can cause a required reduction in operating hours of the heat pump, which in regards would require a higher heat pump capacity. The only downside which can be found for the water-water heat pump is that the design complexity will be somewhat higher than with an air-water heat pump.

Based on the mentioned operations, a water-water heat pump according to concept 3 is selected to further investigate in this research.

Appendix V | Pump power calculation assumptions

Table 6 Overview of assumed pressure drops for different components

Component	**Pressure drop**	**Source**
HX (all)	50 kPa @ design flow rate	RHDHV internal expertise
Dry cooler coil	50 kPa @ 3.65 kg/s	Scaled from selected dry cooler spec sheet
1 solar collector (applied 3 in series)	13 kPa @ 0.0333 kg/s	[36]
ATES	550 kPa @ 85 m^3/h	Design document and estimate based on data from [43]
Piping	120 Pa/m @ design flow rate	General design guideline
HP con. and evap.	140 kPa @ max flow rate	Multiple Carrier spec sheets

Table 7 Overview of assumed n factors for different components

Component	**n [-]**	**Source**
HX	1.85	[45]
Dry cooler	1.85	Assumed same as HX
Solar collector	1.55	Derived from [36]
ATES	0.5	Estimate derived from data of [43]
Piping	2.0	General assumption
HP con. and evap.	1.85	Assumed same as HX

Appendix VI | Operational modes explanation

Table 8 Description of the different operational modes

Operational mode	Heat demand	Heat generation	Cold demand	Cold generation	Buffer well (when relevant)
0					
1	Y				
2	Y	Y <demand			
3	Y	Y >demand			
4	Y	Y <demand		Y	Charging
5	Y	Y <demand		Y	Discharging
6	Y	Y >demand		Y	
7			Y		
8			Y	Y <demand	
9			Y	Y >demand	
10		Y	Y	Y <demand	Charging
11		Y	Y	Y <demand	Discharging
12		Y	Y	Y >demand	
13	Y		Y		
14	Y	Y <demand	Y		
15	Y	Y >demand	Y		Charging
16	Y	Y >demand	Y		Discharging
17	Y		Y	Y <demand	
18	Y		Y	Y >demand	Charging
19	Y		Y	Y >demand	Discharging
20	Y	Y <demand	Y	Y <demand	
21	Y	Y >demand	Y	Y <demand	Charging
22	Y	Y >demand	Y	Y <demand	Discharging
23	Y	Y >demand	Y	Y >demand	
24	Y	Y <demand	Y	Y >demand	Charging
25	Y	Y <demand	Y	Y >demand	Discharging
26		Y			
27				Y	
28		Y	Y		Charging
29		Y	Y		Discharging
30	Y			Y	Charging
31	Y			Y	Discharging

Appendix VII | ISSO 74 ATG method

The indoor building user comfort is assessed using the ATG method described in ISSO 74 [58]. The English meaning of the Dutch ATG abbreviation is adaptive temperature limit. The ATG method provides a relation between running mean outdoor temperature and a comfort range based on operational indoor room temperature. A distinction is made between different comfort classes. The ATG graph is visible in Figure 67, together with indication of class A/B and class C. This is the graph of a Beta building. These are buildings with visible cooling, as is the case for the Mijnbouwstraat.

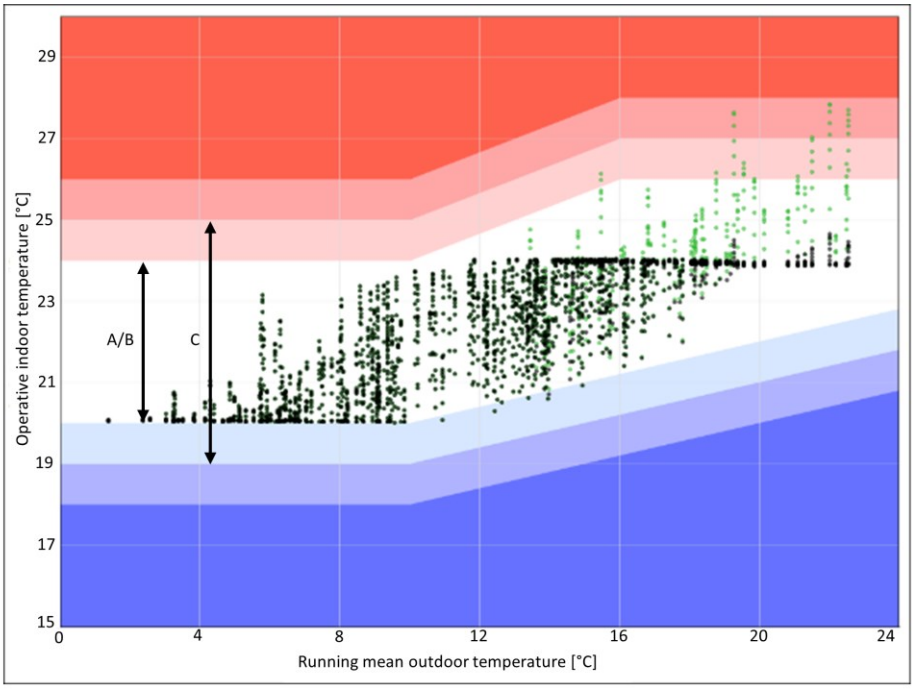

Figure 67 Display of ISSO 74 ATG graph (original from [59])

The ATG comfort assessment method has been modeled in Simulink as it is described in the ISSO 74 publication. The operative temperature is calculated by taking the arithmetic mean of the room air temperature and room radiant temperature. The running mean outdoor temperature is calculated over the last seven days with the weight factors as specified in ISSO 74. For each room, the average operative temperature per hour relative to the ATG graph is assessed during occupancy hours. If the operative temperature falls out of the specified ATG comfort class range, one over or under heating hour is registered for that room.

Appendix VIII | TCO calculation assumptions and overviews

Table 9 Triplet direct construction cost calculation

Triplet direct construction costs	**Number**	**Unit**	**Price per unit**	**Net cost**	**Material surcharge**	**Third party surcharge**	**Total**	**Source of price estimation / comments**
					10%	8%		
Solar collectors								
3364 m2 of flat plate solar collectors	1346	Panels	600	€ 807,360	€ 80,736			Estimate based combination of multiple internet sources [41], [60]–[64]
2090 m2 frames for installation on flat roof East/West 10°	836	Panels	120	€ 100,320	€ 10,032			Rough estimate based combination of multiple internet sources, also including PV frames due to almost no available data.
1274 m2 frames for installation on tilted roofs	510	Panels	90	€ 45,864	€ 4,586			Rough estimate based combination of multiple internet sources, also including PV frames due to almost no available data.
Pipe work to/from roof to technical room (DN100)	180	m	350	€ 63,000	€ 6,300			Internal RHDHV expertise
Pipe work between solar collectors	150	m	250	€ 37,500	€ 3,750			Based on Internal RHDHV expertise value
Sum of all circulation pumps	-	-	-	€ 16,783	€ 1,678			Grundfos website selection tool
HX @50 m3/h - 50kPa - LMDT =1K				€ 7,000	€ 700			Estimate based on internal document with key figures
Installation work placing solar collectors flat roofs	627	Hours	65	€ 40,755				45 min per collector estimate
Installation work placing solar collectors tilted roofs	510	Hours	65	€ 33,124				60 min per collector estimate
Installation work Other	200	Hours	65	€ 13,000				Estimate
Total						€ 101,799	**€ 1,374,288**	
ATES								
ATES subsurface side wells, inc. pumps, piping, and HXs @85 m3/h	3	Wells	170000	€ 510,000	€ 51,000	€ 44,880	**€ 605,880**	Reference value is €4000 m3/h for a doublet. Triplet assumed to be 1.5 that. Source are [65] and 2 internal RHDHV cost calculations
Dry cooler								
Dry cooler Güntner Twin=25°C Twout=8°C Tamb=0°C P=260 kW				€ 15,500	€ 1,550			Güntner selection tool
Circulation pump 3.65 kg/s @ 70 kPa (MAGNA3 40-120 F)				€ 2,873	€ 287			Grundfos selection tool
Pipework	75	m	250	€ 18,750	€ 1,875			Based on Internal RHDHV expertise value
HX @32 m3/h - 50kPa - LMDT =1K				€ 5,500	€ 550			Estimated on internal document with key figures

Installation and placement costs				€ 8,000				Estimate based internal RHDHV cost calculation for other project
Total							**€ 54,885**	
Heat pump								
Water-water heat pump 125 kW (price all inclusive)	125	kW	600	€ 75,000	€ 7,500			Internal RHDHV expertise and internal RHDHV cost calculations
Piping	25	m	350	€ 8,750	€ 875			Internal RHDHV expertise
Total							**€ 92,125**	
Technical room								
Hot generation pump @50 m3/h - 50kPa (MAGNA3 65-150 F)				€ 5,348	€ 535			Grundfos selection tool
Cold generation pump @21.6 m3/h - 50kPa (MAGNA3 40-150 F)				€ 3,404	€ 340			Grundfos selection tool
Hot bridge pump 85 m3/h @ 50 kPa (TP 100-110/4 A-F-A-BQQE-JW3)				€ 5,760	€ 576			Grundfos selection tool
Cold bridge pump 85 m3/h @ 50 kPa (TP 100-110/4 A-F-A-BQQE-JW3)				€ 5,760	€ 576			Grundfos selection tool
Buffer vessel 5000L	2		6000	€ 12,000	€ 1,200			Estimate based on internet search and internal document with key figures
Installation, pipe work, valves, etc				€ 360,000	€ 36,000			Based on internally made cost estimate for Mijnbouwstraat. For doublet is 300k. For triplet multiplied by 1.20 due to increased complexity and connections
Expansion vessel 1000L (inc. Installation)	2		4200	€ 8,400	€ 840			Estimated on internal document with key figures
Partial flow filters (inc. Installation)	2		4500	€ 9,000	€ 900			Estimate from [66] + installation estimate
Vacuum degasser (inc. Installation)	2		4700	€ 9,400	€ 940			Estimate from [67] + installation estimate
Electrical supplies				€ 35,000	€ 3,500			Estimate
Total							**€ 499,479**	
Control equipment				€ 403,200	€ 40,320		**€ 443,520**	Based on internally made cost estimate for Mijnbouwstraat. 336K for doublet. For triplet multiplied with 1.20 due to increased complexity
15% unforeseen cost margin							**€ 460,527**	15% of unforeseen cost over the total costs are taken into account
Grand total							**€ 3,530,705**	

Table 10 Doublet direct construction cost calculation

Doublet direct construction costs	**Number**	**Unit**	**Price per unit**	**Net cost**	**Material surcharge**	**Third party surcharge**	**Total**	**Source of price estimation / comments**
					10%	8%		
ATES								
ATES subsurface side wells, inc. Pumps, piping, and HXs @85 m3/h	2	€/Well	170000	€ 340,000	€ 34,000	€ 29,920	**€ 403,920**	Reference value is €4000 m3/h for a doublet. Triplet assumed to be 1.5 that. Source are [65] and 2 internal RHDHV cost calculations
Water-water heat pump								
2x water-water heat pump 300 kW (price all inclusive)	600	kW	600	€ 360,000	€ 36,000			Internal RHDHV expertise and internal RHDHV cost calculations
Piping	25	m	350	€ 8,750	€ 875			Internal RHDHV expertise
Total							**€ 405,625**	
Air-water heat pump								
2x air-water heat pump 200 kW (price all inclusive)	400	kW	600	€ 240,000	€ 24,000			Internal RHDHV expertise and internal RHDHV cost calculations
Piping	120	m	350	€ 42,000	€ 4,200			Internal RHDHV expertise
Total							**€ 310,200**	
Technical room								
Bridge pump				€ 5,760	€ 576			Grundfos selection tool
Buffer vessel 2000L	2		3000	€ 6,000	€ 600			Estimate based on internet search and internal document with key figures
Installation, pipe work, valves, etc.				€ 300,000	€ 30,000			Based on internally made cost estimate for Mijnbouwstraat. For doublet is 300k. For triplet multiplied by 1.20 due to increased complexity and connections
Expansion vessel 1000L (inc. Installation)	2		4200	€ 8,400	€ 840			Estimated on internal document with key figures
Partial flow filters (inc. Installation)	2		4500	€ 9,000	€ 900			Estimate from [66] + installation estimate
Vacuum degasser (inc. Installation)	2		4700	€ 9,400	€ 940			Estimate from [67] + installation estimate
Electrical supplies				€ 35,000	€ 3,500			Estimate
Total							**€ 410,916**	

Control equipment				€ 336,000	€ 33,600		**€ 369,600**	Based on internally made cost estimate for Mijnbouwstraat. 336K for doublet. For triplet multiplied with 1.20 due to increased complexity
15% unforeseen cost margin							**€ 285,039**	15% of unforeseen cost over the total costs are taken into account
Grand total							**€ 2,185,300**	

Table 11 TCO components life time expectancy assumptions

Component	**Assumed life time expectancy**	**Source(s)**
Solar collectors	25	[68], [69]
ATES	30	[47]
Dry cooler	25	[70], [71] (for cooling towers, but expected to be similar for dry cooler)
Heat pump	20	[72]–[74]
Technical room + control equipment	30	Assumed estimate

Table 12 TCO maintenance costs assumptions

Component	**Assumed maintenance cost (as part of direct construction costs of component)**	**Source(s)**
ATES	4%	[65] and internal RHDHV cost calculation
Solar collectors	0.8%	Based on [75] (slightly lowered due to large scale 1.01% to 0.8%)
All other	2%	Internal RHDHV cost calculation

Table 13 TCO calculation triplet basis scenario

Triplet basis scenario				**Triplet NEN5060 Energy year**			**Triplet NEN5060 energy year + 30%**			**Triplet NEN5060 energy year reduced hot well efficiency + 30%**		
Disc.	Year	Investment costs	Maintenance costs	Energy costs Low	Energy costs Mid	Energy costs High	Energy costs Low	Energy costs Mid	Energy costs High	Energy costs Low	Energy costs Mid	Energy costs High
	0	€ 3,530,705										
1.00	1	€ 0	€ 57,030	22595.30	39976.30	57357.30	23523.89	41619.19	59714.49	27652.56	48923.76	70194.96
0.99	2	€ 0	€ 56,476	3065.25	5423.13	7781.02	3984.82	7050.07	10115.32	8073.41	14283.72	20494.04
0.98	3	€ 0	€ 55,928	3035.49	5370.48	7705.47	3946.14	6981.62	10017.11	7995.03	14145.05	20295.07
0.97	4	€ 0	€ 55,385	3006.02	5318.34	7630.66	3907.82	6913.84	9919.86	7917.40	14007.72	20098.03
0.96	5	€ 0	€ 54,847	2976.83	5266.71	7556.58	3869.88	6846.72	9823.55	7840.54	13871.72	19902.90
0.95	6	€ 0	€ 54,315	2947.93	5215.57	7483.21	3832.31	6780.24	9728.18	7764.41	13737.04	19709.67
0.94	7	€ 0	€ 53,787	2919.31	5164.94	7410.56	3795.10	6714.42	9633.73	7689.03	13603.67	19518.31
0.93	8	€ 0	€ 53,265	2890.97	5114.79	7338.61	3758.26	6649.23	9540.20	7614.38	13471.60	19328.81
0.92	9	€ 0	€ 52,748	2862.90	5065.13	7267.36	3721.77	6584.67	9447.57	7540.46	13340.81	19141.16
0.92	10	€ 0	€ 52,236	2835.11	5015.96	7196.81	3685.64	6520.74	9355.85	7467.25	13211.28	18955.32
0.91	11	€ 0	€ 51,729	2807.58	4967.26	7126.94	3649.85	6457.44	9265.02	7394.75	13083.02	18771.29
0.90	12	€ 0	€ 51,226	2780.32	4919.03	7057.74	3614.42	6394.74	9175.06	7322.96	12956.00	18589.04
0.89	13	€ 0	€ 50,729	2753.33	4871.27	6989.22	3579.33	6332.66	9085.99	7251.86	12830.21	18408.57
0.88	14	€ 0	€ 50,237	2726.60	4823.98	6921.36	3544.58	6271.17	8997.77	7181.45	12705.65	18229.84
0.87	15	€ 0	€ 49,749	2700.13	4777.15	6854.17	3510.16	6210.29	8910.42	7111.73	12582.29	18052.85
0.86	16	€ 0	€ 49,266	2673.91	4730.77	6787.62	3476.08	6150.00	8823.91	7042.68	12460.13	17877.58
0.86	17	€ 0	€ 48,787	2647.95	4684.84	6721.72	3442.34	6090.29	8738.24	6974.31	12339.16	17704.01
0.85	18	€ 0	€ 48,314	2622.24	4639.35	6656.46	3408.92	6031.16	8653.40	6906.60	12219.36	17532.13
0.84	19	€ 0	€ 47,845	2596.78	4594.31	6591.84	3375.82	5972.60	8569.39	6839.54	12100.73	17361.92
0.83	20	€ 76,537	€ 47,380	2571.57	4549.70	6527.84	3343.04	5914.62	8486.19	6773.14	11983.25	17193.35
0.82	21	€ 0	€ 46,920	2546.61	4505.53	6464.46	3310.59	5857.19	8403.80	6707.38	11866.90	17026.43

0.81	22	€ 0	€ 46,465	2521.88	4461.79	6401.70	3278.45	5800.33	8322.21	6642.26	11751.69	16861.12
0.81	23	€ 0	€ 46,014	2497.40	4418.47	6339.55	3246.62	5744.01	8241.41	6577.77	11637.60	16697.42
0.80	24	€ 0	€ 45,567	2473.15	4375.57	6278.00	3215.10	5688.25	8161.40	6513.91	11524.61	16535.31
0.79	25	€ 1,130,826	€ 45,124	2449.14	4333.09	6217.05	3183.88	5633.02	8082.16	6450.67	11412.72	16374.77
0.78	26	€ 0	€ 44,686	2425.36	4291.02	6156.69	3152.97	5578.33	8003.69	6388.04	11301.92	16215.80
0.78	27	€ 0	€ 44,252	2401.81	4249.36	6096.91	3122.36	5524.17	7925.99	6326.02	11192.19	16058.36
0.77	28	€ 0	€ 43,823	2378.50	4208.11	6037.72	3092.04	5470.54	7849.03	6264.60	11083.53	15902.45
0.76	29	€ 0	€ 43,397	2355.40	4167.25	5979.10	3062.02	5417.43	7772.83	6203.78	10975.92	15748.06
0.75	30	-€ 896,301	€ 42,976	2332.54	4126.79	5921.05	3032.30	5364.83	7697.37	6143.55	10869.36	15595.17
	Sum	**€ 3,841,767**	**€ 1,490,501**	**€ 100,397**	**€ 177,626**	**€ 254,855**	**€ 124,666**	**€ 220,564**	**€ 316,461**	**€ 232,571**	**€ 411,473**	**€ 590,374**
	TCO			**€ 5,432,665**	**€ 5,509,894**	**€ 5,587,123**	**€ 5,456,935**	**€ 5,552,832**	**€ 5,648,729**	**€ 5,564,840**	**€ 5,743,741**	**€ 5,922,642**

Table 14 TCO calculation doublet scenario

Doublet basis scenario				**Doublet NEN5060 Energy year**		
Disc.	Year	Investment costs	Maintenance costs	Energy costs Low	Energy costs Mid	Energy costs High
	0	€ 2,185,300				
1.00	1	€ 0	€ 46,084	23795.20	42099.20	60403.20
0.99	2	€ 0	€ 45,636	23564.18	41690.47	59816.76
0.98	3	€ 0	€ 45,193	23335.40	41285.71	59236.02
0.97	4	€ 0	€ 44,754	23108.84	40884.88	58660.91
0.96	5	€ 0	€ 44,320	22884.49	40487.94	58091.39
0.95	6	€ 0	€ 43,890	22662.31	40094.85	57527.39
0.94	7	€ 0	€ 43,463	22442.28	39705.58	56968.87
0.93	8	€ 0	€ 43,041	22224.40	39320.09	56415.78
0.92	9	€ 0	€ 42,624	22008.63	38938.34	55868.05
0.92	10	€ 0	€ 42,210	21794.95	38560.30	55325.64
0.91	11	€ 0	€ 41,800	21583.35	38185.92	54788.50
0.90	12	€ 0	€ 41,394	21373.80	37815.19	54256.57
0.89	13	€ 0	€ 40,992	21166.29	37448.05	53729.81
0.88	14	€ 0	€ 40,594	20960.79	37084.48	53208.16
0.87	15	€ 0	€ 40,200	20757.29	36724.43	52691.58
0.86	16	€ 0	€ 39,810	20555.76	36367.89	52180.01
0.86	17	€ 0	€ 39,423	20356.19	36014.80	51673.41
0.85	18	€ 0	€ 39,041	20158.56	35665.14	51171.72
0.84	19	€ 0	€ 38,662	19962.84	35318.88	50674.91
0.83	20	€ 594,707	€ 38,286	19769.03	34975.98	50182.92

0.82	21	€ 0	€ 37,915	19577.10	34636.40	49695.71
0.81	22	€ 0	€ 37,546	19387.03	34300.13	49213.23
0.81	23	€ 0	€ 37,182	19198.80	33967.12	48735.43
0.80	24	€ 0	€ 36,821	19012.41	33637.34	48262.27
0.79	25	€ 0	€ 36,463	18827.82	33310.76	47793.70
0.78	26	€ 0	€ 36,109	18645.03	32987.36	47329.69
0.78	27	€ 0	€ 35,759	18464.01	32667.09	46870.17
0.77	28	€ 0	€ 35,412	18284.75	32349.94	46415.12
0.76	29	€ 0	€ 35,068	18107.22	32035.86	45964.49
0.75	30	-€ 269,713	€ 34,727	17931.43	31724.83	45518.23
	Sum	**€ 2,510,294**	**€ 1,204,420**	**€ 621,900**	**€ 1,100,285**	**€ 1,578,670**
	TCO			**€ 4,336,614**	**€ 4,814,998**	**€ 5,293,383**

Table 15 TCO calculation triplet more optimized business case scenario

Triplet optimized business case optimized scenario				**Triplet NEN5060 Energy year**			**Triplet NEN5060 energy year + 30%**			**Triplet NEN5060 energy year reduced hot well efficiency + 30%**		
Disc.	Year	Investment costs	Maintenance costs	Energy costs Low	Energy costs Mid	Energy costs High	Energy costs Low	Energy costs Mid	Energy costs High	Energy costs Low	Energy costs Mid	Energy costs High
	0	€ 3,370,573										
1.00	1	€ 0	€ 55,916	€ 22,842	€ 40,413	€ 57,984	€ 23,845	€ 42,187	€ 60,530	€ 27,872	€ 49,312	€ 70,753
0.99	2	€ 0	€ 55,373	€ 3,310	€ 5,856	€ 8,402	€ 4,303	€ 7,613	€ 10,923	€ 8,291	€ 14,669	€ 21,046
0.98	3	€ 0	€ 54,835	€ 3,278	€ 5,799	€ 8,320	€ 4,261	€ 7,539	€ 10,816	€ 8,210	€ 14,526	€ 20,842
0.97	4	€ 0	€ 54,303	€ 3,246	€ 5,743	€ 8,240	€ 4,220	€ 7,466	€ 10,711	€ 8,131	€ 14,385	€ 20,640
0.96	5	€ 0	€ 53,776	€ 3,214	€ 5,687	€ 8,160	€ 4,179	€ 7,393	€ 10,607	€ 8,052	€ 14,246	€ 20,439
0.95	6	€ 0	€ 53,254	€ 3,183	€ 5,632	€ 8,080	€ 4,138	€ 7,321	€ 10,504	€ 7,974	€ 14,107	€ 20,241
0.94	7	€ 0	€ 52,737	€ 3,152	€ 5,577	€ 8,002	€ 4,098	€ 7,250	€ 10,402	€ 7,896	€ 13,970	€ 20,044
0.93	8	€ 0	€ 52,225	€ 3,122	€ 5,523	€ 7,924	€ 4,058	€ 7,180	€ 10,301	€ 7,820	€ 13,835	€ 19,850
0.92	9	€ 0	€ 51,718	€ 3,091	€ 5,469	€ 7,847	€ 4,019	€ 7,110	€ 10,201	€ 7,744	€ 13,700	€ 19,657
0.92	10	€ 0	€ 51,215	€ 3,061	€ 5,416	€ 7,771	€ 3,980	€ 7,041	€ 10,102	€ 7,668	€ 13,567	€ 19,466
0.91	11	€ 0	€ 50,718	€ 3,032	€ 5,364	€ 7,696	€ 3,941	€ 6,973	€ 10,004	€ 7,594	€ 13,436	€ 19,277
0.90	12	€ 0	€ 50,226	€ 3,002	€ 5,312	€ 7,621	€ 3,903	€ 6,905	€ 9,907	€ 7,520	€ 13,305	€ 19,090
0.89	13	€ 0	€ 49,738	€ 2,973	€ 5,260	€ 7,547	€ 3,865	€ 6,838	€ 9,811	€ 7,447	€ 13,176	€ 18,905
0.88	14	€ 0	€ 49,255	€ 2,944	€ 5,209	€ 7,474	€ 3,827	€ 6,772	€ 9,716	€ 7,375	€ 13,048	€ 18,721
0.87	15	€ 0	€ 48,777	€ 2,916	€ 5,158	€ 7,401	€ 3,790	€ 6,706	€ 9,621	€ 7,303	€ 12,921	€ 18,539
0.86	16	€ 0	€ 48,303	€ 2,887	€ 5,108	€ 7,329	€ 3,753	€ 6,641	€ 9,528	€ 7,232	€ 12,796	€ 18,359
0.86	17	€ 0	€ 47,834	€ 2,859	€ 5,059	€ 7,258	€ 3,717	€ 6,576	€ 9,436	€ 7,162	€ 12,672	€ 18,181
0.85	18	€ 0	€ 47,370	€ 2,831	€ 5,010	€ 7,188	€ 3,681	€ 6,512	€ 9,344	€ 7,093	€ 12,549	€ 18,005
0.84	19	€ 0	€ 46,910	€ 2,804	€ 4,961	€ 7,118	€ 3,645	€ 6,449	€ 9,253	€ 7,024	€ 12,427	€ 17,830
0.83	20	€ 76,537	€ 46,455	€ 2,777	€ 4,913	€ 7,049	€ 3,610	€ 6,387	€ 9,163	€ 6,956	€ 12,306	€ 17,657
0.82	21	€ 0	€ 46,004	€ 2,750	€ 4,865	€ 6,980	€ 3,575	€ 6,325	€ 9,074	€ 6,888	€ 12,187	€ 17,485

0.81	22	€ 0	€ 45,557	€ 2,723	€ 4,818	€ 6,913	€ 3,540	€ 6,263	€ 8,986	€ 6,821	€ 12,068	€ 17,316
0.81	23	€ 0	€ 45,115	€ 2,697	€ 4,771	€ 6,845	€ 3,506	€ 6,202	€ 8,899	€ 6,755	€ 11,951	€ 17,147
0.80	24	€ 0	€ 44,677	€ 2,671	€ 4,725	€ 6,779	€ 3,472	€ 6,142	€ 8,813	€ 6,689	€ 11,835	€ 16,981
0.79	25	€ 1,020,649	€ 44,243	€ 2,645	€ 4,679	€ 6,713	€ 3,438	€ 6,083	€ 8,727	€ 6,625	€ 11,720	€ 16,816
0.78	26	€ 0	€ 43,813	€ 2,619	€ 4,633	€ 6,648	€ 3,405	€ 6,023	€ 8,642	€ 6,560	€ 11,606	€ 16,653
0.78	27	€ 0	€ 43,388	€ 2,593	€ 4,588	€ 6,583	€ 3,372	€ 5,965	€ 8,558	€ 6,496	€ 11,494	€ 16,491
0.77	28	€ 0	€ 42,967	€ 2,568	€ 4,544	€ 6,520	€ 3,339	€ 5,907	€ 8,475	€ 6,433	€ 11,382	€ 16,331
0.76	29	€ 0	€ 42,550	€ 2,543	€ 4,500	€ 6,456	€ 3,306	€ 5,850	€ 8,393	€ 6,371	€ 11,272	€ 16,172
0.75	30	-€ 812,356	€ 42,137	€ 2,519	€ 4,456	€ 6,394	€ 3,274	€ 5,793	€ 8,312	€ 6,309	€ 11,162	€ 16,015
	Sum	**€ 3,655,404**	**€ 1,461,388**	**€ 106,853**	**€ 189,047**	**€ 271,242**	**€ 133,059**	**€ 235,411**	**€ 337,764**	**€ 238,313**	**€ 421,631**	**€ 604,950**
	TCO			**€ 5,223,644**	**€ 5,305,839**	**€ 5,388,033**	**€ 5,249,850**	**€ 5,352,203**	**€ 5,454,555**	**€ 5,355,105**	**€ 5,538,423**	**€ 5,721,741**

Appendix IX | Simplified overview of whole simulation model

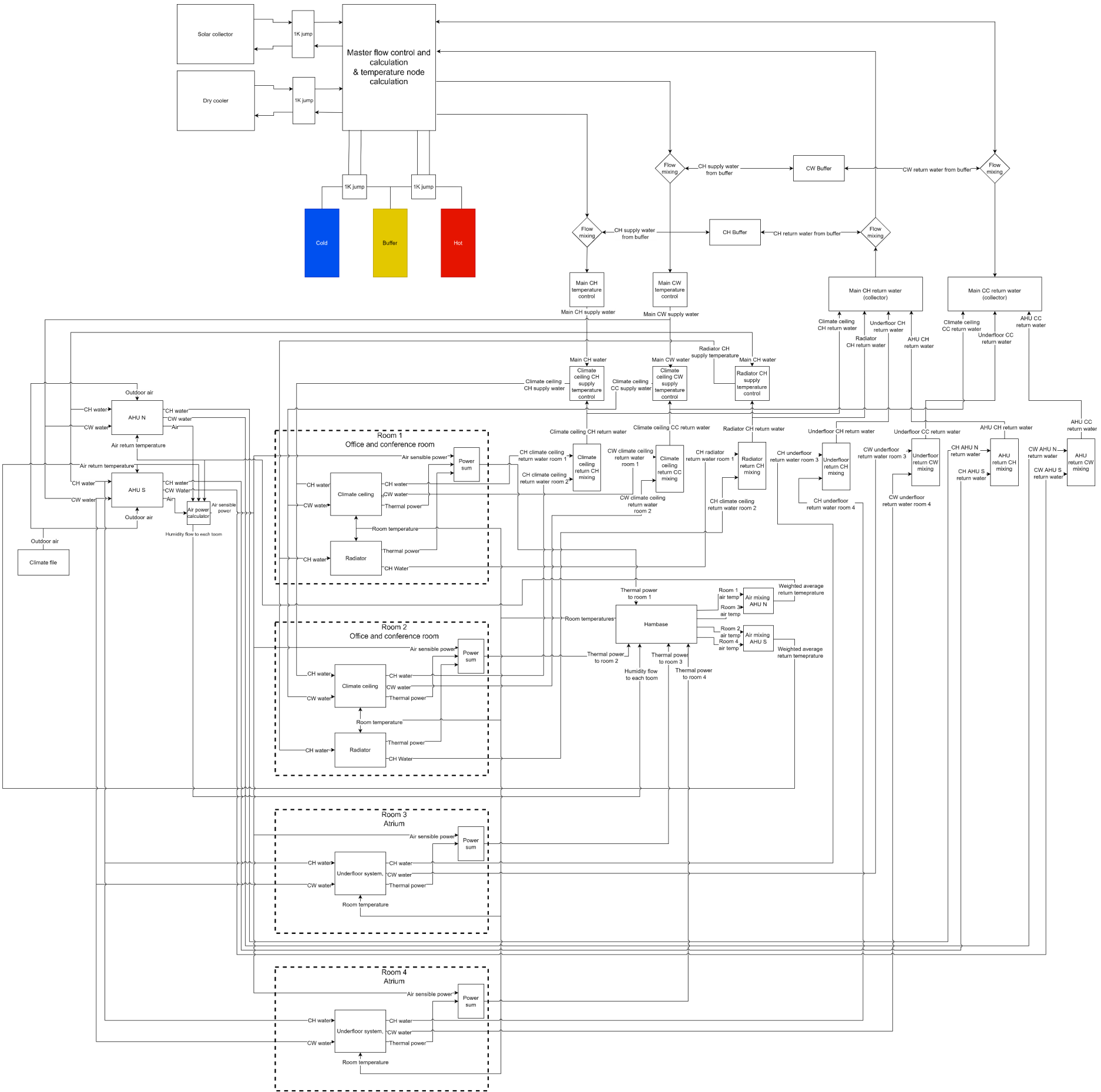

Figure 68 Simplified overview of simulation model